RES2DINV ver. 2025.1

Rapid 2D Resistivity & IP inversion

Wenner (α,β,γ), dipole-dipole, inline pole-pole, pole-dipole, equatorial dipole-dipole, offset pole-dipole, Wenner-Schlumberger, gradient and non-conventional arrays

On land, borehole, cross borehole, surface/borehole, aquatic and time-lapse surveys

AGS™ I Res2DInv™

https://www.seequent.com/products-solutions/res2dinv-and-res3dinv/

March 2025

Email: support@seequent.com

Notice of Copyright
RES2DINV is copyrighted by (C) Seequent, 2025. All rights reserved. No part of this document may be reproduced without written permission of Seequent.

Table of Contents

Cover i
1 Introduction 1
2 Computer system requirements 2
3 Copy protection 3
4 Theory 3
5 Software installation 4
6 Using the program – a quick start 5
7 .Dat data file format 6
7.1 Index-based data format 6
7.1.1 Wenner, pole-pole, equatorial dipole-dipole arrays 6
7.1.2 Schlumberger, dipole-dipole and pole-dipole arrays 8
7.1.3 Topography data for index-based format data files 10
7.2 General array data format 11
7.3 Remote electrodes of the pole-pole and pole-dipole arrays 16
7.4 Cross-borehole data format 19
7.5 IP data format 24
7.6 Time-lapse data files 26
7.7 Incorporating data noise estimates 28
7.8 Fixing resistivities 29
7.9 Aquatic surveys 30
7.9.1 Underwater surveys 31
7.9.2 Surveys with floating electrodes 35
7.10 Incorporating boundaries of known layers 37
7.10.1 Specifying and fixing resistivity of regions above and below a sharp boundary 39
7.11 Global or GPS coordinates 40
7.12 Extending the model horizontal range 43
8 Data tab 44
8.1 Open data 44
8.2 Unsupported data types 44
8.3 Data Import 44
9 Inversion tab 46
9.1 Discretization 46
9.1.1 Model 46
9.1.1.1 Allow parameters to exceed data points 47
9.1.1.2 Use extended model 47
9.1.2 Vertical 47
9.1.2.1 Thickness of first layer 47
9.1.2.2 Layer thickness increase factor 47
9.1.2.3 Model depth range 47
9.1.3 Horizontal 47
9.1.3.1 Width of blocks 48
9.1.3.2 Make blocks equal width 48
9.1.3.3 Model refinement 48
9.1.3.4 Generate model blocks from sensitivity values 51
9.1.4 Forward modelling 51
9.1.4.1 Vertical mesh size 51
9.1.4.2 Horizontal mesh size 52
9.2 Stopping criteria 52
9.2.1 Convergence limit 52
9.2.2 RMS convergence limit 53
9.2.3 Number of iterations 53
9.3 Inversion methodology 53

9.3.1 Settings 53
9.3.1 Calculate model resolution 53
9.3.1.1 Reduce effect of side blocks 54
9.3.1.2 Data space 54
9.3.1.3 Use fast Jacobian calculation for dense data sets 54
9.3.1.4 Always use Finite-element settings* 54
9.3.1.5 Use smoothing of model resistivities* 54
9.3.1.6 Combine Marquardt & smoothness constraints* 55
9.3.1.7 Local optimization option* 55
9.3.2 LS solver types 55
9.3.2.1 Type of optimization method 55
9.3.2.2 Convergence limit for Incomplete Gauss-Newton 55
9.3.3 Data/model norm 56
9.3.3.1 Data norm (L1, L2) 56
9.3.3.2 L1 data norm cutoff factor 56
9.3.3.3 Model norm (L1/L2) 56
9.3.3.4 L1 model norm cutoff factor 57
9.3.4 Parameter range 57
9.3.3.1 Limit resistivity values 57
9.3.3.2 DC upper limit factor 57
9.3.3.3 DC lower limit factor 57
9.3.3.4 IP upper limit 58
9.3.3.5 IP lower limit 58
9.3.4 Long survey lines 58
9.3.4.1 Use fast method to calculate Jacobian matrix 58
9.3.4.2 Use fast method to calculate Jacobian matrix 58
9.3.4.3 Use sparse inversion method 58
9.3.5 Reference model* 58
9.3.5.1 Use reference model* 59
9.3.5.2 Damping factor for reference* 59
9.3.5.3 Type of reference resistivity* 59
9.4 Damping settings 59
9.4.1 DC 59
9.4.1.1 Initial damping factor 59
9.4.1.2 Minimum damping factor 60
9.4.1.3 Enable first layer damping 60
9.4.1.4 Extra damping for first layer 60
9.4.1.5 Damping factors for changes in distance between blocks 60
9.4.1.6 Adjust damping factors for changes in distance between blocks 60
9.4.1.7 Increase of damping factor 60
9.4.1.8 Automatic calculation of damping factor with depth 60
9.4.2 IP 60
9.4.2.1 IP damping factor 60
9.4.2.2 Automatic IP damping factor 61
9.4.3 Flatness filters 61
9.4.3.1 Vertical to horizontal flatness ratio 61
9.4.3.2 Use diagonal filter 61
9.4.4 L-curve* 61
9.3.4.1 Use L-curve method* 62
9.4.4.2 Use same norm in L-curve* 62
9.4.4.3 Allow damping factor to increase during iterations* 62
9.5 Topography 62
9.5.1 Type of topography modelling 63

9.5.2 Topography distortion damping 66
9.5.3 Type pf topography trend removal 66
9.6 IP settings 67
9.6.1 Type of IP model transformation 67
9.6.2 Use IP model refinement 67
9.6.3 Joint or separate of IP inversion 68
9.6.4 Use IP data in resistivity inversion 68
9.6.5 Weight for IP data 68
9.6.6 Type of IP smoothness constraint 68
9.6.7 Apparent IP cutoff value 68
9.7 Time-lapse settings 69
9.7.1 Time-lapse inversion constraint 69
9.7.2 Time-lapse damping factor 69
9.7.3 Reduce time-lapse damping 69
9.8 Floating Electrodes 69
9.81 Floating electrodes survey inversion 70
9.82 Resistivity variation within water layer 70
9.83 Water resistivity variation damping 71
9.9 Borehole 72
9.9.1 Borehole model refinement 73
9.9.2 Type of borehole damping method 73
10. Results/Model tab 74
10.1 Model export 74
11. Compare tab 75
11.1 Display properties 75
12. Program settings 76
Acknowledgements 78
References 79
Appendix A Array types in RES2DINV 82
Appendix B Special OhmMapper Note 84
Appendix D Surveys with electrodes suspended in a water layer 85
Appendix G Setup for GDB import/export 87
DISCLAIMER 88
SUPPORT 88
What's New 89

List of Figures

Figure 1. Sequence of measurements to build up a pseudo section using a computer controlled multi-electrode survey setup. 1
Figure 2. Two possible arrangements of the blocks used in a 2-D model together with the data points in the pseudo section. 2
Figure 3. Parameters that specify the location and length of an array in the index-based data format. 6
Figure 4. Arrangement of electrodes for the equatorial dipole-dipole array. 6
Figure 5. Arrangement of the electrodes for the dipole-dipole and pole-dipole arrays. (a) Dipole-dipole array with integer '*n*' factor. (b) Example of dipole-dipole array with non-integer "*n*" value. Arrangement of the electrodes for (c) the "forward" and (d) "reverse" pole-dipole arrays. 9
Figure 6. Arrangement of electrodes for the offset pole-dipole array. 10
Figure 7. Some possible non-conventional arrays. (a) Non-symmetrical four-electrode Wenner-Schlumberger or gradient type of array. (b) Dipole-dipole array with dipoles of unequal size. (c) A possible but probably non-viable electrode configuration. (d) Highly non-symmetrical dipole-dipole array. 11
Figure 8. Arrangement of the electrodes along a survey line such that the true horizontal distance between adjacent electrodes is constant regardless of the slope of the ground surface. Note that the distance between adjacent electrodes along the ground surface is greater at the steeper part of the slope. 15
Figure 9. A schematic diagram of the arrangement of the electrodes in an actual field pole-pole measurement. 16
Figure 10. A schematic diagram of the arrangement of the electrodes along the survey line in a pole-pole survey with positions of the C2 and P2 electrodes specified. 17
Figure 11. Arrangement of the electrodes in a cross-borehole survey. (a) The default standard model where the dimensions of the model blocks are equal to the spacing between the electrodes. (b) An alternative model with finer blocks with dimensions about half the spacing between the electrodes. 19
Figure 12. The model obtained after the inversion of the BOREHOLE.DAT data set. The option to use finer blocks with half the size of the spacing between the electrodes was used. 21
Figure 13. Model obtained from the inversion of data from a cross-borehole survey to map the flow of a saline tracer. Note the low resistivity zones near the surface (where the tracer was injected) and below a depth of 7 meters. The locations of the borehole electrodes are shown by small black dots. 21
Figure 14. Magusi River ore body resistivity and I.P sections. (a) Apparent resistivity pseudo section, (b) resistivity model section, (c) apparent metal factor pseudo section and (d) metal factor model section. 26
Figure 15. Fixing the resistivity of rectangular and triangular regions of the inversion model... 30
Figure 16. Five possible situations for aquatic surveys. 30
Figure 17. Hat Head land and underwater survey. (a) Apparent resistivity pseudo section (Wenner array) from the Hat Head tidal creek survey. (b) Calculated resistivity pseudo section and (c) the inversion model. Note the creek between the 65 meter and 95 meter have the electrodes are underwater. 32
Figure 18. Lake Lelia underwater survey apparent resistivity pseudo section and model resistivity section. Courtesy of Technos Inc., USA. 32
Figure 19. Models for the Clifton survey from the different inversion methods are shown together. Note the boundary between the high resistivity sand layer and the underlying low resistivity clay layer is much better resolved in the blocky and sharp boundary inversion methods. 37
Figure 20. Different possible arrangement of model blocks for the same data set. (a) Using wider blocks at sides and bottom, (b) blocks of equal width, (c) model blocks extended to ends of survey line. 50

Figure 21. Example of inversion models using the standard and half-sized model blocks. (a) The apparent resistivity pseudo section for the PIPESCHL.DAT data set. The inversion models using (b) blocks with a width of 1.0 meter that is the same as the actual unit electrode, and (c) using narrower blocks with a width of 0.5 meter. 51
Figure 22. Schematic diagram of mesh and model cells used by forward modeling routine. This example has 4 nodes between adjacent electrodes. 52
Figure 23. Example of inversion results using the smooth and robust inversion model constraint. (a) Apparent resistivity pseudo section. The inversion models produced by (b) the conventional least-squares smoothness-constrained method (L2) and (c) the robust or blocky inversion method. 57
Figure 24. Types of roughness filters. (a) Horizontal and vertical components only. (b) Diagonal components as well. 61
Figure 23. Example L-curve plot to determine the optimum damping factor for the BLUERIDGE.DAT data set. (a) Variation of model roughness with data misfit for a range of spatial damping factor values (a few values are shown near the corresponding points), (b) variation of the curvature of the L-curve with the damping factor. 62
Figure 26. Example of the model for the Rathcrogan Mound data set. (a) Measured apparent resistivity pseudo section. (b) Inverse model section with topography. 64
Figure 27. Different methods to incorporate topography into a 2-D inversion model. (a) Schematic diagram of a typical 2-D inversion model with no topography. Model mesh discretization with a distorted grid to match the actual topography where (b) the subsurface nodes are shifted vertically by the same amount as the surface nodes, (c) the shift in the subsurface nodes is gradually reduced with depth or (d) rapidly reduced with depth, and (e) the model obtained with the inverse Schwartz-Christoffel transformation method. 65
Figure 28. Topography linear trend removal for the Rathcrogan mound data set. 66
Figure 29. Example of inversion model with a fixed water layer. The inversion results of the WATER_FLOAT.DAT data is shown where the resistivity water layer (represented by the top blue layer in the model section) is fixed and model extends from below the water bottom. 70
Figure 30. Arrangement of model blocks and the water bottom boundary for an arrangement with the water layer incorporated into the inversion model. 72
Figure 31. Inversion model for the survey with floating electrodes along the along the São Francisco River in Brazil. The thin black line indicates the water bottom boundary. 72
Figure 32. Histogram and scatter plots for the inversion results of the IPMAGUSI.DAT data sets. 74
Figure 33. Display properties sections for the LANDFIL.DAT data set. (a) Apparent resistivity pseudo section. (b) Inversion model section. (c) Model resolution section. (d) Sensitivity section (e) Uncertainty section. 77
Figure 34. Arrangement of the electrodes for some commonly used arrays and their geometric factors. 82
Figure 35. Normal, reverse and offset pole-dipole array arrangements. 83
Figure 36. Example OhmMapper data set and inversion model. (a) Apparent resistivity pseudo section measured with an OhmMapper mobile resistivity surveying system. (b) Model section obtained by RES2DINV 84
Figure 37. Mesh used to model water layer. 85
Figure 38. Example data set and inversion model for a survey with a streamer suspended in a water layer. (a) Apparent resistivity pseudo section and (b) inversion model section. 85

List of Tables

Table 1. List of files and file types installed with the RES2DINV program. 4
Table 2. Example Wenner array data file format. 7
Table 3. Example equatorial dipole-dipole array data file. 7
Table 4. Example Wenner-Schlumberger array data file. 8
Table 5. Example dipole-dipole array data file. 8
Table 6. Example pole-dipole array data file. 9
Table 7. Example offset pole-dipole array data file. 10
Table 8. Example of index-based data file with topography. 11
Table 9. Example data file with general array format. 12
Table 10. Example general array format file with topography. 13
Table 11. Example general array data format file with topography in a separate section. 13
Table 12. Example gradient array data file. 16
Table 13. Pole-pole data file with remote electrodes specified. 18
Table 14. Example borehole data set. 21
Table 15. Example data set with inclined boreholes. 23
Table 16. Example borehole data set with topography. 24
Table 17. Example data file with IP values as chargeability. 25
Table 18. Example time-lapse data set with 3 time series. 27
Table 19. Example data file with noise estimates. 28
Table 20. Example data file with fixed regions. 29
Table 21. Example data file for aquatic survey with bottom electrodes. 31
Table 22. Underwater survey data file in general array format. 33
Table 23. Survey across a dam with only electrodes on the dam side underwater. 34
Table 24. Underwater survey data file with two water layers. 35
Table 25. Survey data file with floating electrodes. 36
Table 26. Example survey data file with known boundaries. 38
Table 27. Example data file with sharp boundary and specified resistivity of regions above and below boundary. 39
Table 28. Example data file with global coordinates. 40
Table 29. Example data file with index-based format and topography and global coordinates. 41
Table 30. Example data file with general array format, topography and global coordinates. 41
Table 31. Example aquatic survey data file with global coordinates. 42
Table 32. Example data file with extended model range. 43
Table 33. Data file with standard unit electrode spacing. 48
Table 34. Data file with half the standard unit electrode spacing. 49
Table 35. Array types and their number codes. 82
Table 36. Example data file for a survey electrodes suspended in a water layer. 86

1 Introduction

RES2DINV is a program that will automatically determine a two-dimensional (2-D) resistivity model for the subsurface for data obtained from 2-D electrical imaging surveys (Dahlin 1996). It is a 64-bit Windows based program that supports multi-core CPUs.

Figure 1 shows an example of the electrodes arrangement and measurement sequence that can be used for a 2-D electrical imaging survey. Many different multi-electrode systems have been developed over the past 25 years using different arrangements of the cables and measurement strategies (Loke 2018, Loke et al. 2013). This program is designed to invert large data sets (with about 200 to 100000 data points) collected with a system with a large number (25 to 16000) of electrode positions along the survey line. The survey is usually carried out with a system where the electrodes are arranged along a line with a constant spacing between adjacent electrodes. However, the program can also handle data sets with a non-uniform electrode spacing.

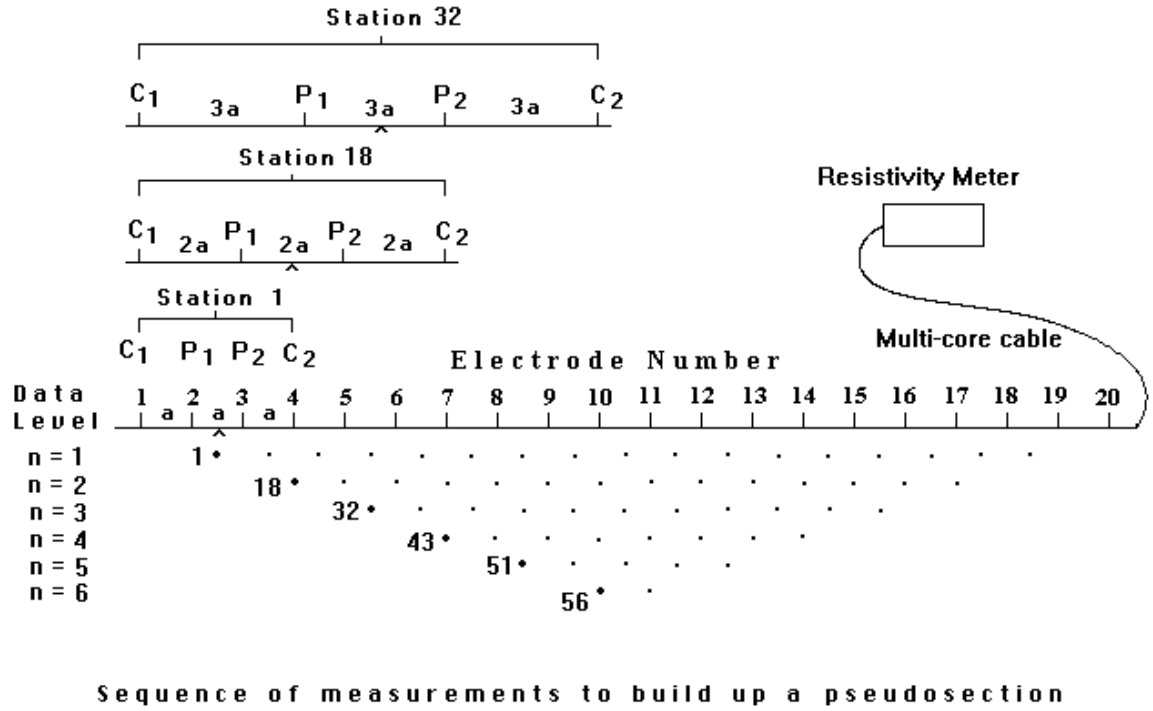

Figure 1. Sequence of measurements to build up a pseudo section using a computer controlled multi-electrode survey setup.

The 2-D model used by the inversion program consists of a large number of rectangular blocks. Figure 2a shows an arrangement of the blocks that is loosely tied to the distribution of the data points in the pseudo section. The distribution and size of the blocks are automatically generated by the program using the distribution of the data points as a rough guide. The depth of the bottom row of blocks is set to be approximately equal to the median depth of investigation (Edwards 1977) of the data points with the largest electrode spacing. Figure 2b shows an alternative arrangement with blocks of uniform width extending to the ends of the survey line.

A finite-difference or finite-element modelling subroutine is used to calculate the apparent resistivity values, and a non-linear smoothness-constrained least-squares optimization technique is used to calculate the resistivity of the model blocks (deGroot-Hedlin and Constable 1990). This program can be used for surveys using the Wenner, pole-pole, dipole-dipole, pole-dipole, Wenner-Schlumberger, and gradient arrays (Appendix A). In addition to these common arrays, the program supports non-conventional arrays with an almost unlimited number of possible electrode configurations (Loke et al. 2010a,b). Besides normal surveys carried out with the electrodes on the ground surface, the program also supports aquatic and cross-borehole surveys.

Copyright 2025, Seequent

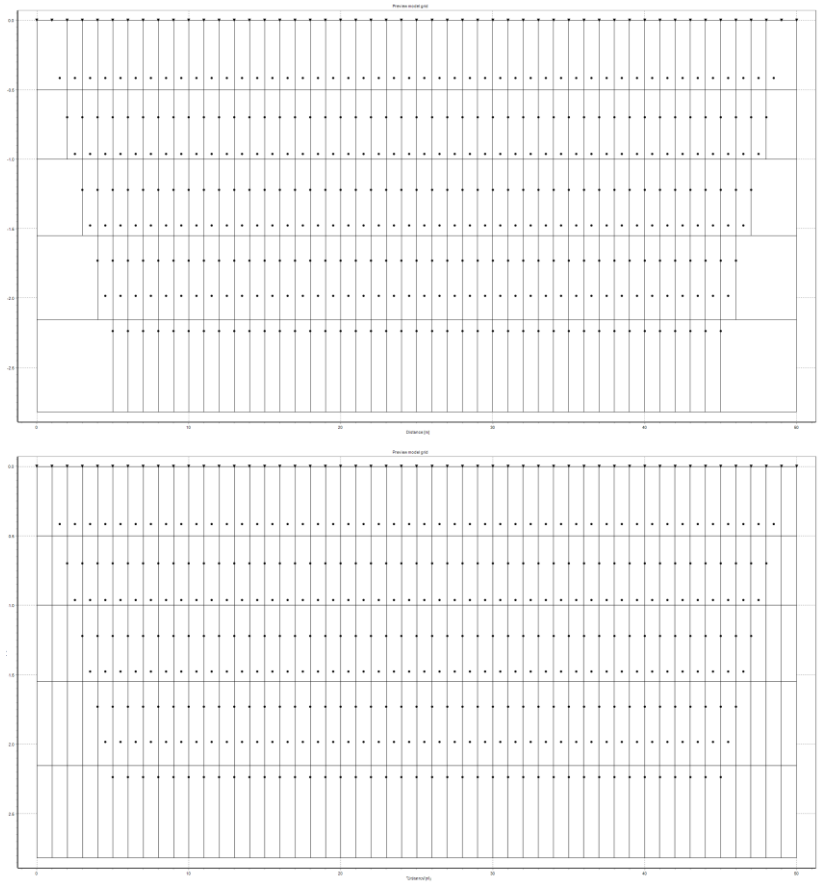

Figure 2. Two possible arrangements of the blocks used in a 2-D model together with the data points in the pseudo section.

2 Computer system requirements

This program is designed to run Windows 10 or later operating systems. On a modern multi-core PC, it will take less than a half a minute to invert the data set obtained from a survey with 100 electrodes.

System requirements: A windows PC with a 64-bit multi-core CPU, at least 4 GB RAM and a 64-bit version of Windows is required. However, it is recommended that you use a PC with at least 8 GB RAM. The program can access more than 8 GB RAM. This greatly increases the data and model size that can be processed.

It is recommended that you use a PC with an Intel (rather than an AMD) CPU as the RES2DINV program is optimized for this type of CPU. These optimizations can significantly reduce the calculation time for large data sets. The program uses the hard disk to store temporary swap files. If you have more than one hard disk drive, the program will automatically select the drive with the largest amount of free space as the drive to store the swap files. The amount of free hard-disk space should be at least 4 times the RAM.

There should not be too many background programs running while executing this program. By shutting down the other programs, more memory will be available to this program. This will reduce memory to hard disk swapping that slows down the program.

Copyright 2025, Seequent

3 Copy protection

The program uses the Seequent ID license system. Without a license, you cannot use the software.

4 Theory

The inversion routine used by the program is based on the smoothness-constrained least-squares method (deGroot-Hedlin and Constable 1990, Sasaki 1992, Loke et al. 2003). The smoothness-constrained least-squares method is based on the following equation.

$$(\mathbf{J}^T\mathbf{J} + \lambda \mathbf{F}) \Delta\mathbf{q}_k = \mathbf{J}^T\mathbf{g} - \lambda \mathbf{F}\, \mathbf{q}_{k-1} \quad (4.1)$$

where

$\mathbf{F} = \alpha_x \mathbf{C_x}^T \mathbf{C_x} + \alpha_z \mathbf{C_z}^T \mathbf{C_z}$
$\mathbf{C_x}$ = horizontal roughness filters, $\mathbf{C_z}$ = vertical roughness filter
$\mathbf{J}$ = Jacobian matrix of partial derivatives, $\mathbf{J}^T$ = transpose of $\mathbf{J}$
λ = damping factor, $\mathbf{q}$ = model vector, $\mathbf{g}$ = data misfit vector
α_x = weight for horizontal filter, α_z = weight for vertical filter
k = iteration number

One advantage of this method is that the damping factor and roughness filters can be adjusted to suit different types of data. A detailed description of the different variations of the smoothness-constrained least-squares method can be found in the free tutorial notes by Loke (2018). The different program options are described in sections 9.

Starting from an initial model (usually a homogenous earth model), the program calculates the change in the model parameters ($\Delta\mathbf{q}_k$) that will reduce the difference between the calculated and measured apparent resistivity values ($\mathbf{g}$). It adjusts the resistivity of the model blocks subject to the smoothness constraints used. A measure of this difference is given by the root-mean-squared (RMS) error. However, the model with the lowest possible RMS error sometimes shows large and unrealistic variations in the model resistivity values and might not always be the "best" model from a geological perspective. In general, the most prudent approach is to choose the model at the iteration after which the RMS error does not change significantly. This usually occurs between the 3rd and 6th iterations.

Copyright 2025, Seequent

5 Software installation

You can download the programs from the https://my.seequent.com website. You will need a Seequent ID to login and download the installer. The installer RES2DINV package comes in a single compressed installation file and includes the Seequent Connector app that is used to connect to the licensing system.

The default folder for the program is C:\Program Files\AGS\RES2DINV. Table 1 shows a list of some of the files that are installed when you run the SETUP.EXE program.

Table 1. List of files and file types installed with the RES2DINV program.

RES2DINV.EXE	Main inversion program
RES2DINVx64.EXE	Legacy RES2DINV version
RES2DINV.PDF	Manual in PDF format
RES2DINVX64.PDF	Manual for the old RES2DINV version in PDF format
.dat-files	Input files containing data from DC (IP) surveys in a format that can be read by RES2DINV. In this manual, you can find numerous examples where different data files are used for inversions with different settings and configurations in the demo_data folder.
.r2r-files	Output files containing inversion results.

Copyright 2025, Seequent

6 Using the program – a quick start

Click the RES2DINV icon to start the program. The program will then display the following Main Window.

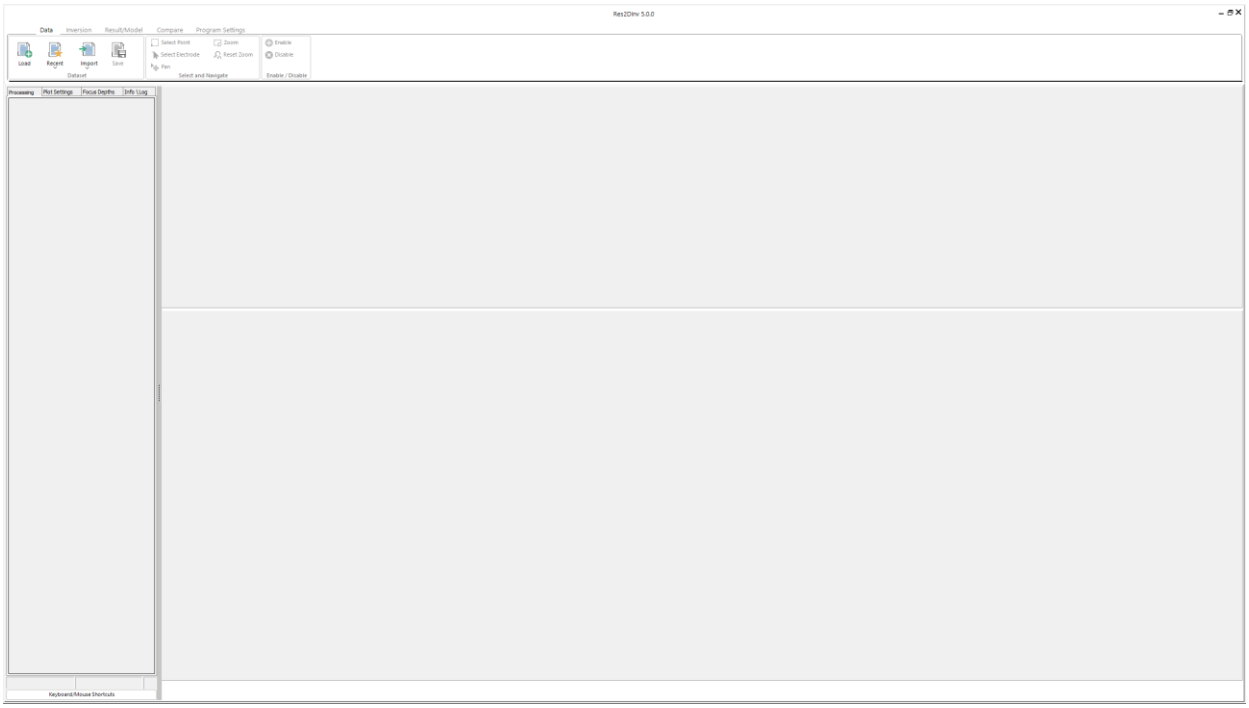

You can select an option by clicking it with the mouse cursor. If this is the first time you are using the program, try loading one of the smaller demo data files such as the BLOCKDIP.DAT provided with the program. Click the "**Load**" icon, navigate to the 'demo_data' folder where the RES2DINV program is installed. After loading the file, go to the "**Inversion**" tab, and then choose the '**Run inversion**' option. The inversion subroutine will start. Wait for the data to be inverted. After the inversion process has been completed, the program will display the apparent resistivity and inversion model sections.

Copyright 2025, Seequent

7 .Dat data file format

When you select the "**Load**" option under Dataset, a list of files in the current folder that has an extension of DAT will be displayed. It is assumed that the files follow the format required by this program. Most field equipment systems, such as the ABEM Terrameter and Iris Instrument systems, come with a utility program to convert the raw data into the format required by the RES2DINV program. This program can also import data formats from a number of field instruments (section 8.3). The apparent resistivity values are given in a text file. You can use any text editor, such as the Windows Notepad program, if you are creating the data file manually. The data are arranged in an ASCII delimited manner where a comma or blank space or LF/CR is used to separate different numerical data items. If there is a problem in running this program, one possible cause is that the input data was arranged in a wrong format.

There are two main types of data format used by this program, an index-based and a general array format. The older index-based format is only used for conventional arrays such as the Wenner, Wenner-Schlumberger, pole-pole, pole-dipole and dipole-dipole arrays. The general array format can be used for any array, including non-conventional arrays.

7.1 Index-based data format

The index-based data format use a maximum of three parameters to specify an array (Figure 3). The first parameter is the location of the first (leftmost) electrode or the mid-point of the array. The second parameter is the spacing between the P1 and P2 potential electrodes (the '*a*' spacing). The third parameter (only applicable to the pole-dipole, dipole-dipole and Wenner-Schlumberger arrays) is the ratio of the distance of the current electrode from the nearest potential electrode to the P1-P2 spacing (the '*n*' value). The three parameters are illustrated in Figure 3 for the dipole-dipole array as an example.

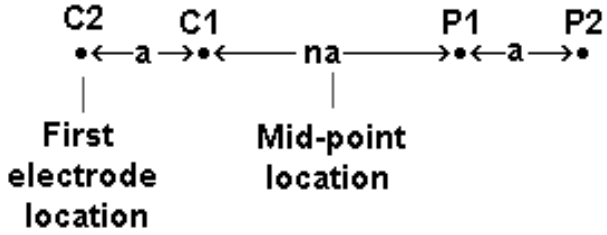

Figure 3. Parameters that specify the location and length of an array in the index-based data format.

7.1.1 Wenner, pole-pole, equatorial dipole-dipole arrays

For the Wenner, pole-pole and equatorial dipole-dipole arrays, it is always assumed that the '*n*' factor is always equals to 1 and thus need not be listed in the data file. As an example of a data file without the '*n*' factor, Table 2 shows the data format for the example file LANDFILL.DAT with comments about information in the data lines.

The data file BLOCKPOL.DAT gives an example of a pole-pole array data set. The arrangement of the electrodes for the equatorial dipole-dipole array is shown in the Figure 4.

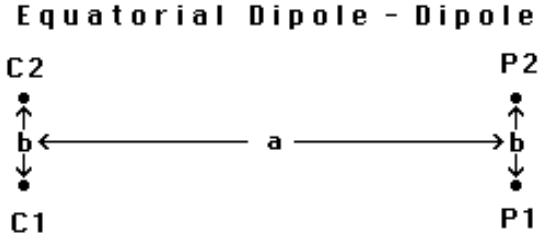

Figure 4. Arrangement of electrodes for the equatorial dipole-dipole array.

Copyright 2025, Seequent

Table 2. Example Wenner array data file format.

LANDFILL.DAT file	*Comments*
LANDFILL SURVEY	*Name of survey line*
3.0	*Unit electrode spacing*
1	*Array type, 1 for Wenner*
334	*Number of data points*
1	*Type of x-location for data points, 1 for mid-point*
0	*Flag for IP data, 0 for none (1 if present)*
4.50 3.0 84.9	*First data point. For each data point, list the x-location,*
7.50 3.0 62.8	*'a' electrode spacing, apparent resistivity value*
10.50 3.0 49.2	*Third data point*
13.50 3.0 41.3	*Fourth data point*
...	*Same format for other data points*
...	
75.00 48.0 52.5	*Last data point*
0,0,0,0,0	*Ends with a few zeros. Flags for other options.*

The apparent resistivity value ρ_a for this array is given by

$$\rho_a = 2\pi\, a\, s\, R / (s-a) \qquad (7.1)$$

where $s = (a^2 + b^2)^{0.5}$ and R is the measured resistance. This array differs from other arrays where the electrodes are arranged in a single line. Each reading is characterized by two spacings. The first spacing, *a*, is the distance between the current electrodes pair C1-C1 and the potential pair P1-P2. The second spacing, *b*, is the spacing between the C1 and C2 electrodes. This program has a restriction that the spacing between the P1-P2 pair must be the same as that between the C1-C2 pair. An example of a data file for this array is the data file FAULTEQU.DAT in Table 3. For this array, it is necessary to include the '*b*' spacing between the C1-C2 electrodes pair after the array number. It is assumed all the readings in the data file use the same '*b*' spacing. If different '*b*' spacings are used, please refer to Appendix B in the RES3DINV manual.

Table 3. Example equatorial dipole-dipole array data file.

FAULTEQU.DAT file	*Comments*
Equatorial dipole-dipole array	*Name of survey line*
1.0	*Unit electrode spacing (a)*
8	*Array type, 8 for equatorial dipole-dipole*
1.5	*The 'b' spacing between the C1-C2 pair*
285	*Number of data points*
1	*Type of x-location for data points, 1 for mid-point*
0	*Flag for IP data, 0 for none (1 if present)*
0.50 1.00 2.74	*First data point. For each data point, list the*
1.50 1.00 2.74	*x-location, 'a' electrode spacing, and the*
...	*apparent resistivity value*
...	
..	*Same format for other data points*
..	
47.00 6.00 1.02	*Last data point*
0,0,0,0,0	*Ends with a few zeros. Flags for other options.*

Copyright 2025, Seequent

7.1.2 Schlumberger, dipole-dipole and pole-dipole arrays

The dipole-dipole, pole-dipole and Wenner-Schlumberger arrays data sets have a slightly different format since an extra parameter, the dipole separation factor '*n*', is needed. Table 4 shows an example for the Wenner-Schlumberger array.

Table 4. Example Wenner-Schlumberger array data file.

PIPESCHL.DAT file	*Comments*
Underground pipe survey	*Name of survey line*
1.0	*Unit electrode spacing*
7	*Array type, 7 for Wenner-Schlumberger*
173	*Number of data points*
1	*Type of x-location for data points, 1 for mid-point*
0	*Flag for IP data, 0 for none (1 if present)*
1.50 1.00 1 641.1633	*First data point. For each data point, list the x-location,*
2.50 1.00 1 408.0756	*'a' electrode spacing, the 'n' factor and the*
3.50 1.00 1 770.0323	*apparent resistivity value*
4.50 1.00 1 675.3062	*Fourth data point*
...	
..	*Same format for other data points*
..	
2.50 1.00 2 206.2745	*31st data point, note 'n' value of 2*
...	
19.00 2.00 5 896.3058	*Last data point, note a=2.0 and n=5*
0,0,0,0,0	*Ends with a few zeros. Flags for other options.*

Table 5 describes the data file format for the dipole-dipole array.

Table 5. Example dipole-dipole array data file.

BLOCKDIP.DAT file	*Comments*
Block	*Name of survey line*
1.0	*Unit electrode spacing*
3	*Array type, 3 for dipole-dipole*
173	*Number of data points*
1	*Type of x-location for data points, 1 for mid-point*
0	*Flag for IP data, 0 for none (1 if present)*
1.50 1.00 1 641.1633	*First data point. For each data point, list the x-location,*
2.50 1.00 1 408.0756	*'a' electrode spacing, the 'n' factor and the*
3.50 1.00 1 770.0323	*apparent resistivity value*
...	
..	*Same format for other data points*
..	
2.50 1.00 2 206.2745	*31st data point, note 'n' value of 2*
...	
19.00 2.00 5 896.3058	*Last data point, note a=2.0 and n=5*
0,0,0,0,0	*Ends with a few zeros. Flags for other options.*

In most cases, the *'n'* dipole separation factor is an integer value. However, it is possible for the '*n'* factor to have non-integer values although all the electrodes still have a constant inter-electrode spacing. This can occur when the spacing '*a'* between the P1-P2 pair is twice (or more) the unit electrode spacing. For the example shown in Figure 5b, the unit electrode spacing for the survey line is 1 meter. The '*a'* spacing has a value of 2 meters, while the distance between the C1 and P1 electrodes is 3 meters. In this case, the '*n'* factor has a value of 1.5. The data file, DIPOLEN5.DAT, gives an example of a dipole-dipole data set with non-integer '*n'* values. For cases where the fractional part of the *n* factor has is an infinite series in decimal notation, the '*n'* value should be given to at least four decimal places. For example, if the '*n'* value is one and one-third, it should be given as 1.3333.

Copyright 2025, Seequent

If the location of the first electrode is used in the data format, it should be the leftmost electrode; such as the C2 electrode in Figure 5a and Figure 5b, C1 in Figure 5c and P2 in Figure 5d.

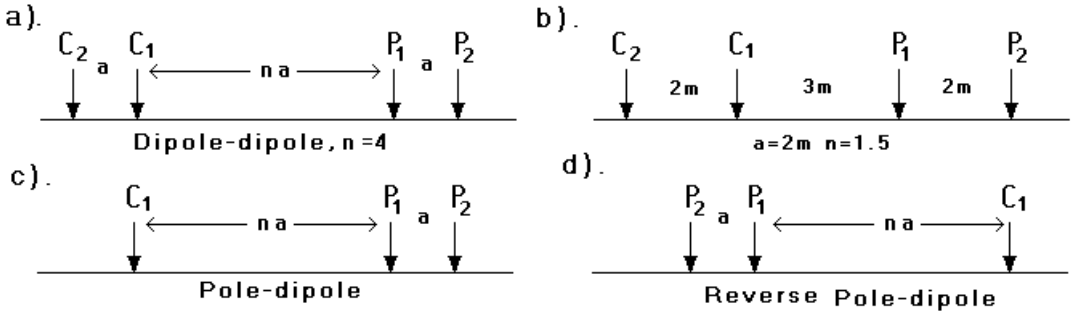

Figure 5. Arrangement of the electrodes for the dipole-dipole and pole-dipole arrays. (a) Dipole-dipole array with integer '*n*' factor. (b) Example of dipole-dipole array with non-integer "*n*" value. Arrangement of the electrodes for (c) the "forward" and (d) "reverse" pole-dipole arrays.

There are two other issues involved with the pole-dipole array. The first is that the current electrode can be to the left (normal arrangement) or to the right (reverse arrangement) of the potential electrodes. To distinguish between the two arrangements, a positive value is used for the '*n*' factor in the normal arrangement, and a negative value for the 'reverse' arrangement. The pole-dipole array is an asymmetrical array, and over symmetrical structures the apparent resistivity anomalies in the pseudo section are also asymmetrical. In some situations, the asymmetry in the measured apparent resistivity values could influence the model obtained after inversion. One method to eliminate the effect of this asymmetry is to repeat the measurements with the electrodes arranged in the reverse manner. By combining the measurements with the "forward" and "reverse" pole-dipole arrays, any bias in the model due to the asymmetrical nature of this array would be removed. The file PDIPREV.DAT is an example data set that combines measurements made with the "forward" and "reverse" pole-dipole arrays (Table 6). There is no common standard to define the position of the pseudo section *x* plotting position for the pole-dipole array as it is a non-symmetrical array. There are two possible conventions, to use the mid-point between the P1-P2 electrodes or the mid-point between the C1-P2 electrodes. This program uses the mid-point between the C1-P2 electrodes to define the *x*-location of the array.

Table 6. Example pole-dipole array data file.

PDIPREV.DAT file	*Comments*
Forward and reverse pole-dipole array	*Name of survey line*
7.0	*Unit electrode spacing*
6	*Array type, 6 for pole-dipole*
162	*Number of data points*
0	*Type of x-location for data points, 0 for first electrode*
0	*Flag for IP data, 0 for none (1 if present)*
0,63,1,0.8277	*x-location, 'a' spacing, 'n' factor, apparent resistivity,*
0,56,1,0.8236	*2nd data point*
0,49,1,0.8888	*3rd data point*
..	*Same format for other data points*
..	
0,63,-1,2.298	*82nd data point, 'n' value of -1for reverse pole-dipole*
...	
0,7,-1,102.4	*Last data point, note a=7.0 and n=-1*
0,0,0,0,0	*Ends with a few zeros. Flags for other options.*

Another variation of the pole-dipole array is the offset pole-dipole array. This array was originally designed to carry out 3-D IP surveys rapidly (White *et al.*, 2003), thus data from such surveys are normally processed with the 3-D inversion program RES3DINV. Support is provided for the array in this program so that users have the option of inverting each line individually. The arrangement of the electrodes is shown in the Figure 6. The arrangement is similar to that used by the normal pole-dipole

Copyright 2025, Seequent

array except that the current electrode is not on the same line as the potential electrodes but offset at a distance "*b*" from the survey line. This arrangement was used to reduce the EM coupling between the current electrode and the potential dipole. The RES2DINV program does not support the case when the C1 electrode is immediately below the P1 electrode (i.e., *n*=0). For a data set with this arrangement, you will need to use the RES3DINV program. Another restriction is that the '*b*' offset distance is the same for all the data points. If different '*b*' values are used in the survey, you will also need to use the RES3DINV program. The file OFF_PDP.DAT gives an example of the data format for this array. Table 7 shows the initial part of this data file with comments about the format. The data format is essentially the same as the normal pole-dipole array, except the array number is 10 and the offset distance is given immediately after the array number.

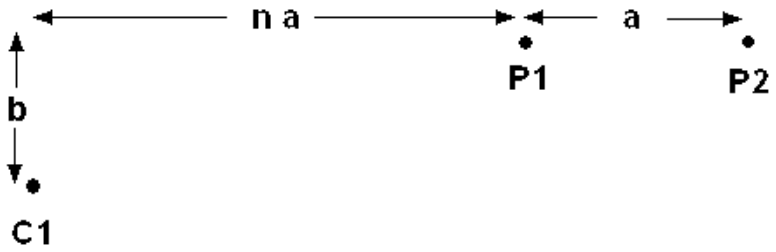

Figure 6. Arrangement of electrodes for the offset pole-dipole array.

Table 7. Example offset pole-dipole array data file.

OFF_PDP.DAT file	*Comments*
Blocks with IP	*Title*
2.00	*Unit electrode spacing*
10	*Array type (10 for offset pole-dipole)*
1.00	*Offset of current electrode from survey line*
530	*Number of data points*
1	*1 for mid-point of array given as x-location*
1	*1 to indicate IP present*
Chargeability	*Type of IP data*
Msec	*IP unit*
0.10,1.00	*Delay, integration time*
2.0 2.0 1.0 100.7976 -0.9118	*For each data point, we have*
4.0 2.0 1.0 102.0548 -1.8678	*x-location, "a" dipole spacing, "n" factor,*
6.0 2.0 1.0 104.9487 -4.3391	*apparent resistivity, apparent IP*
8.0 2.0 1.0 111.0159 -9.0335	
…..	*Other data points*
…..	
53.0 2.0 -10.0 109.3857 5.5469	*Last data point*
0,0,0,0,0	*A few zeros to end the file*

7.1.3 Topography data for index-based format data files

The topography data is entered immediately after the main section with the apparent resistivity values. The file GLADOE2.DAT is an example with topographical data. The bottom section of this file with a description of the format for topographical data is given in Table 8. Note that the topography data is placed immediately after the apparent resistivity data points. The first item is a flag to indicate whether the file contains topography data. If there is no topography data, its value is 0. Enter 1 or 2 if topographical data is present. In the case where the actual horizontal and vertical coordinates of topography data points along the survey line are given, enter 1. ***Even if the actual horizontal distances are given in the topography data section, you must still use the x-distance along the ground surface in the apparent resistivity data section. The index-based always assumes that the x-distances in the main data section are surface distances regardless of the x-distances used in the topography section.***

In most surveys the distances of the points along the ground surface, and not true horizontal distances, are actually measured with a tape or using a cable with takeouts at regular intervals. In this case, enter a value of 2 for the topography data flag. This is followed by the number of topographical data points.

Copyright 2025, Seequent

It is not necessary to measure the elevation for each electrode. For example, the data in the GLADOE2.DAT file involves 161 electrodes but only the elevations at 26 points are given. The maximum number of topographical data points you can have is 4000. For each data point, the horizontal location and the elevation are entered into the data file. After the last topographical data point, the number of the topographical data point where the first electrode is located is given. In the above example, the first electrode was located at -40 meters, which corresponds to the 2nd topographical data point. Note that the elevation of the first electrode is required. If this was not measured in the field, you can estimate it from the elevations of the neighboring data points. In most cases, the first topographical data point corresponds to the first electrode and the last topographical data point corresponds to the last electrodes. An example data file with this arrangement is RATHCRO.DAT. By tying the first and last topographical data points to the first and last electrodes, this will help to avoid errors in the data format.

Table 8. Example of index-based data file with topography.

GLADOE2.DAT file	*Comments*
237 2 39.207	*Last four data points*
203 2 14.546	*with x-location of the data point, electrode spacing*
227 2 31.793	*and measured apparent resistivity values*
233 2 30.285	
2	*Topography data flag. If no topography data, place 0 here.*
26	*Number of topography data points*
-100 33	*Horizontal and vertical coordinates of 1st,*
-40 34.5	*2nd topography data point*
-20 35.0	*This is followed by similar data for*
0 35.209	*the remaining topography data points*
..	
..	
..	
300 33	*Last topography data point*
2	*The topography data point number with the first electrode*
0,0,0,0,0	*A few zeros to end the file*

7.2 General array data format

This feature is to cater for electrode arrangements that do not fall under the usual array types or electrode arrangements, or unusual ways of carrying out the surveys. There are probably an infinite number of possible electrode configurations that are limited only by the imagination of the user but in most cases they are likely to be slight variations of the standard arrays. Figure 7 shows four possible non-standard configurations. One possibility is a non-symmetrical variation of a symmetrical array, such as the Wenner-Schlumberger or the dipole-dipole array (Figure 7a,b,d). Such a configuration could arise from surveys with multi-channel resistivity meters where measurements are made with several pairs of potential electrodes for a common pair of current electrodes. While the program gives the user greater latitude in the electrode arrangement, some arrays that are technically possible but would have very low potential signals should be avoided.

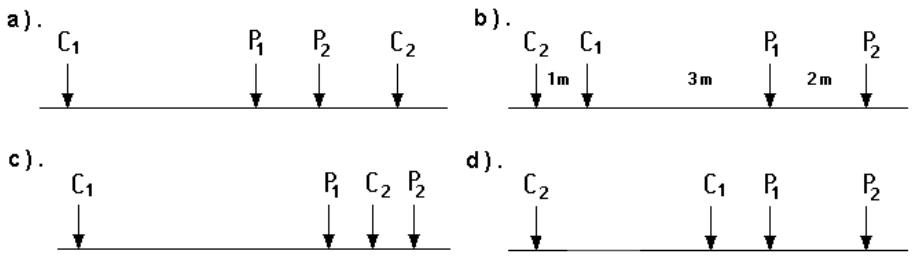

Figure 7. Some possible non-conventional arrays. (a) Non-symmetrical four-electrode Wenner-Schlumberger or gradient type of array. (b) Dipole-dipole array with dipoles of unequal size. (c) A possible but probably non-viable electrode configuration. (d) Highly non-symmetrical dipole-dipole array.

Copyright 2025, Seequent

To accommodate the various possibilities, a general array data format where the positions of all the four electrodes are listed is used. The *x*-location as well as the elevation of all the electrodes used in a measurement must be given. The file MIXED.DAT is an example data file with such a format. This is a synthetic data set with a mixture of measurements using the Wenner-Schlumberger and dipole-dipole arrays. The initial part of this data file with comments about the format is given in Table 9.

The sub-array type indicator is used when the electrode configuration follows one of the conventional arrays, for example the Wenner-Schlumberger array. As an example, the file MIXEDWS.DAT has the data for a Wenner-Schlumberger array only but the information is arranged in a general array format. In this case the sub-array number is 7. The file RATHCMIX.DAT (Table 10) has the data for the Rathcrogan mound (Waddell and Barton, 1995) for the Wenner array but in a general array format (thus it has sub-array number of 1). For these data sets, the apparent resistivity values can be displayed in the form of a pseudo section. Table 10 lists the data format used for this data set. The file MIXED.DAT is a combined data set with measurements using the Wenner-Schlumberger and dipole-dipole array. In this case, there is no consistent array type, so the sub-array number is given as 0.

Table 9. Example data file with general array format.

MIXED.DAT file	*Comments*
Mixed array	*Name of survey line*
1.0	*Unit electrode spacing*
11	*Array type (11 for general array)*
0	*Array type, 0 non-specific*
Type of measurement (0=app. resistivity,1=resistance)	*Header*
0	*0 to indicate apparent resistivity*
407	*Number of data points*
1	*Type of x-location, 1 for true horizontal distance*
0	*Flag for IP data, 0 for none (1 if present)*
4 0.0 0.0 3.0 0.0 1.0 0.0 2.0 0.0 10.158	*The format for each data point is :-*
4 1.0 0.0 4.0 0.0 2.0 0.0 3.0 0.0 10.168	*Number of electrodes used,*
4 2.0 0.0 5.0 0.0 3.0 0.0 4.0 0.0 10.184	*x- and z-location of C1, C2, P1, P2,*
4 3.0 0.0 6.0 0.0 4.0 0.0 5.0 0.0 10.225	*Apparent resistivity or resistance value*
4 4.0 0.0 7.0 0.0 5.0 0.0 6.0 0.0 10.337	
..	
..	*Same format for other data points*
..	
4 27.0 0.0 26.0 0.00 33.0 0.0 34.0 0.0 6.765	*Last data point*
0,0,0,0,0	*Ends with a few zeros.*

Concerning the indicator for the type of *x*-location, there are two possible values. A value of 1 is used if the *x*-location values are the true horizontal distances, while a value of 2 is used if it is the distance along the ground surface. This is similar to the convention used for topography data for the index-based format (Section 7.1.3).

In the RATCMIX.DAT file, the topography information is included as the elevation for each electrode in every data line. In some cases, it might be more convenient to enter the topography information in a separate list, much like for data in the index-based format. One example with data in the general array format but with the topography in a separate list after the apparent resistivity data lines is given in the file RATCMIX_Sep_Topo.DAT. Part of the file is shown in Table 11. Note the addition of an extra header line "*Topography in separate list*" that indicates the topography information is in a separate list after the apparent resistivity data lines. Note also in the data lines, the elevation for each electrode is given as 0.00. The program will calculate the elevation for the electrodes from the topography information.

Copyright 2025, Seequent

Table 10. Example general array format file with topography.

RATHCMIX.DAT file	*Comments*
Rathcrogan	*Name of survey line*
2.0	*Unit electrode spacing*
11	*Array type (11 for general array)*
1	*Sib-array type, 1 for Wenner*
Type of measurement (0=app. resistivity,1=resistance)	*Header*
0	*0 to indicate apparent resistivity*
399	*Number of data points*
2	*Type of x-location, 2 for surface distance*
0	*Flag for IP data, 0 for none (1 if present)*
4 -36.0 0.044 -30.0 0.503 -34.0 0.134 -32.0 0.311 116.0	*First data point, note non-zero elevation after x-location of each electrode.*
4 -34.0 0.134 -28.0 0.712 -32.0 0.311 -30.0 0.503 118.0	*Second data point*
..	*Same format for other data points*
..	
..	
4 58.0 0.385 94.0 -3.270 70.0 -2.095 82.0 -2.853 1160.0	*Second last data point*
4 60.0 -0.093 96.0 -3.340 72.0 -2.274 84.0 -2.914 1680.0	*Last data point*
0,0,0,0,0	*Ends with a few zeros.*

Table 11. Example general array data format file with topography in a separate section.

RATCMIX_Sep_Topo.DAT file	*Comments*
Rathcrogan	*Name of survey line*
2.0	*Unit electrode spacing*
11	*Array type (11 for general array)*
1	*Sib-array type, 1 for Wenner*
Type of measurement (0=app. resistivity,1=resistance)	*Header*
0	*0 to indicate apparent resistivity*
399	*Number of data points*
2	*Type of x-location, 2 for surface distance*
0	*Flag for IP data, 0 for none (1 if present)*
4 -36.0 0.0 -30.0 0.0 -34.0 0.0 -32.0 0.0 116.0	*First data point, note non-zero elevation after x-location of each electrode.*
4 -34.0 0.0 -28.0 0.0 -32.0 0.0 -30.0 0.0 118.0	*Second data point*
..	*Same format for other data points*
..	
..	
4 58.0 0.0 94.0 0.0 70.0 0.0 82.0 0.0 1160.0	*Second last data point*
4 60.0 0.093 96.0 0.0 72.0 0.0 84.0 0.0 1680.0	*Last data point*
Topography in separate list	*Extra header required for general array*
2	*2 to indicate surface distance*
67	*Number of topography data points*
-36,0.044	*Horizontal and vertical coordinates of 1st,*
-34,0.134	*2nd topography data point*
..	*This is followed by similar data for*
..	*the remaining topography data points*
96,-3.34	*Last topography data point*
1	*The topography data point number with the first electrode*
0,0,0,0,0	*Ends with a few zeros.*

Copyright 2025, Seequent

The measurement can be given in terms of resistance or apparent resistivity. If there is no topography, i.e., the z-locations are all equal to zero or the same, the conventional formula can be used to calculate apparent resistivity. The geometric factor *k* is given by the following equation

$$k = 2\pi / [(1/r_1) - (1/r_2) - (1/r_3) + (1/r_4)] \quad (7.2)$$

where r_1 is the distance between the C1 and P1 electrodes, r_2 is the distance between the C1 and P2 electrodes, r_3 is the distance between the C2 and P1 electrodes and r_4 is the distance between the C2 and P2 electrodes. In the case when there is no topography, the distance between two electrodes is simply the difference in the *x*-locations of the two electrodes.

In the case where topography is present, there is no widely accepted convention. To be consistent with the format used earlier, two different conventions are used depending on the type of *x*-location given in the data file. If the *x*-locations are given as distances along the surface (i.e., not true horizontal distances), the distance between two electrodes is calculated by using the difference in the values of the *x*-locations only.

If the *x*-locations are true horizontal distances, the default option is that the true distance between two electrodes is used in the calculation of the geometric factor. For example, if the C1 and P1 electrodes are located at (x_1,z_1) and (x_2,z_2) respectively, then

$$r_1 = (r_x^2 + r_z^2)^{0.5} \quad (7.3)$$

where $r_x = x_1 - x_2$

$r_z = z_1 - z_2$

In the case where the ground surface has a constant slope, both conventions will give the same geometric factor.

To accommodate a situation where the *x*-locations are true horizontal distances, but the geometric factor was calculated using only the x-positions, a couple of extra lines must be inserted in the data file just after the flag to indicate the type of measurement, as shown in the table below. A flag value of '0' is used to indicate only the horizontal distances between the electrodes are used to calculate the geometric factor.

Example file	*Comments*
….	*Initial part of file is same*
….	*as in previous examples*
11	*Array type (11 for general array)*
0	*Sib-array type, 1 for Wenner*
Type of measurement (0=app. resistivity,1=resistance)	*Header*
0	*0 to indicate apparent resistivity*
Type of geometric factor (0=Horizontal distance,1=Linear distance)	*Extra header for situation where horizontal distances are used for the geometric factor*
0	*0 for horizontal distance, 1 for linear distance*
300	*Number of data points*
1	*Type of x-location, 1 for true horizontal distances*
0	*Flag for IP data, 0 for none*
….	*Rest of file follows normal format*
….	

Note that in the general array data format, the *z*-location is the elevation of the electrode which is positive in the upwards direction. This unfortunately is different from the format for the borehole data set where the *z*-values are positive in the downwards direction.

Copyright 2025, Seequent

Figure 8 shows an interesting arrangement where the electrodes are arranged such that the *true horizontal* distances between adjacent electrodes are constant. When the slope of the ground surface is not constant, this results in an arrangement where the distance between adjacent electrodes as measured along the ground surface is not constant but depends on the slope. In areas where the slope is steeper, the distance between adjacent electrodes along the ground surface is greater. To accommodate such an arrangement, the general array format can be used. In this case, the indicator for the type of *x*-location must be 1 since the true horizontal distances are given in the data. Very often, the survey is carried out with one of the conventional arrays, such as the Wenner-Schlumberger, so the appropriate sub-array number should also be given.

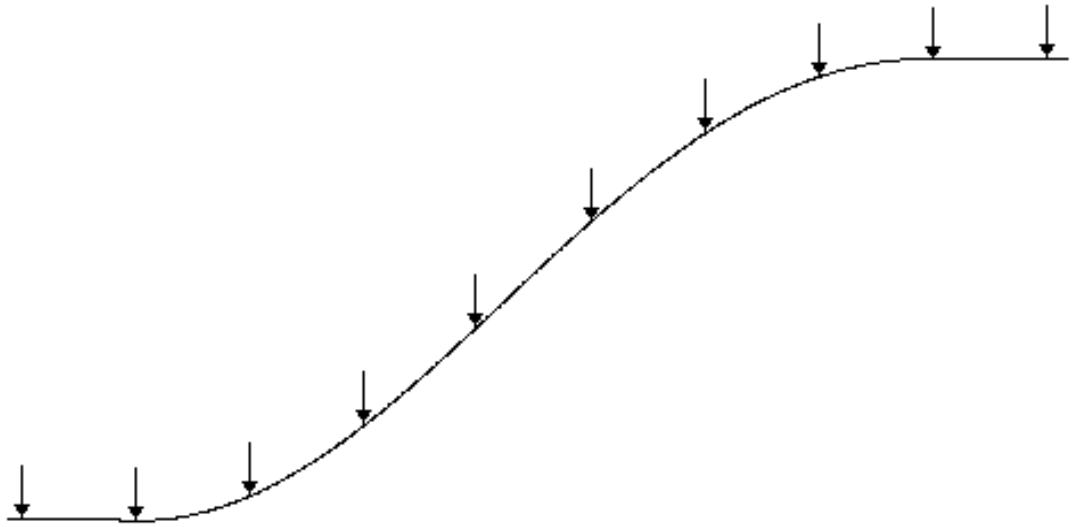

Figure 8. Arrangement of the electrodes along a survey line such that the true horizontal distance between adjacent electrodes is constant regardless of the slope of the ground surface. Note that the distance between adjacent electrodes along the ground surface is greater at the steeper part of the slope.

In some cases, the 2-D data set is generated from a series of collinear 1-D sounding lines. In such a situation, the distance between adjacent electrodes is not constant, whether as measured along the surface or in the true horizontal direction. For such a case, the general array format (with a sub-array type of 0) can be used.

For data sets with a sub-array type of 0, the data cannot be displayed in the form of a pseudo section, nor can it edited with the "Exterminate bad data points" option. To remove bad data points from the data set, you need to first carry out an inversion of the entire data set. However, you should use the "Robust data constraint" (see section 9.3.3.1) to ensure that bad data points do not have a large effect on the inversion results. Next, use the Error Statistics tool. This will display a histogram where the data points are grouped according to the difference between the measured and calculated apparent resistivity values. This allows you to remove the data points where a large difference occurs, for example more than 100 percent. After removing the noisier data points, save the trimmed data set in a file and carry out the inversion again with the trimmed data set.

The multiple gradient array is becoming popular with multi-channel systems (Dahlin and Zhou 2006). The data for the gradient array must be given in the general array format with a sub-array number of 15. A listing of the example GRADIENT.DAT file with comments about the format is given in Table 12.

Copyright 2025, Seequent

Table 12. Example gradient array data file.

GRADIENT.DAT file	*Comments*
Gradient array	*Name of survey line*
1.0	*Unit electrode spacing*
11	*Array type (11 for general array)*
15	*Sib-array type, 1 for Wenner*
Type of measurement (0=app. resistivity,1=resistance)	*Header*
0	*0 to indicate apparent resistivity*
1792	*Number of data points*
1	*Type of x-location, 2 for surface distance*
0	*Flag for IP data, 0 for none*
4 0.0,0.0 9.0,0.0 1.0,0.0 2.0,0.0 5.0588	*First data point*
4 1.0,0.0 10.0,0.0 2.0,0.0 3.0,0.0 5.0724	*Second data point*
..	
..	*Same format for other data points*
..	
4 46.0,0.0 118.0,0.0 78.0,0.0 86.0,0.0 4.2571	*Second last data point*
4 48.0,0.0 120.0,0.0 80.0,0.0 88.0,0.0 4.2258	*Last data point*
0,0,0,0,0	*Ends with a few zeros.*

7.3 Remote electrodes of the pole-pole and pole-dipole arrays

In theory, the pole-pole array has only 2 electrodes, the positive current electrode C1 and the positive potential electrode P1. In practice, such an array does not exist since all field measurements are made using an array with 4 electrodes (Figure 9).

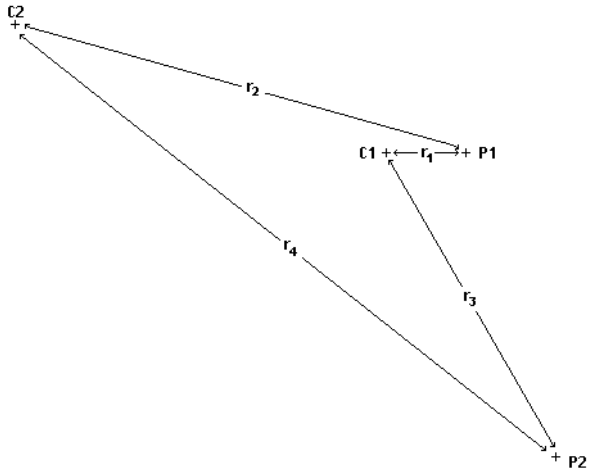

Figure 9. A schematic diagram of the arrangement of the electrodes in an actual field pole-pole measurement.

To minimize the effects of the C2 and P2 electrodes, it is generally recommended that the distance of these two electrodes from the C1 and P1 electrodes should be at least 10 times (and preferably 20 times) the maximum C1-P1 spacing r_1. In some cases, when large spacings between the C1 and P1 electrodes are used, this requirement is not met for all measurements. This could lead to distortions in the inversion model (Robian et al. 1997). To overcome this problem, the RES2DINV program allows the user to incorporate the effects of the C2 and P2 electrodes in the inversion.

To calculate the apparent resistivity value measured with the non-ideal pole-pole array, two possible geometric factors can be used. One method is to use the same equation as the ideal pole-pole array. This gives an approximate geometric factor since the resulting apparent resistivity value is not the same as the true resistivity for a homogeneous half-space. Alternatively, the exact geometric factor that takes into account the positions of the C2 and P2 electrodes can be used.

Copyright 2025, Seequent

Approximate Geometric factor (ideal pole-pole array) = $2.\pi.r_1$

Exact Geometric factor = $2\,\pi$ / [$(1/r_1)$ - $(1/r_2)$ - $(1/r_3)$ + $(1/r_4)$] (7.4)

The program supports both conventions. A possible arrangement of the electrodes in a pole-pole survey is shown in Figure 10. In this case, the C2 and P2 electrodes are fixed throughout the survey. The measurements are made by using different pairs of electrodes along the survey line as the C1 and P1 electrodes. For a survey line with *n* electrodes, there are *n(n+1)/2* possible combinations. For example, if there are 25 electrodes in the survey line, there are 300 possible combinations. In practice, not all the possible measurements are made. Instead, a maximum distance between the C1 and P1 electrodes is set depending on the maximum depth of investigation needed (Edwards 1977). In many cases, this maximum distance is 6 to 10 times the unit electrode spacing along the survey line. To avoid the possibility of negative or zero apparent resistivity values, the distance of the C2 and P2 electrodes must be at least 3 times the maximum C1 to P1 spacing used. For example, if the unit electrode spacing is 1 meter, and the maximum C1-P1 spacing is 10 meters, then the C2 and P2 electrodes must be at least 30 meters from the survey line. Note that as the distance of the C2 and P2 electrodes from the survey line decreases, the effective maximum depth of investigation of the survey also decreases. It might be significantly less than the depth of investigation for the ideal pole-pole array (Edwards 1977).

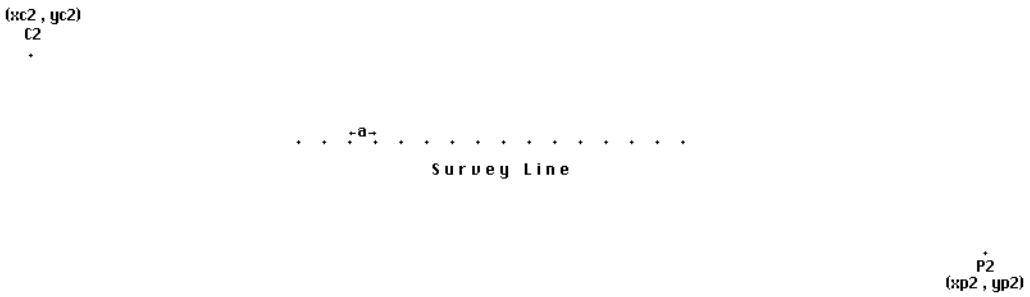

Figure 10. A schematic diagram of the arrangement of the electrodes along the survey line in a pole-pole survey with positions of the C2 and P2 electrodes specified.

The file POLPOLFX.DAT is an example data file with pole-pole measurements where the locations of the C2 and P2 remote electrodes are specified. A description of the format used is given in Table 13. Although the *z*-locations of the electrodes are also included in the file data format for completeness, the values are presently not used by the program. The program at present estimates the heights at the remote electrodes from the heights of the electrodes along the survey line. However, in future, they might be used to accommodate extreme cases where slope of the ground at the remote electrodes is very different from that along the survey line.

The data format is the same as that for normal pole-pole surveys except for the section (after the array number) which contains information about the location of the second current and potential electrodes. The data line “Exact Geometric factor used” is used to indicate that the apparent resistivity values in the data file were calculated used the exact geometric factor. If the approximate geometric factor was used, this data line should be given as “Approximate Geometric factor used”. The file POLDPLFA.DAT is an example data file for a pole-dipole survey where the approximate geometric factor was used in calculating the apparent resistivity values. Note that in this file, only the location of the second current electrode C2 is given.

For the pole-pole array, the effect of the C2 electrode is approximately proportional to the ratio of the C1-P1 distance to the C2-P1 distance. If the effects of the C2 and P2 electrodes are not taken into account, the distance of these electrodes from the survey line must be at least 20 times the largest C1-P1 spacing used to ensure that the error is less than 5%. In surveys where the inter-electrode spacing along the survey line is more than a few meters, there might be practical problems in finding suitable locations for the C2 and P2 electrodes to satisfy this requirement. Thus, the error in neglecting the effects of the remote electrodes is greatest for the pole-pole array. As a general guide, if the distances of the C2 and P2 electrodes from the survey line are more than 20 times the largest C1-P1 spacing used, the array can be treated as an ideal pole-pole array for interpretation purposes. Otherwise, the coordinates of the C2 and P2 electrodes should be recorded so that their effects can be determined by this program. However, it should be noted that as the distance of the P2 electrode from the survey line increases, the telluric noise

Copyright 2025, Seequent

picked up by the P1-P2 pair also increases. This factor should also be taken into account when positioning the P2 electrode.

For the pole-dipole array, the effect of the C2 electrode is approximately proportional to the *square* of ratio of the C1-P1 distance to the C2-P1 distance (Loke 2018). Thus, the pole-dipole array is less affected by the C2 remote electrode. If the distance of the C2 electrode is more than 5 times the largest C1-P1 distance used, the error caused by neglecting the effect of the C2 electrode is less than 5% (the exact error also depends on the location of the P2 electrode for the particular measurement). So, as a general guide, if the distance of C2 electrode from the survey line is more than 5 times the largest C1-P1 spacing, it can be treated as an ideal pole-dipole array. Otherwise, enter the coordinates of the C2 electrode into the data file. For the pole-dipole array, only the header and coordinates of the C2 electrode is required in the data file.

Table 13. Pole-pole data file with remote electrodes specified.

POLPOLFX.DAT file	*Comments*
Blocks Model	*Name of survey line*
2.0	*Unit electrode spacing*
2	*Array type (2 for pole-pole)*
Remote electrodes included	*Header to indicate position of remote electrodes included in data file*
C2 remote electrode X, Y and Z location	*Header for C2 electrode location*
-50.000,20.000,0.0	*x-, y- and z-location of C2 electrode*
P2 remote electrode X, Y and Z location	*Header for P2 electrode location.*
120.000,0.000,0.0	*x-, y- and z-location of P2 electrode*
Exact Geometric factor used	*Type of geometric factor used*
295	*Number of data points*
1	*1 indicates center of array is given*
0	*0 for no IP*
1.00 2.00 10.13	*x-location, electrode spacing apparent resistivity for 1st data point*
3.00 2.00 10.18	*Second data point*
..	*The rest follows standard index-based*
..	*format.*
..	

Copyright 2025, Seequent

7.4 Cross-borehole data format

The resolution of electrical surveys carried out with electrodes on the ground surface decreases exponentially with depth. One method to obtain reasonably good resolution at depth is by making measurements with the electrodes in boreholes. Cross-borehole surveys are much less frequently carried out compared to surface-based surveys, so unlike surface surveys, there are at present no common standards with regards to the arrangement of the electrodes. The cross-borehole option in this program is intended for shallow surveys with the arrangement of the electrodes placed in a certain general pattern (Sasaki 1992). The basic arrangement of the electrodes is shown in the Figure 11. The RES2DINV programs support up to 100 boreholes.

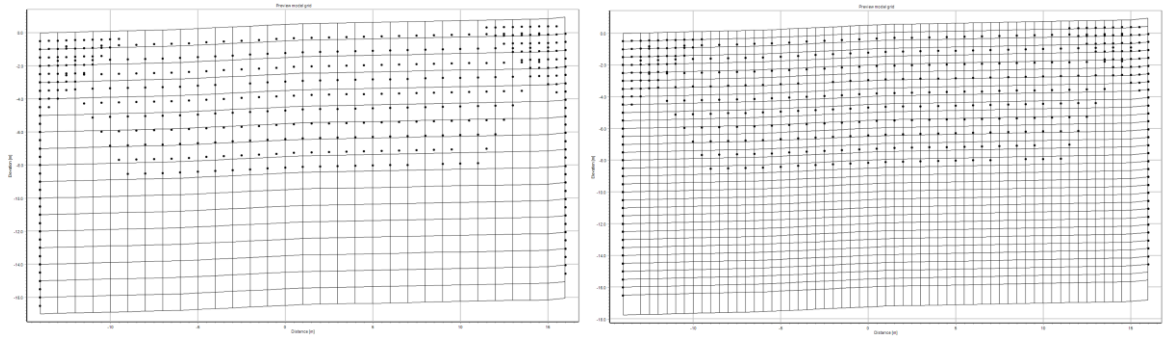

Figure 11. Arrangement of the electrodes in a cross-borehole survey. (a) The default standard model where the dimensions of the model blocks are equal to the spacing between the electrodes. (b) An alternative model with finer blocks with dimensions of about half the spacing between the electrodes.

The electrodes are divided into 2 sets with (i) surface electrodes, (ii) electrodes in the boreholes. It is assumed that the boreholes do not have a metal casing which would severely alter the pattern of the current flow. The program divides the subsurface into a number of quadrilateral blocks (Figure 11). Note that the positions of the surface and borehole electrodes control the way the subsurface is divided into the model blocks. The file BOREDIFF.DAT is an example data file with cross-borehole measurements. A description of the format used is given in Table 14. Note that in this example, the measurements are made with the pole-dipole array where only the C1, P1 and P2 electrodes are used. It is assumed the boreholes are vertical. Thus, the x-locations of all the electrodes in the same borehole are the same in Table 14. The array number is 12 for cross-borehole survey data with the measurements given as apparent resistivity values. You can also enter the data as resistance measurements, in which case the array number is 13. This might be more convenient as most resistivity meters give the readings as a resistance value in ohm, and furthermore the geometric factor for arrays with subsurface electrodes is different from the geometric factor for conventional surface arrays. The file BORERES.DAT gives an example where the measurements are given as resistance values. An interesting field data set where the pole-pole array was used, and the measurements are also given as resistance values, is BORELUND.DAT from Lund University, Sweden.

If only two electrodes are used in a measurement, only the *x*- and *z*-locations of the C1 and P1 electrodes are given in the data file (see the file BOREHIP.DAT which also contains IP measurements). However, if all four electrodes are used, the *x*- and *z*-locations of the C1, C2, P1 and P2 electrodes must be given in this order. You can combine measurements made with different numbers of electrodes in the same data file.

When the program reads in a file with resistance values, you have a choice of inverting the data set using apparent resistivity values, or directly use the resistance values. Using resistance values directly in the inversion has the advantage of allowing you to use readings where the apparent resistivity value does not exist (due to an infinite geometric factor). After reading in a data file, the program will attempt to filter out suspicious readings with potentially high noise levels if the measurements are given as apparent resistivity values, or if you had chosen the option to use apparent resistivity values in the inversion. If you choose to carry out the inversion using resistance values, the readings are not filtered.

The geometric factor for subsurface electrodes is different from that used for surface electrodes. For a 4-electrode measurement with electrodes C1, C2, P1 and P2 located at (x_{c1},z_{c1}), (x_{c2},z_{c2}), (x_{p1},z_{p1}) and (x_{p2},z_{p2}), respectively (*z* indicating depth beneath surface), the geometric factor *k* is given by

$$k=4\pi/[1/r_{C1P1}+1/r_{C1'P1}-1/r_{C1P2}-1/r_{C1'P2}-1/r_{C2P1}-1/r_{C2'P1}+1/r_{C2P2}+1/r_{C2'P2}] \quad (7.5)$$

(Wilkinson et al., 2008)

where distances between electrodes and electrode reflections (‘) are given by:

Copyright 2025, Seequent

$r_{C1P1}=|(x_{c1},z_{c1})-(x_{p1},z_{p1})|$
$r_{C1'P1}=|(x_{c1},-z_{c1})-(x_{p1},z_{p1})|$
$r_{C1P2}=|(x_{c1},z_{c1})-(x_{p2},z_{p2})|$
$r_{C1'P2}=|(x_{c1},-z_{c1})-(x_{p2},z_{p2})|$
$r_{C2P1}=|(x_{c2},z_{c2})-(x_{p1},z_{p1})|$
$r_{C2'P1}=|(x_{c2},-z_{c2})-(x_{p1},z_{p1})|$
$r_{C2P2}=|(x_{c2},z_{c2})-(x_{p2},z_{p2})|$
$r_{C'2P2}=|(x_{c2},-z_{c2})-(x_{p2},z_{p2})|$

The depth of the electrodes in Borehole 1 can be different from the corresponding electrodes in Borehole 2. In practice, to get the best results the depths should not differ too much. This program requires that the number of electrodes in both boreholes must be the same. In practice, this restriction is not a significant problem. You can be easily overcome this restriction by inserting dummy electrodes into the data set if the number of electrodes in one borehole is less (in the section where the *x*- and *z*-location of the electrodes in the borehole are given).

The program also requires that a surface electrode is located at the top of both boreholes. If they do not physically exist, just insert dummy electrodes at the appropriate locations in the data file. Also, there should be at least a few surface electrodes between the two boreholes, as well as at least two surface electrodes to the left of borehole 1, and another two to the right of borehole 2. If such electrodes were not used in the field survey, just insert dummy electrodes into the data file to satisfy the requirements of this program.

By default, the program will subdivide the subsurface into quadrilateral blocks such that the dimensions of the blocks are equal to the spacing between the electrodes (Figure 11a). However, you can also choose to use a model where the dimensions of the blocks are about half the spacing between the electrodes (Figure 11b). Using the model with a finer discretization could significantly improve the inversion results in some cases (Sasaki 1992). This setting can be enabled in the inversion settings under Borehole – Borehole model refinement.. However, since the resolution of electrical measurements decreases rapidly with distance from the measuring electrodes, the refinement does not always improve modeling result.. In fact, in certain cases, it could result in unnatural oscillations in the model resistivity values, particularly near the electrodes. This is as a result of the well-known trade-off between model resolution and model variance in geophysical inversion.

Figure 12 shows the model obtained after the inversion of the BOREHOLE.DAT data set. This is a synthetic data set produced by a forward modeling program with a high resistivity block in between the two boreholes. The option to use finer blocks with half the size of the spacing between the electrodes was used in the inversion of this data set. Figure 13 shows the inversion results from an interesting field data set. This data set is one from a number that were collected by a survey to study the flow of fluids through the UK Chalk aquifer in east Yorkshire by using a saline tracer (Slater et al. 1997). There is a low resistivity zone near the surface where the saline solution was irrigated onto the ground, and also prominent low resistivity zones below a depth of 7 meters due to the saline tracer that had flowed downwards. Another interesting feature of this data set is that no surface electrodes were used. All the surface electrodes given in the BORELANC.DAT data file are dummy electrodes; two to the left of borehole 1 and another two to the right of borehole 2.

If IP measurements were also made, you need to enter a value of 1 at the 6th line in the data file, and two more data lines after that which gives the type of IP measurement used and the two parameters associated with it (see section 7.5). Next, enter the IP value after the apparent resistivity value for each data point. The file BOREHIP.DAT is an example cross-borehole data file with IP measurements.

The file boreholes_inclined.dat gives an example of the data format with non-vertical boreholes (Table 15). Note the addition of an additional header line ‘Inclined boreholes present’ just before the section with the positions of the boreholes to indicate that non-vertical boreholes are present. For inclined boreholes, the subdivision of the subsurface into model blocks is no longer tied directly to the positions of the electrodes. You can also use this format for vertical boreholes where the corresponding electrodes at different boreholes are at different depths. This avoids inclined or skewed model blocks when there are significant differences in the borehole electrodes depths.

Copyright 2025, Seequent

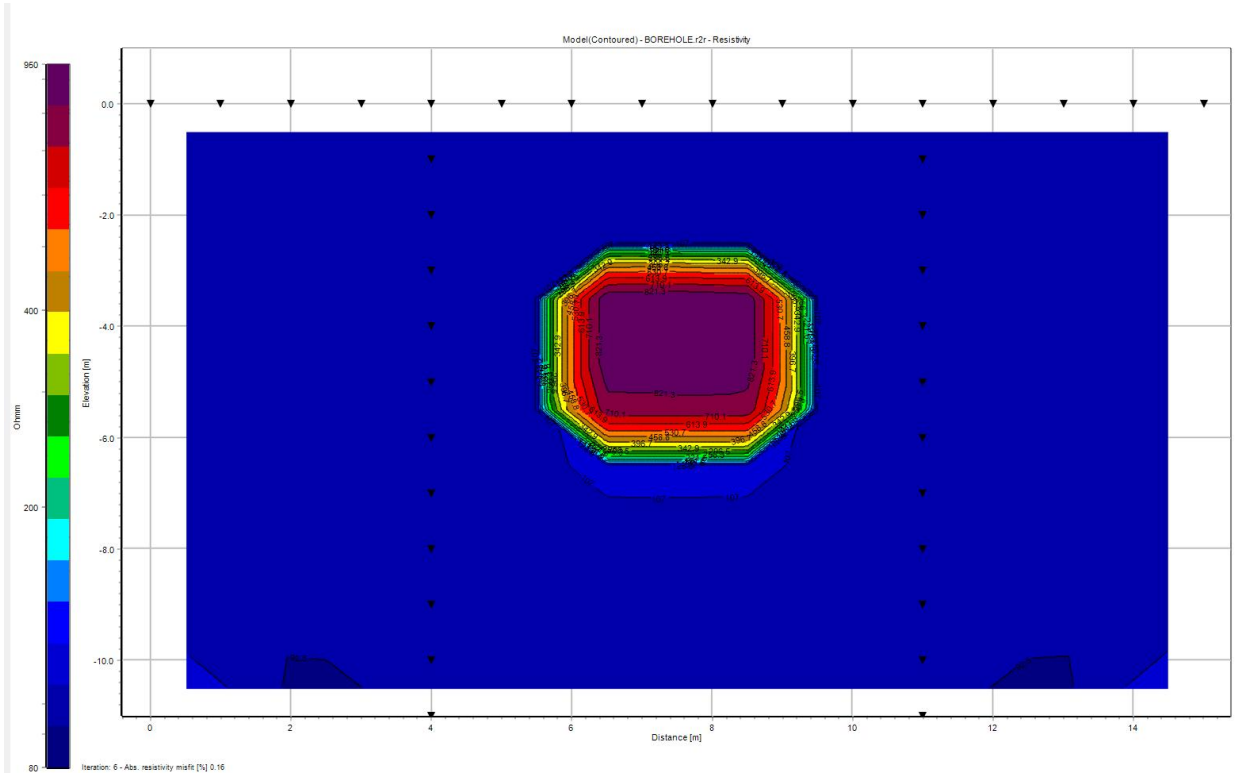

Figure 12. The model obtained after the inversion of the BOREHOLE.DAT data set. The option to use finer blocks with half the size of the spacing between the electrodes was used.

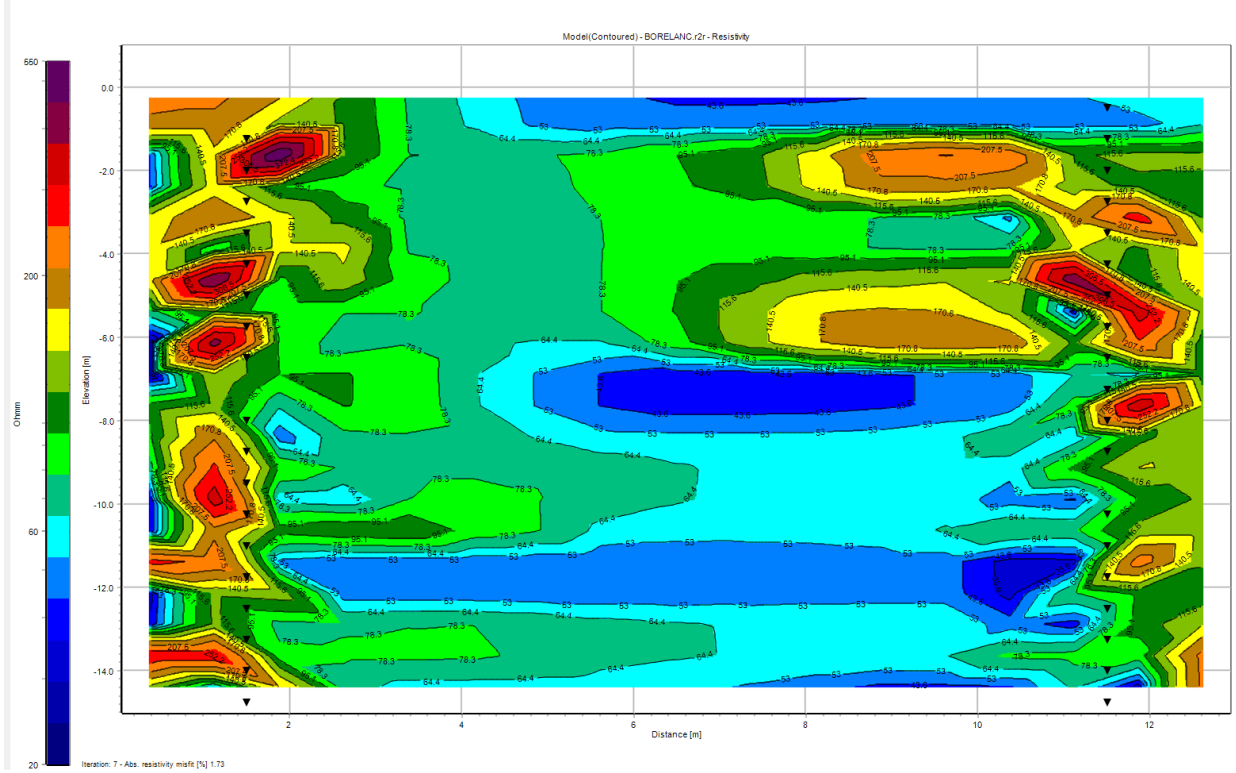

Figure 13. Model obtained from the inversion of data from a cross-borehole survey to map the flow of a saline tracer (borelanc.dat). Note the low resistivity zones near the surface (where the tracer was injected) and below a depth of 7 meters. The locations of the borehole electrodes are shown by small black dots.

Table 14. Example borehole data set.

BOREDIFF.DAT file	*Comments*
Borehole electrodes at different depths	*Name of survey line*

Copyright 2025, Seequent

1.0	*Unit electrode spacing*
12	*Array number 12 for cross-borehole survey*
840	*Number of data points*
2	*2 to indicate XZ location format is used*
0	*0 for no IP*
Surface Electrodes	*Header for surface electrodes*
16	*Number of surface electrodes*
0.0, 0.0	*x- and z-location of first surface electrode*
1.0, 0.0	*Location of second surface electrode*
..	*Note 0.0 z value for surface electrode*
..	*Similar format for other surface electrodes*
..	
15.0, 0.0	*Last surface electrode*
Number of boreholes	*Header*
2	*Two boreholes in this data set*
Borehole 1 Electrodes	*Header for first borehole*
10	*Number of electrodes in first borehole*
4.0, 1.0	*x- and z-location of first electrode*
4.0, 2.0	*x- and z-location of second electrode*
4.0, 3.0	*Note electrodes are listed from the topmost*
..	*below the surface downwards*
..	*Similar format for other borehole electrodes*
..	
4.0, 10.0	*Last electrode in first borehole*
Borehole 2 Electrodes	*Header for second borehole*
10	*Number of electrodes in second borehole*
11.0, 1.5	*x- and z-location of first electrode*
11.0 2.5	*x- and z-location of second electrode*
..	
..	*Similar format for other borehole electrodes*
11.0, 10.5	*Last electrode in second borehole*
Measured data	*Header for section with the measurements*
3 0.0 0.0 1.0 0.0 2.0 0.0 101.5718	*The format for each data point is :-*
3 0.0 0.0 2.0 0.0 3.0 0.0 99.5150	*Number of electrodes used in measurement,*
3 0.0 0.0 3.0 0.0 4.0 0.0 99.2303	*x- and z-location of C1, C2, P1, P2*
3 0.0 0.0 4.0 0.0 5.0 0.0 99.1325	*electrodes, apparent resistivity value.*
..	
..	*Same format for other data points*
...	
3 11.0 11.0 11.0 3.5 11.0 2.50 120.8297	*Last data point*
0,0,0,0	*End with a few zeros.*

Copyright 2025, Seequent

Table 15. Example data set with inclined boreholes.

boreholes_inclined.dat file	*Comment*
Example bipole-bipole configurations	*Title*
4.0	*Unit electrode spacing*
12	*Array number for borehole survey*
2555	*Number of data points*
2	*2 to indicate XZ location format used*
0	*0 for o IP*
Surface Electrodes	*Header*
26	*Number of surface electrodes*
0.0, 0.0	*x, z location of 1st surface electrode*
4.0, 0.0	*x, z location of 2nd surface electrode*
..	
..	
100.0, 0.0	*Last surface electrode*
Inclined boreholes present	*Extra header to indicate inclined borehles*
Number of boreholes	*Header*
2	*Two boreholes present*
Borehole 1 Electrodes	*Header for first borehole*
20	*Number of electrodes in first borehole*
20.0, 4.0	*x, z location of 1st electrode in borehole 1*
20.0, 8.0	*x, z location of 2nd electrode in borehole 1*
..	
..	*Same format for other borehole electrodes*
..	
20.0, 80.0	*Last electrode in first borehole*
Borehole 1 Electrodes	*Header for second borehole*
20	*Number of electrodes in borehole*
80.0, 4.0	*First electrode in second borehole*
80.0, 8.0	*Second electrode in second borehole*
80.0, 12.0	
80.0, 16.0	
80.0, 20.0	
80.0, 24.0	
80.5, 28.4	*Note x-location is different, non-vertical*
80.0, 32.0	
..	
..	*Other borehole electrodes*
..	
80.0, 80.0	*Last electrode in second borehole*
Measured Data	*Header for start of apparent resistivity data*
4 4.0, 0.0 0.0,0.0 8.0,0.0 12.0, 0.0 101.6895	*First data value*
...	*Format is the same as before*

Copyright 2025, Seequent

The file BOREHOLE_TOPO.DAT is a field example of a cross-borehole data set with topography. The initial part of this data file with a description of the format is given in Table 16.

Table 16. Example borehole data set with topography.

BOREHOLE_TOPO.DAT file	*Comment*
BOREHOLE WITH TOPOGRAPHY	*Name of survey line*
1.0	*Unit electrode spacing*
12	*Array number 12 for cross-borehole survey*
570	*Number of data points*
2	*2 to indicate XZ location format used*
0	*0 for o IP*
Topography Present	*Header to indicate topography is present*
Topography information mode (0=wrt to surface electrodes)	*Header*
0	*Indicates depths of borehole electrodes are given with respect to the surface electrode at the top of the borehole*
Type of x-distances	*Header*
2	*2 to indicate x-distances are along the surface*
Surface Electrodes	*Header*
31	*Number of surface electrodes*
-14.0000 0.00	*x, z location of 1st surface electrode*
-13.0000 0.03	*x, z location of 2nd surface electrode*
-12.0000 0.05	*Note non-zero z value*
..	
..	*Same format for other electrodes*
..	
16.0000 0.95	*Last surface electrode*
Borehole 1 electrodes	*Header for first borehole*
17	*Number of electrodes in borehole*
-14.0000 1.0000	*x, z location of 1st electrode in borehole 1*
-14.0000 2.0000	*x, z location of 2nd electrode in borehole 1*
..	*Rest of the file follows the usual format*
..	*for a cross-borehole data file*

Note that the topography information is given in the *z*-coordinates of the surface electrodes. The file BOREHOLE_Global.dat is an example where the true or GPS coordinates (section 7.11) of the electrodes on the surface are also available.

7.5 IP data format

The data collected from IP (Induced Polarization) surveys consists of two sets, the normal apparent resistivity measurements and an apparent IP data. The files IPMODEL.DAT, IPMAGUSI.DAT, IPSHAN.DAT and IPKENN.DAT are example data files with both resistivity and IP data. This program supports four different types of IP data; (i) time domain chargeability measurements, (ii) frequency domain percent frequency effect measurements, (iii) phase angle measurements and (iv) metal factor IP values.

The file IPMODEL.DAT has the IP data as chargeability values using the index-based format for the positions of the electrodes. The first part of the file with comments is listed in Table 17. A value of "1", instead of "0", is entered into the sixth line to indicate that IP data is present. This is followed by 3 data lines that give information about the nature of the IP data. The seventh line with the word *'Chargeability'* shows that the IP data is given in terms of chargeability. Many IP instruments measured the chargeability be integrating the area under the IP decay curve. In this case, the unit is in msec (millisecond). The chargeability value obtained by this method is normally calibrated to the Newmont $M_{(331)}$ standard (Summer 1976) so that the chargeability value in msec has the same numerical value as the chargeability given in mV/V. The chargeability in mV/V is defined as the ratio of the secondary voltage immediately after the current is cut off to the primary DC voltage.

Copyright 2025, Seequent

Table 17. Example data file with IP values as chargeability.

IPMODEL.DAT file	*Comments*
Fault and block model	*Name of survey line*
1.0	*Unit electrode spacing*
3	*Array type (3 for dipole-dipole)*
432	*Number of data points*
1	*1 indicates center of array is given*
1	*1 to indicate IP present*
Chargeability	*Type of IP data*
msec.	*IP unit*
0.1,1.0	*Delay, integration time*
1.50 1.00 1 12.04 7.2038	*1st data point : - x-loc., a, n, app. res., app. IP*
2.50 1.00 1 12.03 7.1983	*2nd data point*
..	
..	*Same format for other data points*
..	

IP surveys have traditionally been used in the mineral exploration industry, particularly for metal sulfides, where generators producing high currents of the order of 10 Amperes are used. The apparent IP values from such surveys are usually less than 100 msec. (or mV/V). One recent development is the addition of IP capability to battery-based systems used in engineering and environmental surveys where currents of 1 Ampere or less are normally used. An accompanying phenomenon is the observation of IP values of over 1000 msec. (or less than -1000 msec.) in some data sets. Such values are almost certainly caused by noise due to a very weak IP signal. To check whether such high IP values are real, first check the apparent resistivity pseudo section. If it shows unusually high and low values that vary in an erratic manner, the data is noisy. If the apparent resistivity values are noisy, then the apparent IP values are almost certainly unreliable. Next check the apparent IP pseudo section. If the apparent IP values show an erratic pattern (frequently with anomalous values lined up diagonally with an apex at a doubtful electrode), then the IP values are too noisy to be interpretable.

IP values that are given in other units are converted into chargeability values internally by the program during the inversion process. The relevant conversion equations may be found in the papers by Van Voorhis et al. (1973) and Nelson and Van Voorhis (1973). For frequency domain measurements, the IP value is usually given in Percent Frequency Effect (PFE). This is given as

$$PFE = 100 (\rho_{DC} - \rho_{AC}) / \rho_{AC} \qquad (7.6)$$

where ρ_{DC} and ρ_{AC} are the apparent resistivity values measured at low and high frequencies. The file IPSHAN.DAT is an example of a frequency domain IP data set. In the seventh line, the type of IP data is given as “Percent Frequency Effect”. The 9th data line contains the values of the low and high frequencies used in the measurement. This data set is from a field survey in Burma where the measurements were made with 20 and 40 meter dipoles (Edwards 1977). Like many field data sets, it has a very complex distribution of the data points in the pseudo section. The survey target is a galena deposit in meta-sediments. The geology is rather complex with massive galena deposits together with quartz veins, silicified marbles and clay zones. There is a very wide range of resistivity values.

IP values are also given as phase angles. In this case the unit normally used is milli-radians (mrad). An example of an IP data set with phase angles is given in the file IPKENN.DAT with values from the paper by Hallof (1990). In the seventh line, the type of IP data type is given as “Phase Angle”. The second parameter in the ninth data line contains the values of the frequency at which the phase angles were measured. The first parameter is not used and is normally set to 0. Many modern IP survey instruments can measure the phase angle for several frequencies. In this case, the inversion of is repeated for the phase angle data at each frequency. This will give an idea of the change of the subsurface IP phase angle with frequency for complex resistivity studies.

IP data is sometimes given as a metal factor (MF) value. The MF value can be calculated from either time domain or frequency domain measurements. In the time domain, the metal factor is value is given by

Copyright 2025, Seequent

$$MF = 1000\ M / \rho_{DC} \qquad (7.7)$$

where the chargeability M is given in terms of millisecond (Witherly and Vyselaar 1990). In the frequency domain, it is given as

$$MF = 100000\ (\rho_{DC} - \rho_{AC}) / \rho_{AC}^{\ 2} \qquad (7.8)$$

The file IPMAGUSI.DAT is from a survey over the Magusi River ore body (Edwards 1977) where the survey was conducted with 30.5 meter (100 feet), 61.0 meter (200 feet) and 91.4 meter (300 feet) dipoles. Again, the resulting pseudo section has a very complex distribution of the data points. The measured apparent resistivity and IP pseudo sections, together with the model sections obtained are shown in Figure 14. The ore body shows up as a distinct low resistivity body with high IP values near the middle of the survey line in the model sections. In the inversion of this data set, the robust inversion (L1-norm) method was used (see section 9.3.3) to sharpen the boundary between the ore body and the surrounding rocks. This program uses the complex resistivity method (Kenma *et al.* 2000) for the inversion of IP data.

The inversion program tries to minimize the difference between the observed and calculated equivalent apparent chargeability values. IP values in percent frequency effect and phase angles are directly proportional to the equivalent chargeability values. However, the metal factor value also involves a resistivity value. The model that gives a minimum RMS error for the chargeability values sometimes does not give a minimum RMS error for the metal factor values. However, the actual effect on the inversion model is usually very small.

The file IPGENERAL8.DAT is an example IP data file using the general array data format. The IP data parameters are also given just before the main data section with the apparent resistivity and IP values.

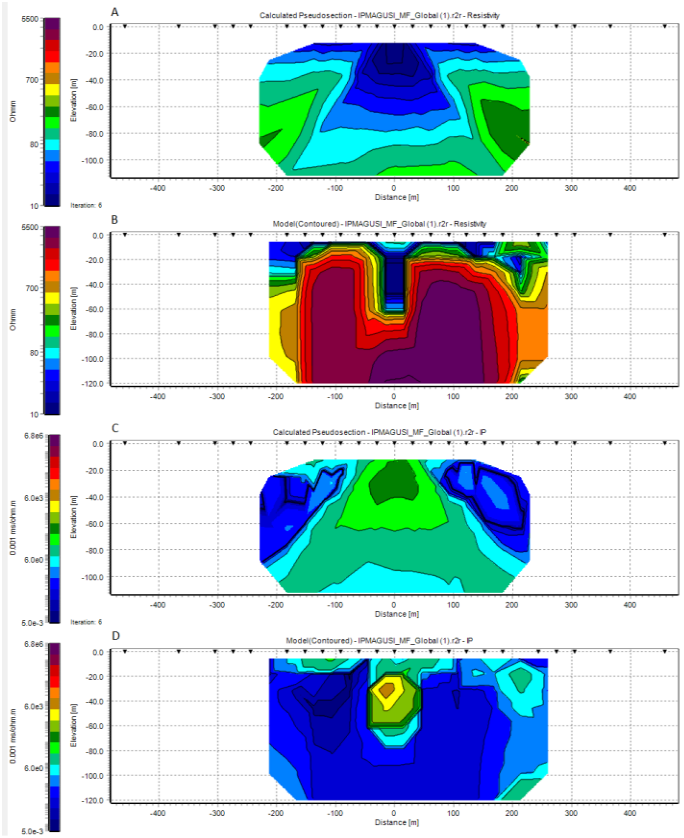

Figure 14. Magusi River ore body resistivity and I.P sections. (a) Apparent resistivity pseudo section, (b) resistivity model section, (c) apparent metal factor pseudo section and (d) metal factor model section.

7.6 Time-lapse data files

In studying the changes of the subsurface resistivity with time, two-dimensional resistivity imaging surveys are often repeated over the same line at different times. Such studies include the flow of

Copyright 2025, Seequent

water through the vadose zone, changes in the water table due to water extraction (Barker and Moore 1998), flow of chemical pollutants and leakage from dams.

The file TIMELAPS.DAT is an example data file with three sets of apparent resistivity data. The upper part of the file together with comments about the data format is listed in Table 18. The data format is largely similar to the normal data set with only one set of readings. For a time-lapse data file, the main difference is the extra section just before the data block with the apparent resistivity values. Here the header "Time sequence data" is used to indicate the presence of the extra data sets corresponding to the later time measurements. The following part of this extra section contains information on the number of time series measurements (3 in this example). The maximum number of time series data sets allowed is 21 (30 for RES2DINV with 16GB RAM). For each data point, the format for the initial part is identical to that used for the normal data sets. The only addition is that after the apparent resistivity value for the first data set, the corresponding apparent resistivity values for the later time data sets are given.

Table 18. Example time-lapse data set with 3 time series.

TIMELAPS.DAT file	*Comment*
Example time-lapse data	*Title*
1.0	*Unit electrode spacing*
7	*Array type, Wenner-Schlumberger in this example*
350	*Number of data points*
1	*Mid-point of x-location of array is given*
0	*No IP data*
Time sequence data	*Header to indicate time-lapse data*
Number of time sections	*Header*
3	*Number of time series*
Time unit	*Header*
Hours	*Unit used in time measurement*
Second time section interval	*Header*
1.0	*Time difference for second time data set*
Third time section interval	*Header*
2.0	*Time difference for third time data set*
1.50 1.00 1.0 11.868 11.868 11.868	*The format for each datum point is as follows:*
2.50 1.00 1.0 11.867 11.867 11.867	*x-location, "a" electrode spacing, "n" factor,*
3.50 1.00 1.0 11.863 11.863 11.863	*apparent resistivity for first data set, apparent*
4.50 1.00 1.0 11.859 11.860 11.860	*resistivity for second data set,*
5.50 1.00 1.0 11.855 11.856 11.856	*apparent resistivity for third data set.*
6.50 1.00 1.0 11.851 11.851 11.851	
...	*Same format for other data points*

If a measurement was missing from a time series, enter 0.0 as the value of the apparent resistivity for that particular time series. The program will assume that a zero value is an indication of a missing data point.

Copyright 2025, Seequent

7.7 Incorporating data noise estimates

Some types of resistivity surveying instruments record an estimate of the random noise for each measurement. This is usually done by repeating the same measurement several times. The data error estimate is then calculated from the standard deviation in the readings. This gives a measure of the repeatability in the readings, i.e., the random noise. Note that this data error estimate does not include sources of systematic errors such as coupling between the cables. A better method to estimate the data error is by using reciprocal measurements.

To include the data error estimate in a data file, the error values are entered after the apparent resistivity value. The file MODEL35_N.DAT is an example of a data file from a surface survey with the error values. Part of the file is shown in Table 19 with an explanation of the changes needed. Note there are two new additions in the data format. Firstly, just before the section of the file with the measured apparent resistivity data points, there are 3 extra lines. The first line 'Error estimate for data present' is a header to indicate that the data file contains the data error estimates. The second new line is a header to explain the use of the next line. The third line contains a flag to indicate to the program the units used in the error estimate. At present, use a value of '0' to indicate that the error value has the same units as the data value. For example, if the measurements are given as ohm.m, then the error values must also be in ohm.m. Measurements in most instruments are given as resistance values (i.e., ohm), or voltage plus current values which can be converted to resistance values. To calculate the apparent resistivity value, the resistance value is multiplied by a geometric factor. The error value recorded by the instrument is probably in the form of a resistance (ohm) value. Thus, the error estimate recorded by the instrument must also be multiplied by the same geometric factor before it is entered into the DAT file format used by this program. The file modelip_5%_noise.dat gives an example of an IP data set with noise estimates. The use of the flag for the unit used by the error value makes it possible for future versions of the program to allow the use of other units for the error value, for example the data in ohm.m while the error in ohm. Another possibility is the error given as a percentage value.

Table 19. Example data file with noise estimates.

MODEL35_N.DAT file	*Comments*
Block Model	*Title*
1.00	*Unit electrode spacing*
7	*Array type, 7 for Wenner-Schlumberger*
230	*Number of data points*
1	*Mid-point of x-location of array is given*
0	*No IP data*
Error estimate for data present	*Header to indicate error values present*
Type of error estimate (0=same unit as data)	*Header for type of error*
0	*0 to indicate it is same unit as data vaue*
1.500 1.000 1.000 10.0145 0.1434	*x-loc., 'a' value, 'n' value, apparent*
2.500 1.000 1.000 9.9706 0.1882	*resistivity, data point error value*
3.500 1.000 1.000 10.3357 0.1761	
..	
..	*Other data points follow same format*
..	

To invert data with noise estimates, the least-squares equation in (4.1) is modified to the following equation

$$(\mathbf{J^T W_d^T W^T J W_d^T W^T} + \lambda \mathbf{F}) \Delta \mathbf{q_k} = \mathbf{J^T W_d^T W^T g} - \lambda \mathbf{F}\, \mathbf{q_{k-1}} \qquad (7.9)$$

where $\mathbf{W_d}$ is a diagonal weighting matrix that incorporates the effect of the data errors. Data points with a smaller error are given a greater weight in the inversion process. In an ideal situation, the noise estimate should be measured (for example by reciprocal measurements). However, in most field surveys such

Copyright 2025, Seequent

noise estimates are not measured due to time constraints. In such a situation, the best option is probably to use the 'Robust data constraint' option (section 9.3.3) so that the effect of outliers in the data on the inversion model is minimized. With this option, a linear weight is given to the difference between the measured and calculated apparent resistivity values. This makes the inversion result less sensitive to outliers compared to the normal least-squares constraint where the square of the difference between the measured and calculated apparent resistivity values is used.

7.8 Fixing resistivities

In some cases, the true resistivity of a section of the subsurface might be known, for example from borehole resistivity measurements. This program allows you to fix the resistivity of up to 1000 sections of the subsurface. The shape of the section to be fixed must be rectangular or triangular. The data to fix the model resistivity values are entered into the input data file after section with the topography information.

As an example, part of the example data file MODELFIX.DAT is listed Table 20. The first item after the topography data section is the number of regions where the resistivity is to be specified. In the example above, 2 regions are specified. If a value of 0 is given (default value), then there are no regions where the resistivity is specified by the user. Next, the shape of the region is given, R for rectangular or T for triangular. If a rectangular region is specified, then the X and Z coordinates of the top-left and bottom-right corners of the rectangle are given, as shown in Figure 15.

Table 20. Example data file with fixed regions.

MODELFIX.DAT file	*Comments*
25.0 10.0 12.81	*Last data point*
0	*Topography flag, 0 for no topography*
2	*Number if regions to fix, put 0 if none*
R	*Type of first region, R for rectangular*
24,0.7	*X and Z coordinates of top-left corner of rectangle*
28,2.3	*Coordinates of bottom-right corner of rectangle*
2.0	*Resistivity value of rectangular region*
2.0	*Damping factor weight*
T	*Type of second region, T for triangular*
30,0.0	*X and Z coordinates of first corner of triangle*
30,3.0	*X and Z coordinates of second corner of triangle*
45,3.0	*Coordinates of third corner of triangle*
10.0	*Resistivity value of triangular region*
2.5	*Damping factor weight*
0,0,0	*Ends with a few zeros for other options*

If a triangular region is chosen, the X and Z coordinates of the 3 vertices of the triangle must be given in an anti-clockwise order. After the coordinates of the region to be fixed are given, the next data item is the resistivity of the region. After that, the damping factor weight for the resistivity of the region is needed. This parameter allows you control the degree to which the inversion subroutine can change the resistivity of the region. There is usually some degree of uncertainty in resistivity of the region. Borehole measurements can only give the resistivity of a very limited zone near the borehole. Thus, it is advisable that the program should be allowed (within limits) to change the resistivity of the region. If a damping factor weight of 1.0 is used, the resistivity of the region is allowed to change to the same extent as other regions of the subsurface model. The larger the damping factor weight is used, the smaller is the change that is allowed in the resistivity of the "fixed" region. Normally, a value of about 1.5 to 2.5 is used. If a relatively large value is used, for example 10.0, the change in the resistivity of the region would be very small during the inversion process. Such a large value should only be used if the resistivity and shape of the region is accurately known.

Copyright 2025, Seequent

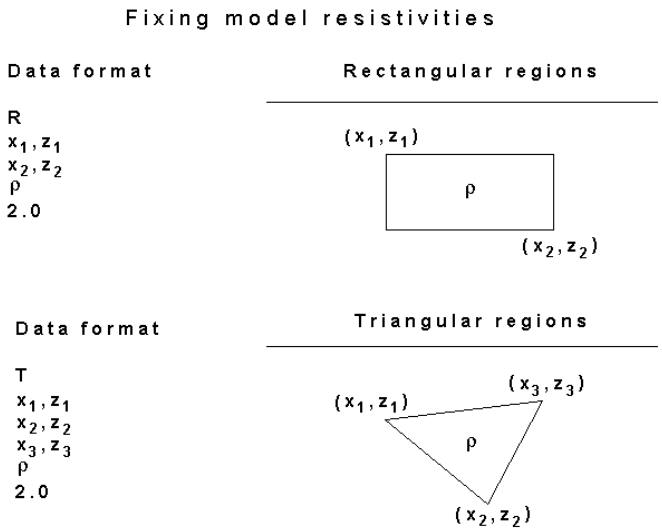

Figure 15. Fixing the resistivity of rectangular and triangular regions of the inversion model.

7.9 Aquatic surveys

(a) Single water layer

The possible situations for aquatic surveys are shown in Figure 16. In 'Case 1' all the electrodes are on the surface of the river or sea bottom and are underwater. In 'Case 2' the water layer covers a limited region and the ground rises above the water surface at some places, such as a survey across a river. In 'Case 4' the water region is limited by a barrier such as a dam wall or levee, and although the electrodes on the right side are below the water surface level, it is known that they are not covered by the water layer. 'Case 3' is for a survey with the electrodes floating on the water surface, such as on a streamer pulled by a boat. 'Case 5' is variation of this type of survey where the electrodes are on a streamer suspended between the surface and the bottom. This places the electrodes closer to the sub-bottom which is being surveyed but is not dragged along the bottom (as in 'Case 1') where it could encounter obstacles.

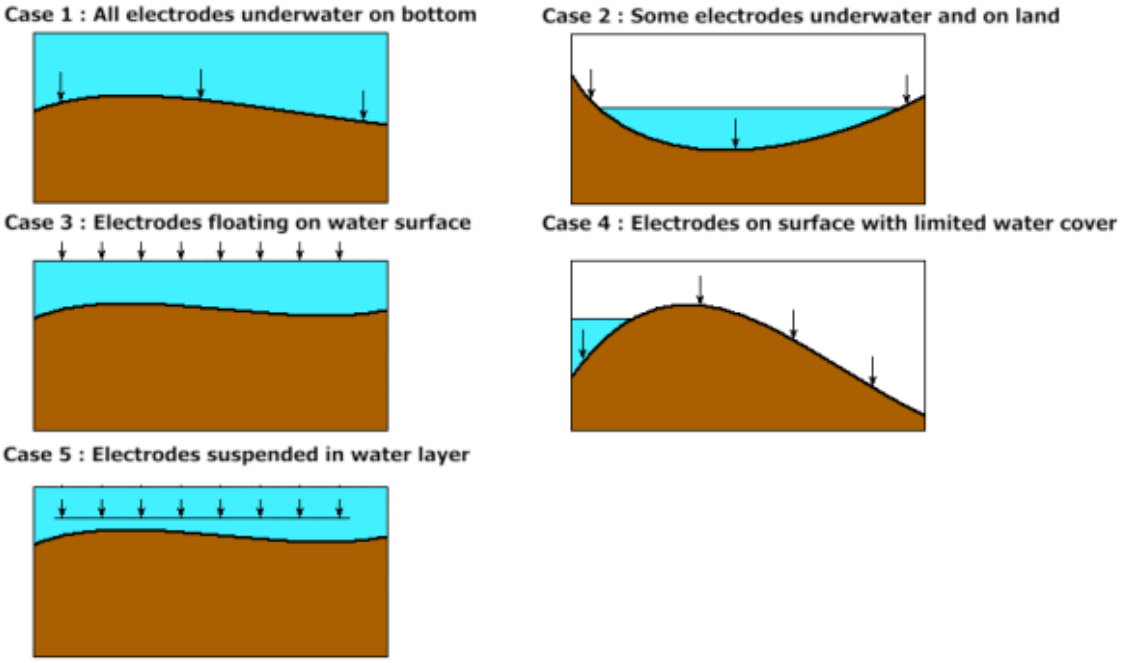

Figure 16. Five possible situations for aquatic surveys.

The information with the aquatic survey parameters are entered in the data file after the main section with the apparent resistivity data, topography and fixed regions.

Copyright 2025, Seequent

7.9.1 Underwater surveys

The data format for surveys with electrodes planted on the water bottom for both cases 1 and 2 are the same. An example data file is HAT_HEAD.DAT that uses the index-based format is listed in Table 21. Note that a flag is included to indicate that the normal geometric factor (as used for a surface survey) is used to calculate apparent resistivity values. If a value of 0 is used for this flag, the exact geometric factor (which includes the thickness of the water layer) must be used to calculate the apparent resistivity values. In the HAT_HEAD.DAT file, some of the electrodes are above the water (Figure 17). In most surveys, all the electrodes are underwater as in the following LAKELELIA.DAT example (Table 22). The program will automatically calculate the thickness of the water layer from the elevation of the sea or river bottom and the elevation of the water surface. This format allows for the second situation shown in Figure 17 where some of the electrodes are above the water surface (i.e., on normal dry land) and some of the electrodes underwater. A common situation where this occurs is a survey that crosses a river. In this case, the program will assume that an electrode with an elevation that is less than the elevation of the water surface is underwater. For the case when some of the electrodes are above the water surface, the surface geometric factor must be used for calculating the apparent resistivity values for all the data points. The topographic modelling is automatically carried out by the program when you invert the data set. The program will automatically adjust the surface of the finite-element grid used to model the subsurface so that it matches the surface of the sediment below the water layer. Figure 18 shows the apparent resistivity pseudo section and inversion model for the LAKELELIA.DAT data set where all the electrodes are underwater. Mobile surveying systems typically produce survey lines that are very long compared to the depth of investigation of the cable array system used.

Table 21. Example data file for aquatic survey with bottom electrodes.

HAT_HEAD.DAT file	*Comments*
LR5 Marine	*Title*
2.5	*Unit electrode spacing*
1	*Array type, Wenner in this example*
392	*Number of data points*
0	*First electrode x-location of array is given*
0	*No IP data*
0 .0 2.5 20.445599	*First data point*
7.5 2.5 167.579387	*Second data point*
..	
..	*Same format for other data points*
..	
2.5 40 25.202095	*Last data point*
2	*Topography flag, surface distance used*
50	*Number of topography points*
0.0 2.36	*x-location and elevation of 1st topography point*
2.5 2.41	*x-location and elevation of 2nd topography point*
..	
..	*Same format for other topography points*
77.5 0.55	
80.0 0.00	*A few points below water surface*
82.5 0.05	
..	
122.5 2.51	*Last topography point*
1	*Indicates first electrode is at first topography data point*
0	*Flag for fixed regions, 0 for no fixed regions in this case*
1	*Flag to indicate aquatic survey with bottom electrodes*
0.18, 0.1, 0, 122.5, 1.5	*Resistivity, IP (if IP data exist in the data file), left and right limits of water layer, elevation of water surface*
1	*1 to indicate normal surface geometric factor used*
0,0,0,0	*Ends with a few zeros for other options*

Copyright 2025, Seequent

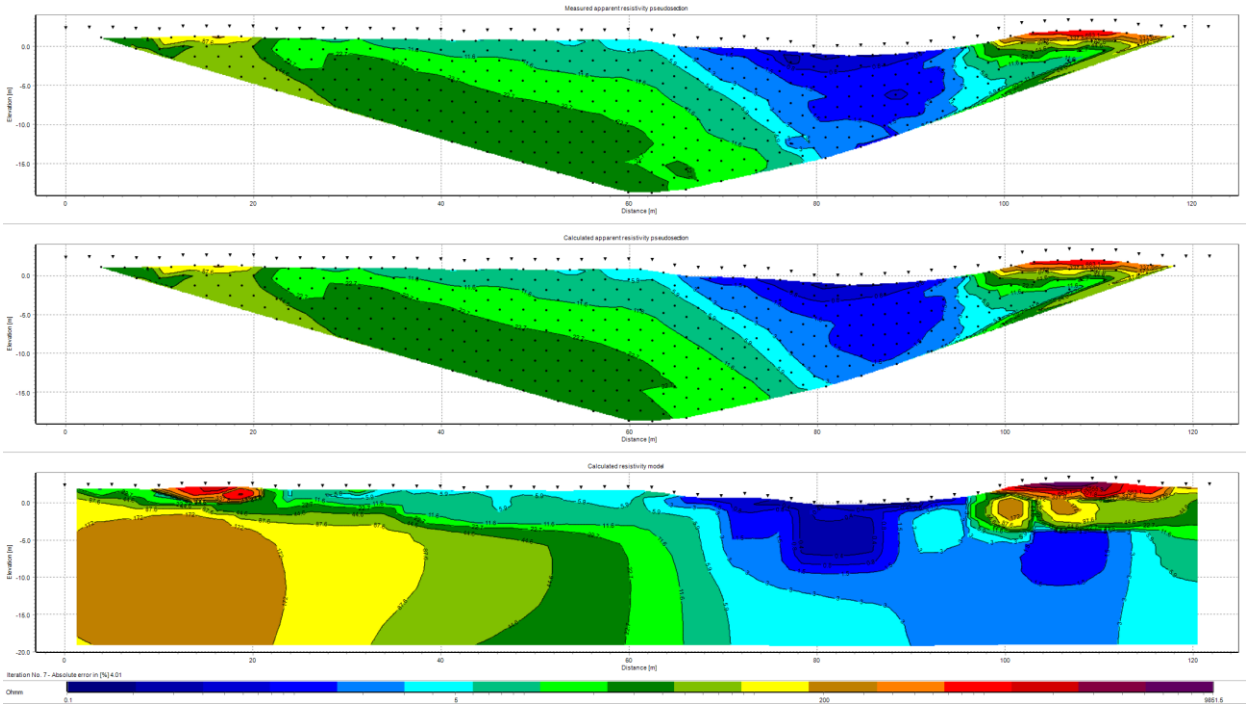

Figure 17. Hat Head land and underwater survey. (a) Apparent resistivity pseudo section (Wenner array) from the Hat Head tidal creek survey. (b) Calculated resistivity pseudo section and (c) the inversion model. Note the creek between the 65 meter and 95 meter have the electrodes are underwater.

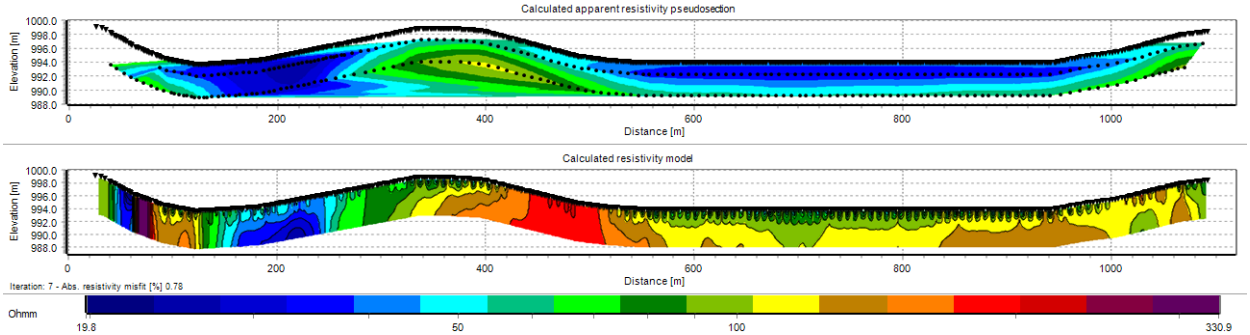

Figure 18. Lake Lelia underwater survey apparent resistivity pseudo section and model resistivity section. Courtesy of Technos Inc., USA.

Copyright 2025, Seequent

Table 22. Underwater survey data file in general array format.

LAKELELIA.DAT file	*Comments*
LAKE LELIA UNDERWATER SURVEY	*Title*
1.50	*Unit electrode spacing*
11	*General array type*
1	*Wenner sub-array*
Type of measurement (0=app. resistivity.1=resistance)	*Header*
0	*0 to indicate apparent resistivity given*
291	*Number of data points*
2	*Indicates surfaces x-distances*
0	*No IP data*
4 82.37,0.0 91.37,0.0 85.37,0.0 88.37,0.0 43.137	*First 4 data points in general*
4 89.55,0.0 98.55,0.0 92.55,0.0 95.55,0.0 36.599	*array data format. Note*
4 96.74,0.0 105.74,0.0 99.74,0.0 102.74,0.0 36.458	*value of 0.0 for electrode*
4 103.92,0.0 112.92,0.0 106.92,0.0 109.92,0.0 37.019	*elevation as it is listed later.*
..	*Similar format for other data*
..	*points*
4 1050.25,0.0 1077.25,0.0 1059.25,0.0 1068.25,0.0 93.072	*Last 2 data points*
4 1056.35,0.0 1083.35,0.0 1065.35,0.0 1074.35,0.0 95.383	
Topography in separate list	*Header to indicate elevation is given separately*
2	*2 to indicate surface x-distances*
38	*Number of topography data points*
26.12 999.09	*Topography x and z values*
..	
..	
1127.76999.09	
1	*First electrode coincides with first topography data point*
0	*0 for no fixed regions*
1	*1 indicates underwater survey*
58.00, 0.1, -2000.00, 2000.00, 1000	*Resistivity, IP (if IP data exist in the data file), left and right limits of water layer, elevation of water surface*
1	*Indicates surface geometric factor used for apparent resistivities*
0,0,0,0	*End with a few zeros*

Copyright 2025, Seequent

A possible situation where the water layer has a limited extent is shown as 'Case 4' in Figure 16. In this example the water is limited to the left side and is blocked by a barrier. Although some electrodes on the right side are below the water surface level, they are not covered by the water layer. Any electrode which is located outside the left and right limits of the water layer specified in the data file is assumed to be not covered by the water. An example data file is the DAM_SURVEY.DAT file (Table 23).

Table 23. Survey across a dam with only electrodes on the dam side underwater.

DAM_SURVEY.DAT file	*Comments*
Survey across a dam	*Title*
5.0	*Unit electrode spacing*
7	*Wenner-Schlumberger array type*
3025	*Number of data points*
0	*Indicates first electrode position given*
0	*No IP data*
0.0000, 5.0000, 1.00000, 13.2933	*First 4 data points in general*
5.0000, 5.0000, 1.00000, 11.5155	*array data format. Note*
10.0000, 5.0000, 1.00000, 10.4964	*value of 0.0 for electrode*
15.0000, 5.0000, 1.00000, 9.8681	*elevation as it is listed later.*
..	*Similar format for other data points*
540.0000, 5.0000, 1.00000, 24.8984	
..	
10.0000, 5.0000, 54.00000, 18.2645	*Last 2 data points*
0.0000, 5.0000, 55.00000, 18.1088	
2	*2 to indicate surface x-distances*
112	*Number of topography data points*
0.0000, 30.0000	*Topography x and z values*
..	
..	
555.0000, 0.0000	*Last topography point*
1	*1st electrode coincides with 1st topography data point*
0	*0 for no fixed regions*
1	*1 indicates underwater survey*
20.00, 0.1, 0.0, 130.0, 71.50	*Resistivity, IP (if IP data exist in the data file), left and right limits of water layer, elevation of water surface*
1	*Indicates surface geometric factor used for apparent resistivities*
0,0,0,0	*End with a few zeros*

Note in the above table, the right limit of the water layer (130.0 m) is much less than the right end of the line at 555.0 m. When the program reads in such a file where the limits of the water layer is less than the line coverage, it will automatically detect such a situation and display a 'Water layer has limited extent' message and set the proper inversion settings.

Another possible situation is shown in Figure 16 (case 5) where the electrodes are on a streamer suspended between the water surface and the bottom. The data format for this case is described in Appendix D.

(b) Stratified water layer

In areas near the coast, the water layer resistivity might have a significant variation with depth. A common situation that arises is a freshwater (higher resistivity) layer overlying a denser more saline (lower resistivity) near the bottom. In some surveys the depth to the water bottom might change significantly along the survey line that makes it important to include the variation of the water resistivity with depth in the model. The example file water-2-layers-diff-a6-n6.dat (Table 24) shows the data format used when there is more than one water layer. Note the slight change in the data format in the bottom section of the file to accommodate more than one water layer. It is assumed that the boundary between the layers is always horizontal. The program allows up to a maximum of 12 water layers that should be sufficient to model almost any water resistivity variation with depth. A field example where it was

Copyright 2025, Seequent

necessary to use more than 5 water layers to accurately model the water resistivity variation with depth in a survey across a river is described in Dahlin *et al.* (2014).

Table 24. Underwater survey data file with two water layers.

water-2-layers-diff-a6-n6.dat file	*Comments*
Model with two water layers	*Title*
1.00	*Unit electrode spacing*
3	*Dipole-dipole array type*
1143	*Number of data points*
1	*Indicates array mid-point given*
0	*No IP data*
1.500 1.000 1.000 32.0955	*First 2 data points*
3.500 1.000 1.000 32.2777	
..	*Similar format for other data*
..	*Points*
25.000 6.000 6.000 87.8598	*Last 2 data points*
26.000 6.000 6.000 87.6574	
2	*Topography flag 2 to indicate surface x-distances*
3	*Number of topography data points*
0.000, -4.000	*Topography x and z values*
25.500, -4.001	
50.000, -4.000	
1	*First electrode coincides with first topography data point*
0	*0 for no fixed regions*
Number of water layers	*Header to indicate more than 1 water layer*
2	*Shows 2 layers*
Layer 1 parameters	*Header for first water layer*
80.000, 0.1, -100.000, 200.000,0.000	*Resistivity, IP (if IP data exist in the data file), left and right limits of water layer, elevation at top of water layer*
Layer 2 parameters	*Header for second water layer*
50.000, 0.1, -100.000, 200.000, -1.620	*Resistivity, IP (if IP data exist in the data file), left and right limits of water layer, elevation at top of 2nd water layer*
1	*Indicates surface geometric factor used for apparent resistivities*
0,0,0,0	*End with a few zeros*

7.9.2 Surveys with floating electrodes

Another possible arrangement for an aquatic survey is a boat dragging a cable with the electrodes floating on the water surface. The main disadvantage of this arrangement is that a large part of the current flows within the water layer, compared to the portion of the current that flows into the material below the water bottom. The main advantage is that the survey is easier and faster to carry out and avoids problems such as the cable being snagged by obstacles on the river bottom. It could be an efficient method in shallow areas where the screening effect due to the water layer is not too large.

One possible way of interpreting such a data set is to treat it as a standard surface data set where the water layer is included as part of the model. This probably gives acceptable results where there is a strong contrast between the water layer and the topmost layer of the sub-bottom materials, and where the data has a low noise level.

However, if the depth of the water bottom was measured during the course of the survey (usually with an echo sounder), and the water resistivity was also measured, the effect of the water layer could be calculated and included in the model. The file WATER_FLOAT.DAT is a synthetic data set which gives an example of the data format. The initial part of the file is identical with that used for normal surface surveys or surveys with electrodes on the water bottom. The difference is in the final section of the file where the water layer parameters are given in Table 25. While this example gives the data in the general array format (section 7.2), the program can also accept data in the index-based format (section 7.1). Most systems for surveys with floating electrodes take measurements at a finer spacing compared to the

Copyright 2025, Seequent

spacing between the electrodes takeouts on the cable. Please refer to section 9.8 for methods to handle such data from mobile survey systems.

As a final note, it has been observed that in some data sets there is mismatch between the coordinates of the electrodes for the measurements and the bottom topography as measured using a profiler and a GPS system. This shows up when using the option to incorporate the water layer in the inversion model by a horizontal shift (usually of 5 to 10 meters) between the bottom topography and steep structures in the inversion model such as small gullies and peaks. This is probably due to differences in the locations of the depth sounder system and the cable with the electrodes.

In a 2-D data file, it is assumed that the survey line is straight. This might be difficult in some areas with strong water currents. If there are significant deviations in the direction of the line, it might be better to use the RES3DINV program to treat the survey as a 3-D data set.

Table 25. Survey data file with floating electrodes.

WATER_FLOAT.DAT file	*Comments*
Survey on water layer and floating electrodes	*Title*
2.0	*Unit electrode spacing*
11	*General array type*
0	*Non-specific sub-array*
Type of measurement (0=app. resistivity.1=resistance)	*Header*
0	*0 to indicate apparent resistivity given*
942	*Number of data points*
1	*Indicates true horizontal x-distances*
0	*No IP data*
4 2.0,0.0 0.0,0.0 4.0,0.0 6.0,0.0 1.86738	*First 3 data points in general*
4 4.0,0.0 2.0,0.0 6.0,0.0 8.0,0.0 1.86843	*array data format. Note water*
4 6.0,0.0 4.0,0.0 8.0,0.0 10.0,0.0 1.87070	*surface at 0.0 meter elevation*
..	
..	*Similar format for other data*
..	*points*
4 46.0,0.0 34.0,0.0 94.0,0.0 106.0,0.0 14.91776	*Last 2 data points*
4 48.0,0.0 36.0,0.0 96.0,0.0 108.0,0.0 15.51526	
0	*No topography information*
0	*No fixed regions*
3	*3 indicates floating electrodes survey*
Water resistivity	*Header*
1.5	*Water resistivity value*
Water elevation	*Header*
0.0	*Elevation of water surface*
18	*Number of water bottom depth points*
0 -1.5	*x-location and elevation of water*
10 -1.5	*bottom below water surface given*
20 -1.5	*for each point*
26 -1.5	
28 -2.0	
30 -2.5	
..	
..	*Similar format for other points*
..	
108 –1.5	*last depth point*
1	*Indicates first electrode is at first depth point*
0,0,0,0	*End with a few zeros*

Copyright 2025, Seequent

7.10 Incorporating boundaries of known layers

In some cases, the depth profile of a boundary between two layers with very different resistivity values is known from other sources; such as borehole data, seismic refraction or GPR surveys. Very frequently, there is a rapid and sharp change across the boundary, such as between a clay and sand layer. If the depth to the boundary is known, this information can be incorporated into the inversion so that the resistivities of the layers can be more accurately determined.

The file CLIFLAYER4.DAT is an example data file where the boundary between a gravel and underlying clay layer is known from a seismic refraction survey (Scott *et al.* 2000). Part of the file is shown in Table 26 with an explanation of the changes needed. In this example there are two boundaries. The program allows up to 30 boundaries that should be sufficient for almost all practical cases. The file MODEL_BOUNDARY_GENERAL.DAT gives an example of a data file with the general array format with only one boundary. Figure 19 shows the inversion of the CLIFLAYER4.DAT data set using different inversion options. The first model using the smooth inversion method (section 9.3.3) shows a gradational transition between the sand and underlying lower resistivity clay layer (Figure 19b). The depth to the boundary is not well determined. The use of the blocky or robust inversion method (section 9.3.3) gives a much sharper boundary (Figure 19c). The addition of the boundary from the seismic refraction survey helps to further sharpen the boundary (Figure 19d).

The greatest limitation of this option at present is that the depths to the layers are fixed throughout the inversion. An option to allow the depths to be automatically changed might be added in a future update.

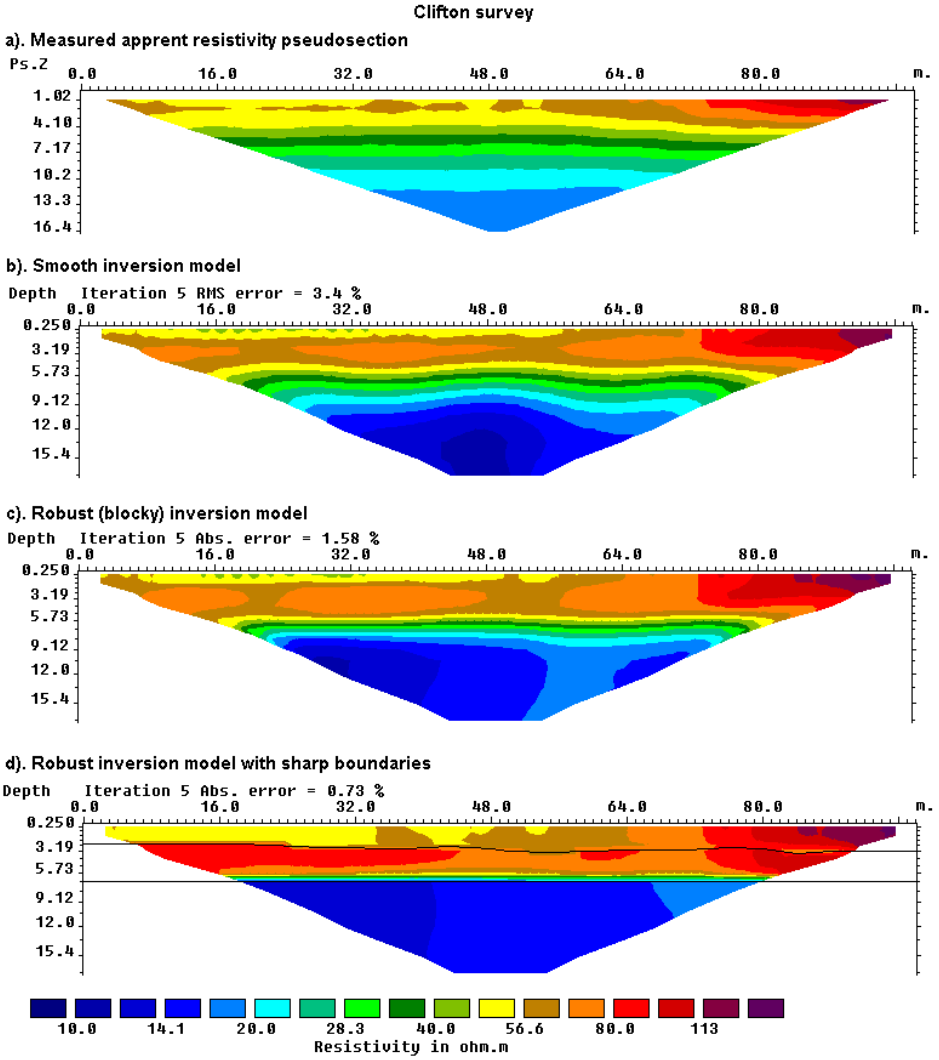

Figure 19. Models for the Clifton survey from the different inversion methods are shown together. Note the boundary between the high resistivity sand layer and the underlying low resistivity clay layer is much better resolved in the blocky and sharp boundary inversion methods.

Copyright 2025, Seequent

Table 26. Example survey data file with known boundaries.

CLIFLAYER4.DAT file	*Comments*
Clifton	*Title*
2	*Unit electrode spacing*
1	*Indicates Wenner array*
392	*Number of data points*
1	Type of x-location (center)
0	*No IP*
3 2 58.63305	*First data point in index-based format*
5 2 56.77204	*Second data point*
..	
..	*Other data points*
50 32 17.94035	*Last data point*
0	*No topography*
0	*No fixed regions*
0	*No aquatic survey*
Sharp layers present	*Header to indicate sharp boundaries present*
Number of boundaries	*Header*
2	*Number of boundaries, two in this case*
Boundary 1 parameters	*Header for first boundary*
Boundary type	*Header for type of boundary*
Layer	*Layer type*
Group weight	*Header for weight, for future use*
1.0	*Enter 1.0 here, not used at present*
Number of points on boundary	*Header*
16	*16 points for this boundary*
x and z coordinates of pts	*Header*
0.0 2.3	*x-location and depth of 1st point*
18.0 2.3	*x-location and depth of 2nd point*
..	
..	*x-location and depth of other points*
..	
92.0 3.2	*x-location and depth of last point*
Boundary 2 parameters	*Header for second boundary*
Boundary type	*Header for type of boundary*
Layer	*Layer type*
Group weight	*Header for weight, for future use*
1.0	*Enter 1.0 here, not used at present*
Number of points on boundary	*Header*
3	*3 points for this boundary*
x and z coordinates of points	*Header*
0.0 6.7	*x-location and depth of 1st point*
45 6.7	*x-location and depth of 2nd point*
92 6.7	*x-location and depth of 3rd point*
0,0,0,0	*End with a few zeros*

Copyright 2025, Seequent

7.10.1 Specifying and fixing resistivity of regions above and below a sharp boundary

In some special cases, the resistivity of the regions above and below the sharp boundary might be known or can be estimated. To estimate the resistivity, an inversion of the data set can be first carried out without the specifying the resistivity of the regions. A common situation is an insulating liner below a landfill. The material within the landfill can have relatively low resistivity values (such as about 100 ohm.m), and the main purpose of the survey is to map the resistivity variations in the landfill materials. The landfill liner might be essentially an insulating boundary where the current cannot penetrate through it, so the resistivity of the region below the liner can be considered more than several thousand ohm.m. This information can be incorporated into the inversion by specifying the depth profile of the liner and the resistivity of the region below it. The bottom part of an example data file is listed in Table 27. The 'Group Weight' value sets the damping factor for the region. A value of 1.0 means the resistivity is allowed to vary freely during the data inversion. A much higher value, such as 20.0, greatly reduces the variations allowed and essentially fixes the resistivity value. This ensures the resistivity of the selected region is kept fixed during the inversion, and in this example the program only changes the resistivity of the region above the boundary to fit the measured data.

Table 27. Example data file with sharp boundary and specified resistivity of regions above and below boundary.

Sharp-Boundary-Resistivity.dat file	*Comments*
21.00 6.00 5.00 325.20636	*Last*
22.00 6.00 5.00 317.22330	*three*
23.00 6.00 5.00 330.36230	d*ata points*
0	*Topography flag, 0=no topography*
0	*No fixed regions*
0	*No aquatic survey*
Sharp layers present	*Header to indicate sharp boundaries present*
Number of boundaries	*Header*
1	*1 boundary in this example*
Boundary 1 parameters	*Third coordinate point*
Boundary type	*Zeros to indicate other options,*
Layer	*such as fixed regions etc.*
Group Weight	
1.000	
Fix resistivity? (0=No,1=Yes)	
1	
Resistivity value	
100.0	
Number of points on boundary	
3	
x and z coordinates of points	
0.000, 4.740	
20.000, 4.741	
44.000, 4.740	
Fix resistivity of region below last boundary? (0=No,1=Yes)	
1	
Group Weight	
20.000	
Fix resistivity?	
1	
Resistivity value	
4000.0	
0,0,0,0,0	

Copyright 2025, Seequent

7.11 Global or GPS coordinates

Two-dimensional resistivity surveys are carried out with the electrodes arranged along a straight line. The coordinates of the electrode positions, and thus the subsurface model resistivity values, are given with respect to the ends of the line in the form of local coordinates. In order to incorporate the results in a map, the true coordinates (in terms of latitudes and longitudes, or northings and eastings) are required. The positions of points along the line can now be easily obtained using Global Positioning System (GPS) receivers. In order to obtain the true coordinates for the model values, the GPS coordinates must first be entered into the data file read by the RES2DINV program. The results can later be extracted from the XYZ file generated from the data inversion file.

The information concerning the GPS coordinates is given in the section immediately after the topography information in the data file. An example for a data file (without topography) using the index-based format for the resistivity data is given in the file BETA_GLOBAL.DAT. The section of the file containing the GPS information is shown in Table 28.

Table 28. Example data file with global coordinates.

BETA_GLOBAL.DAT file	*Comments*
8.750 4.500 10.132	*Last*
7.500 5.000 9.601	*three*
8.000 5.000 9.601	d*ata points*
0	*Topography flag, 0=no topography*
Global Coordinates present	*Header to indicate GPS information present*
Number of coordinate points	*Header*
3	*Number of coordinate points*
Local Longitude Latitude	*Header*
0.0 20.0 10.0	*First coordinate point given as* *Local position along line, GPS Longitude, GPS Latitude*
8.0 26.93 14.0	*Second coordinate point*
15.5 33.42 17.75	*Third coordinate point*
0	*Zeros to indicate other options,*
0	*such as fixed regions etc.*
0	*not present*

An example for a data file with topography using the index-based format is given in the file RATCHRO_GLOBAL.DAT. The section of the file containing the GPS information given after the topography section is shown in Table 29. The file IP_MAGUSI_MF_GLOBAL.DAT is an example of a data file with IP values as well the GPS information.

The file MIXED_GLOBAL.DAT and RATHMIX_GLOBAL.DAT are examples of data files using the general array format containing GPS coordinates. Both data sets have the topography information within each data point line. The section of the RATHMIX_GLOBAL.DAT with the GPS information is shown in Table 30. The file LAKELELIA_GLOBAL.DAT is an example with data in the general array format for an underwater survey with GPS coordinates. It also has the topography information in a separate list from the apparent resistivity data lines. Part of this file is shown in Table 31.

Copyright 2025, Seequent

Table 29. Example data file with index-based format and topography and global coordinates.

RATHCRO_GLOBAL.DAT file	*Comments*
..	*Initial section with main data section and*
..	*topography*
..	
92,-3.207	*Last*
94,-3.27	*Three topography*
96,-3.34	*data points*
1	*First topography point same as first electrode*
Global Coordinates present	*Header to indicate GPS information present*
Number of coordinate points	*Header*
3	*Number of coordinate points*
Local Longitude Latitude	*Header*
-36.0 80100.0 200300.0	*First coordinate point given as* *Local position along line, GPS Longitude, GPS Latitude*
20.0 80148.1 200327.8	*Second coordinate point*
96.0 80213.3 200365.4	*Third coordinate point*
0	*Zeros to indicate other options,*
0	*such as fixed regions etc.*
0	*not present*

Table 30. Example data file with general array format, topography and global coordinates.

RATHMIX_GLOBAL.DAT file	*Comments*
…	*Initial part with main data section*
4 60.0 -0.093 96.0 -3.34 72.0 -2.274 84.0 -2.914 1680.0	*Last apparent resistivity data point*
0	*Put zero for topography flag*
Global Coordinates present	*Header to indicate GPS information present*
Number of coordinate points	*Header*
3	*Number of coordinate points*
Local Longitude Latitude	*Header*
-36.0 80100.0 200300.0	*Local position along line, GPS Longitude and Latitude*
20.0 80148.1 200327.8	*Second coordinate point*
96.0 80213.3 200365.4	*Third coordinate point*
0	*Zeros to indicate other options,*
0	*such as fixed regions etc.*
0	*not present*

Copyright 2025, Seequent

Table 31. Example aquatic survey data file with global coordinates.

LAKELELIA_GLOBAL.DAT file	*Comments*
…	*Initial part with main data section*
Topography in separate list	*Header for topography information*
2	*Topography flag*
38	*Number of topography points*
26.12 999.09	*First topography point*
…..	*Other topography data points*
1127.76999.09	*Last topography point*
1	*1st topography point at 1st electrode*
Global Coordinates present	*Header to indicate GPS information present*
Number of coordinate points	*Header*
4	*Number of coordinate points*
Local Longitude Latitude	*Header*
26.0 100000.0 200000.0	*First coordinate point given as local position along line, GPS Longitude and Latitude*
126.0 100086.6 200086.6	*Second coordinate point*
500.0 100410.5 200237.0	*Third coordinate point*
1092.0 100923.2 200533.0	*Last coordinate point*
0	*Zeros to indicate other options,*
0	*such as fixed regions etc. not present*
1	*Indicates water layer present*
58.00,-2000.00,2000.00,1000,1	*The water layer information*
0,0,0	*End with a few zeros*

Copyright 2025, Seequent

7.12 Extending the model horizontal range

The program automatically sets the left and right ends of the model at the first and last electrode locations for surveys with surface electrodes only. In some situations, there might be large resistivity contrasts just beyond the ends of the survey line (Maurer and Friedel, 2006). This option allows the user to extend the horizontal range of the inversion model used by the program.

The data must be given in the general array data format (section 7.2) for this option to be used. The table below shows the data format using the example MIXEDWS_EXT2.DAT file.

Table 32. Example data file with extended model range.

MIXEDWS_EXT2.DAT file	*Comments*
Mixed array with extended model range	*Title*
1.0	*Unit electrode spacing*
11	*General array type*
7	*Sub-array type, Wenner-Schlumberger*
Type of measurement	*Header*
0	*Indicates apparent resistivity given*
Additional model blocks added beyond ends of survey line	*Header to indicate model extended beyond ends of line*
Number of additional blocks on both sides	*Header*
2	*Indicates 2 blocks added at both ends*
Positions of left additional blocks	*Header for left side*
-2.0,0.0	*x and z position of first extended point on left side*
-1.0,0.0	*x and z position of second extended point on left side*
Positions of right additional blocks	*Header for right side*
35.0,0.0	*x and z position of first extended point on right side*
36.0,0.0	*x and z position of second extended point on right side*
230	*Number of data points*
1	*True horizontal distance*
0	*No IP data*
4 0.0 0.0 19.0 0.0 9.0 0.0 10.0 0.0 10.644	*First data point*
4 1.0 0.0 20.0 0.0 10.0 0.0 11.0 0.0 10.281	*Second data point*
..	
..	*Same format for other data points*
0,0,0,0	*Ends with a few zeros for other options*

Note the format for the additional horizontal positions. Firstly, the *x* positions must be given starting from the left side, or the lowest value. The *z* positions must also be given. If there is no topography, a value of 0.0 is given as in the example. If there is topography, the elevation at the point must be given. The files RATCHMIX_Ext.dat and RATCMIX_Sep_Ext.dat are examples of the data format with topography.

Copyright 2025, Seequent

8 Data tab

All tools and functions in the Data tab are described on the Wiki page that can be accessed by pressing F1 when on the Data tab in Res2Dinv:

https://wiki.ags-cloud.dk/wiki/R2H_DataTab

8.1 Open data

The load option will open a file dialog to select a data file in the .dat format. Select the file to open the data.

8.2 Unsupported data types

RES2DINV version 2025.1 doesn't support:

- Offset pole-dipole array
- Equatorial dipole-dipole

These data types will be implemented in a future update.

8.3 Data Import

Clicking the Import option will show the following list of sub-options. Use this option to read in the raw data file from different instruments and convert the data into the .dat format used by RES2DINV. The supported formats are:

- Instrumentation GDD
- Iris Instruments – AGS format
- Iris Instruments – Binary format
- MAE .tsv
- OYO McOHM
  Zonge .dat
- Geosoft GDB
- AGI SuperSting
- ABEM Terrameter LS – db format

Copyright 2025, Seequent

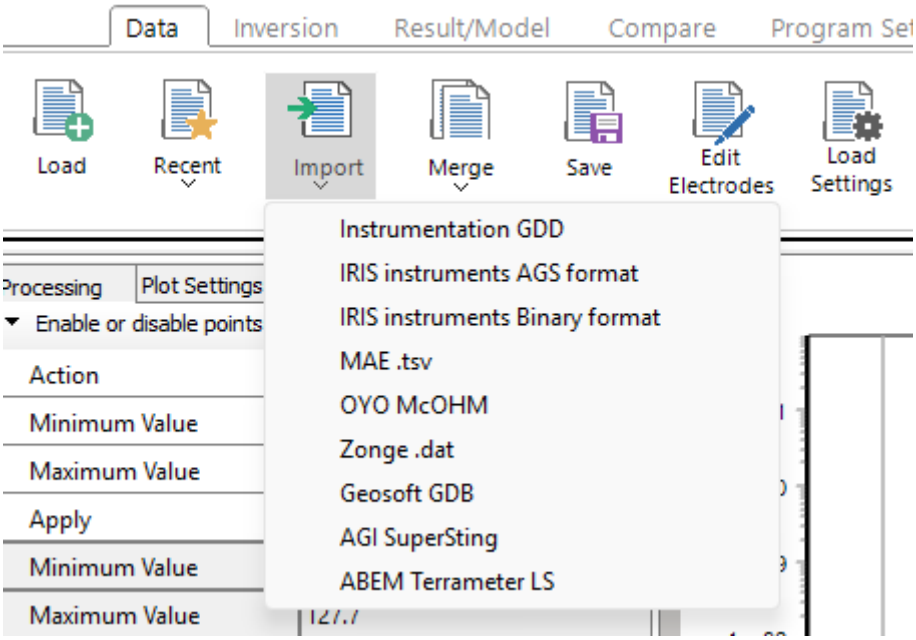

Importing data from Geosoft GDB format

The program supports import of ERT/IP data from a Geosoft GDB file. The importer assumes that the relevant data is present in channels with specific predefined names. For a successful import, at least the position of one current electrode and one potential electrode must be present in the database. These two channels must be named T1X and R1X, respectively. T1X is (true) horizontal position of first current (transmitter) electrode, and R1X is the position of the first potential (receiver) electrode. If only two channels with electrode positions are specified, it will be assumed that all measurements are pole-pole. Similarly, 3 or 4 electrode configurations can be imported if channels named R2X (second potential electrode) and/or T2X (second current electrode), respectively, are present.

Furthermore, it is required that apparent resistivities can be extracted directly or calculated from channels within the database. Apparent resistivities will be loaded directly from a channel named RHOA if present. Alternatively, if no RHOA channel is found, the program will look for two channels named VP and I, which will be assumed to contain measured potential and current (given in Volts and Ampere, respectively).

Topography can also be imported if channels named T1Z, R1Z, … etc. (corresponding to the existing x-position channels) are available. It is assumed that topography and x-position are given with respect to true horizontal coordinates (see above chapter on topographic data formats).

IP data can also be imported if a channel named CHG exists. Res2DInv assumes that such data is given in units of msec and is a result integrating the IP decay curve from 0.1 s to 1.0 s. If these settings need to be changed, they can easily be modified in the resulting .dat-file (see section 7.5).

If the source GDB is divided into multiple lines, the import procedure will generate one Res2DInv .dat-file for each line.

Importing from GDB files requires installation of a set of files. The steps needed for this are described in Appendix G.

Copyright 2025, Seequent

9 Inversion tab

This section covers all the model grid and inversion settings are described in the settings list. All tools and functions on the inversion tab are describe on the Wiki page that can be accessed by pressing F1 when on the Inversion tab in Res2Dinv:

https://wiki.ags-cloud.dk/wiki/R2H_InversionTab

9.1 Discretization

This set of options control the way the program subdivides the subsurface into rectangular cells. By default, the program uses a heuristic algorithm partly based on the position of the data points to generate the size and position of the model blocks. In the default algorithm used, the depth to the deepest layer in the model is set to be about the same as the largest depth of investigation of the data points, and the number of model cells does not exceed the number of data points. The thickness of each deeper layer is increased to reflect the decreasing resolution of the resistivity method with increasing depth. In general, this produces a model where the thickness of the layers increases with depth, and with thicker cells at the sides and in the deeper layers. For most cases, this gives an acceptable compromise. The distribution of the data points in the pseudo section is used as a rough guide in allocating the model cells, but the model section does not rigidly follow the pseudo section. However, the user can change the width and thickness of the cells using a variety of options. The following list of sub-options will be displayed when this option is expanded.

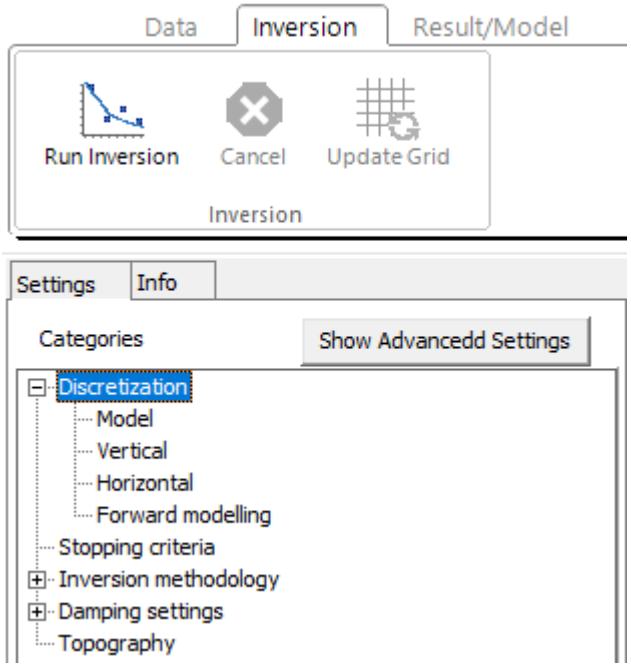

9.1.1 Model

These options will let Res2DInv discretize the model with a finer grid than the distribution of focus points.

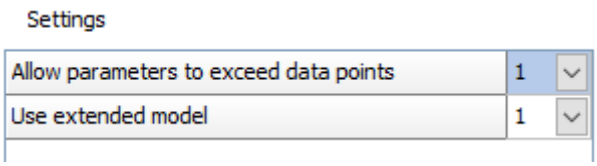

Copyright 2025, Seequent

9.1.1.1 Allow parameters to exceed data points

Allow Res2DInv to use a model where the number of model cells exceeds the number of data points. This is useful to avoid having a model with very wide cells near the bottom for data sets with very sparse data sets. Figure 20 shows such an example with this option enabled.

9.1.1.2 Use extended model

With 'Use extended model' option, model cells of uniform thickness right up to the left and right edges of the survey line are used (Figure 20). A pseudo section is displayed as a trapezoidal shape because it is a crude approximation where each electrode configuration is assigned a focus point at which its apparent resistivity is plotted, as the deeper focus points requires greater electrode separation the trapezoidal shape is a result of this way of displaying data. An inversion, however, models the resistivity distribution under the profile in its entire length (also some distance beyond the profile) to find the distribution of resistivities that is most likely to result in the measured data. Therefore, the inversion result can easily contain information outside of the area covered by the pseudo section.

9.1.2 Vertical

With these options, you can set the thickness of the layers used in the inversion model by setting the thickness of the first layer and the rate at which the thickness of each successive deeper layer increases.

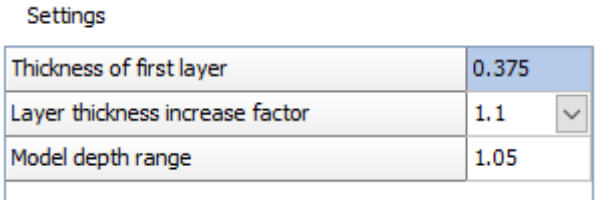

9.1.2.1 Thickness of first layer

Thickness of the first (most surface near) layer in the model as a fraction of the unit electrode spacing.
When Res2DInv reads in a data file, it will normally set the first layer thickness using the minimum pseudodepth of the data points.

9.1.2.2 Layer thickness increase factor

The rate at which the thickness of each successive deeper layer increases. For surface surveys, since the resolution decreases with depth, the thickness of the layers is normally increased by between 5 to 15 % with each deeper layer. This factor can be changed here. 1.1 equals 10%.

9.1.2.3 Model depth range

Res2Dinv normally uses a model where the depth to the deepest layer does not exceed the maximum pseudodepth in the data set. To use a model that spans a deeper depth range, you can change the factor to increase model depth range, for example from 1.05 to 1.30 to increase the model depth range by 30%.

9.1.3 Horizontal

With these options you can set the width of the cells used in the inversion model.

Copyright 2025, Seequent

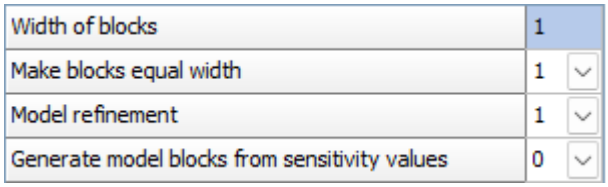

9.1.3.1 Width of blocks

This option allows the user to use model cells that are wider than one unit electrode spacing for all the layers. It is mainly intended for data collected from mobile surveys where a cable with fixed electrodes positions is dragged along during the survey. The distances between the measurement points are often much less than the spacing between the electrode takeouts.

9.1.3.2 Make blocks equal width

Ensure that all the cells have the same width that is equal to the unit electrode spacing.
Figure 20 shows three possible arrangements of the model blocks for the same data set.

9.1.3.3 Model refinement

RES2DINV by default uses a model where the width of the interior model blocks is the same as the unit electrode spacing. This works well in most cases. In situations with large resistivity variations near the ground surface better results can be obtained by using narrower model cells.
This option allows you to choose model cells with widths of half the unit electrode spacing. In almost all cases, this gives the optimum results. By setting this to 0.5, RES2DINV will automatically reduce the unit electrode spacing it uses by half of that given in the data file. Another method is to modify the data file directly using a text editor. The unit electrode spacing is given in the second line of the apparent resistivity data file. For example, the first few lines of the PIPESCHL.DAT file are reproduced in Table 33. In the second data line, the unit electrode spacing is given as 1.0 meter that is the actual spacing used in this survey. When RES2DINV reads in this data file, it will set the width of the model cells to 1.0 meter. The file PIPESCHL_HALF.DAT has the same data except that the unit electrode spacing is now defined as 0.5 meter. The upper part of this file is shown in Table 34.

When RES2DINV reads this file, it will set the model blocks to 0.5 meter width. Figure 21 shows the inversion models for this data set using cells with widths of 1.0 and 0.5 meter. The model with the 0.5 meter block width is able to more accurately model the high resistivity anomalies near the surface between the 3 and 12 meter marks above the pipe, and thus has a slightly lower apparent resistivity RMS data misfit. In most cases with large resistivity variations near the surface, using a model with a cell width of half the actual unit electrode spacing is sufficient. In some cases, using a narrower cell width of one-third or one-quarter the unit might be justified, particularly if the survey was carried out using a pole-dipole or dipole-dipole array with very high '*n*' factors. If the cell width is one-quarter the true unit electrode spacing, or less, oscillations in the model resistivity values in the first few layers can occur. Thus, the use of a cell width of less than one-quarter the true unit electrode spacing is not advisable.

Table 33. Data file with standard unit electrode spacing.

PIPESCHL.DAT file	*Comments*
Underground pipe survey	*Title*
1.00	*Unit electrode spacing*
7	*Wenner-Schlumberger array*
173	*Number of data points*
1	*Mid-point given for x-location*
0	*No IP*
1.50 1.00 1 641.1633	*First data point*
0.0	*Coordinates of the first electrode*
..	*The rest follows the usual data format*

Copyright 2025, Seequent

Table 34. Data file with half the standard unit electrode spacing.

PIPESCHL_HALF.DAT file	*Comments*
Underground pipe survey	*Title*
0.50	*Half the actual unit electrode spacing*
7	*Wenner-Schlumberger array*
173	*Number of data points*
1	*Mid-point given for x-location*
0	*No IP*
1.50 1.00 1 641.1633	*First data point*
0.0	*Coordinates of the first electrode*
..	*The rest follows the usual data format*

Copyright 2025, Seequent

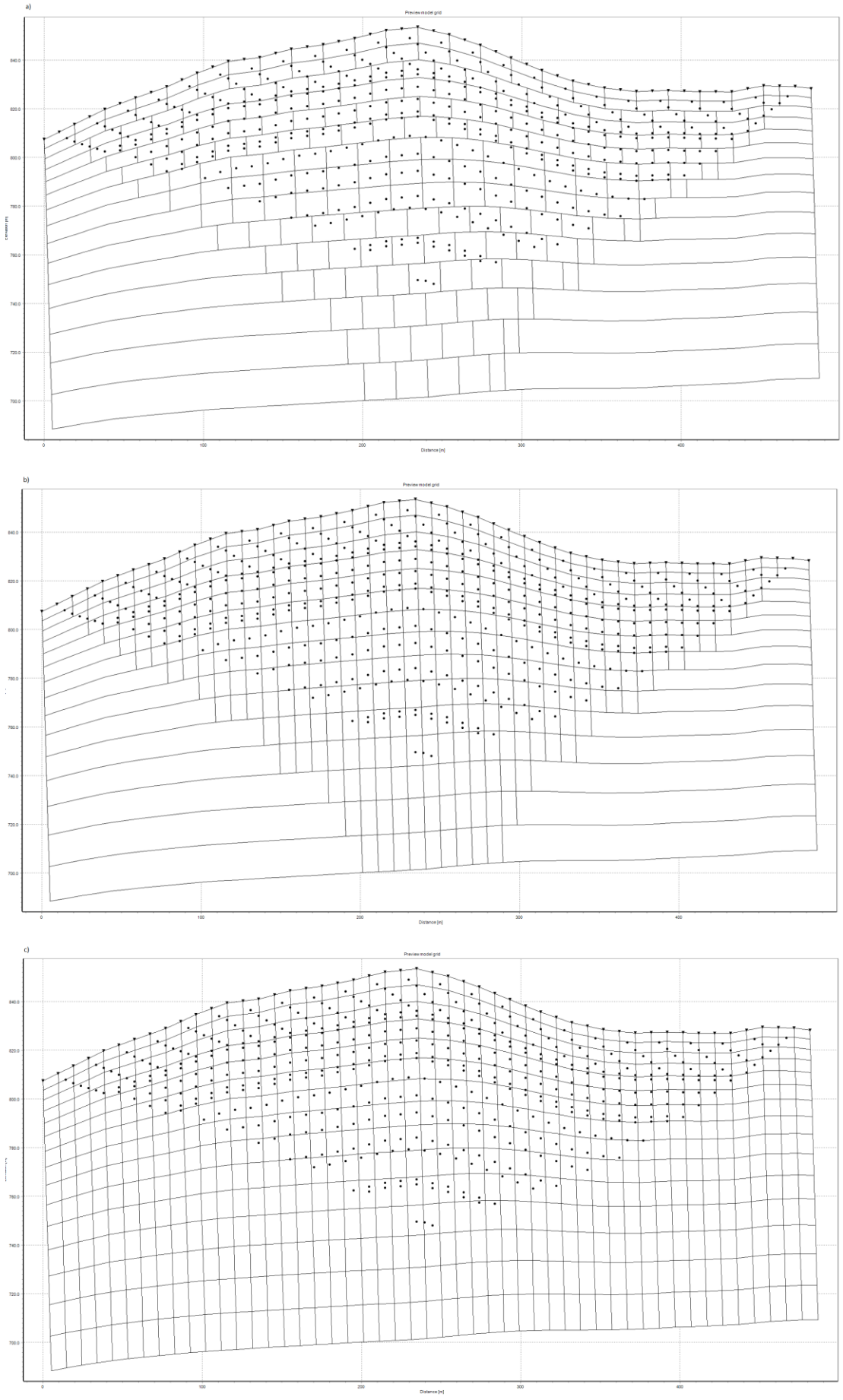

Figure 20. Different possible arrangement of model blocks for the same data set. (a) Using wider blocks at sides and bottom, (b) blocks of equal width, (c) model blocks extended to ends of survey line.

Copyright 2025, Seequent

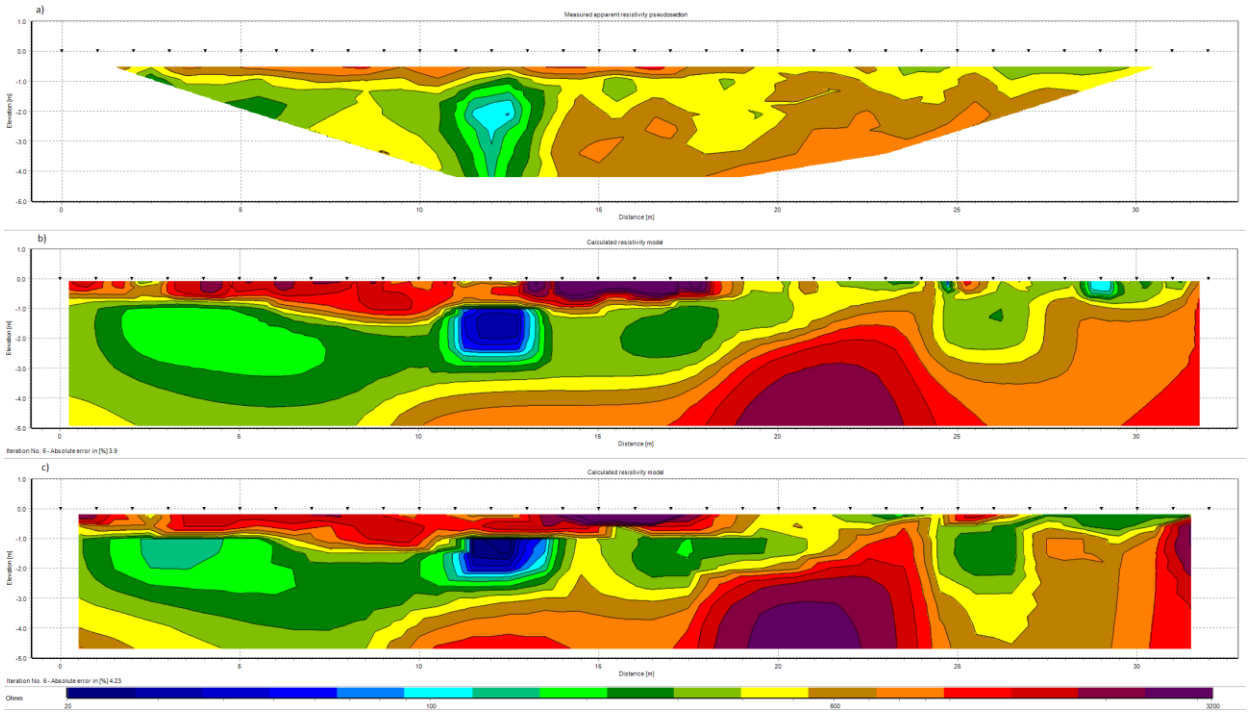

Figure 21. Example of inversion models using the standard and half-sized model blocks. (a) The apparent resistivity pseudo section for the PIPESCHL.DAT data set. The inversion models using (b) blocks with a width of 1.0 meter that is the same as the actual unit electrode, and (c) using narrower blocks with a width of 0.5 meter.

9.1.3.4 Generate model blocks from sensitivity values

This option allocates the arrangement of the blocks in the model using the sensitivity values as a guide. The model created using the sensitivity values increases the width of the blocks near the sides in the deeper parts of the model section in order to increase the sensitivity values of the blocks.

9.1.4 Forward modelling

Settings for the model grid during forward calculations.

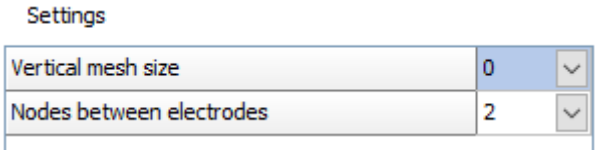

9.1.4.1 Vertical mesh size

This option allows you to use a finer mesh (in the vertical direction) for the finite-difference or finite-element method (2). The model for a survey line on the surface normally uses a finer mesh for the top two layers, and a single mesh line for the deeper layers. This option allows the use of a finer mesh for the deeper layers. The apparent resistivity values calculated will be more accurate with a finer mesh, but the computer time and memory required will be greater. The use of a finer mesh can give better results for cases where subsurface resistivity contrasts of greater than 20:1 is expected. This is particularly useful in areas where a low resistivity layer lies below a high resistivity layer.

Copyright 2025, Seequent

9.1.4.2 Horizontal mesh size

You can choose a mesh grid used by the forward modeling program to have 2 or 4 nodes between adjacent electrodes (Figure 22). With 4 nodes per electrode spacing, the calculated apparent resistivity values would be more accurate (particularly for large resistivity contrasts). However, the computer time and memory required are correspondingly larger. By default, the program will use the 2 nodes option if the data set involves more than 90 electrode positions. In normal surveys with electrodes planted into the ground, the spacing between adjacent electrodes is usually the same as the minimum spacing between two electrodes used in an array. In surveys using a mobile cable system or a streamer in aquatic surveys, the spacing between adjacent electrodes along the survey line can be several times smaller than the minimum spacing between two electrodes used in an array used for the measurements. For such data sets, the '1 node' option can be used to reduce the calculation time and memory required by the forward modeling routine.

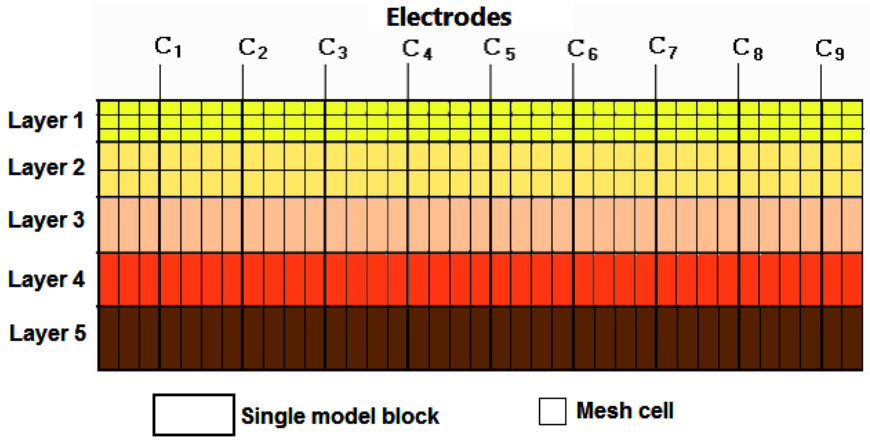

Figure 22. Schematic diagram of mesh and model cells used by forward modeling routine. This example has 4 nodes between adjacent electrodes.

9.2 Stopping criteria

With these settings, it is possible to set the criteria for when an inversion should stop and display the model results.

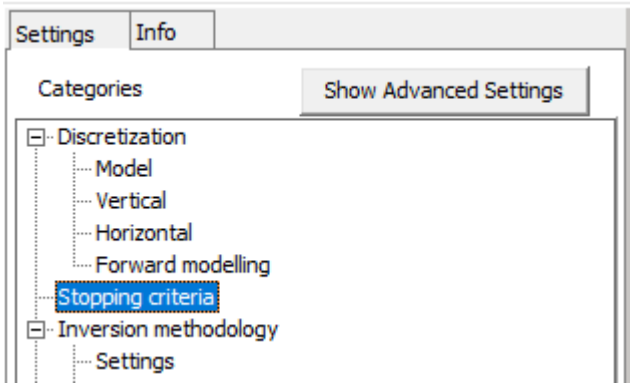

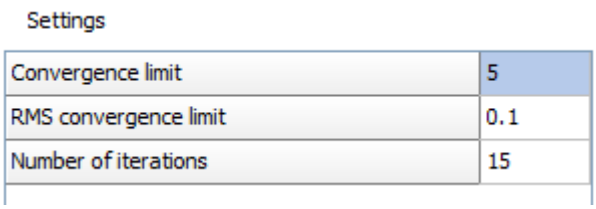

9.2.1 Convergence limit

The relative change in the RMS error between 2 iterations. By default, a value of 5% is used. This is used to accommodate different data sets with different degrees of noise present.

Copyright 2025, Seequent

9.2.2 RMS convergence limit

The RMS data misfit. This sets the percentage RMS error in the inversion of the apparent resistivity data where the program will stop after the model produced has an RMS error less than this limit. Normally a value of between 1% and 5% should be used, depending on the quality of the data.

9.2.3 Number of iterations

This allows the user to set the maximum number of iterations for the inversion. By default, the maximum number of iterations is set to 15. For most data sets, this is probably sufficient.

9.3 Inversion methodology

The following set of options control the path the inversion subroutine takes during the inversion of a data set. The sub-options menu is shown below. The settings marked with a * is advanced settings which we recommend not to change.

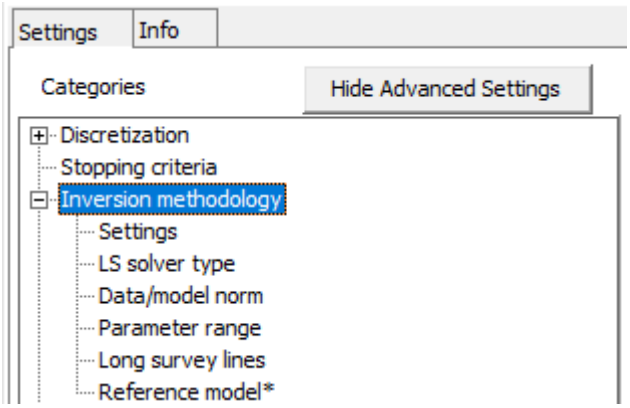

9.3.1 Settings

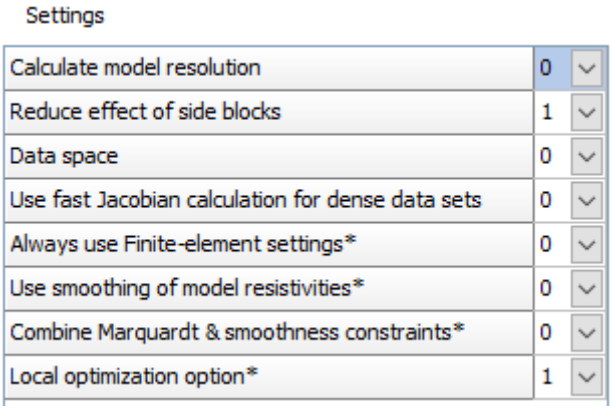

9.3.1 Calculate model resolution

The model resolution matrix is given by

$$\mathbf{R} = (\mathbf{J}^T\mathbf{J} + \lambda \mathbf{F})^{-1} \mathbf{J}^T\mathbf{J} \qquad (11.5)$$

The model resolution of the model blocks are given by the diagonal elements of this matrix. The model resolution matrix **R** may be viewed as a filter through which the inversion method attempts to resolve the subsurface resistivity (Day-Lewis *et al.* 2004). In the ideal case with perfect resolution, the elements of the main diagonal (R_{jj}) are 1.0 while the off-diagonal elements are 0.0. In practice, the model resolution values for most model blocks are much less than 1.0. The time taken to calculate the model resolution matrix is proportional to the cube of the number of model blocks, so it is probably only practical to carry

Copyright 2025, Seequent

out the calculations for models with less than about 30000 blocks. It is probably not practical to calculate the resolution values due to computer time and memory limitations for very large data sets and models. You can enable the calculation of the model resolution values, as well as the point-spread function (Oldenborger and Routh, 2009), using the following dialog box. This gives a measure of how widely the information from a region of the subsurface is spread out to the surrounding model cells in the inverse model.

9.3.1.1 Reduce effect of side blocks

This option affects the calculation of the Jacobian matrix values for the model blocks located at the sides and bottom of the model section. Normally, for a block located at the side, the contributions by all the mesh elements associated with the model block are added up right to the edge of the mesh. This gives a greater weight to the side block compared to the interior blocks. In some cases, particularly when the robust inversion option is used, this can result in unusually a high or low resistivity value for the side block. This option limits the contribution of the mesh elements outside the ends of the survey line to the Jacobian matrix values for the side blocks. The following dialog box shows the different degrees the contribution of the cells outside the survey line to the Jacobian matrix values are truncated. If this option is used, it is recommended to also use the “Make blocks equal width” under the Horizontal Discretization setting.

For borehole data this setting is automatically set to disabled because it will give better model results for borehole data.

9.3.1.2 Data space

By default, Res2Dinv will use the logarithm of the apparent resistivity values as the data parameter when carrying out the inversion. For most cases, this gives the best results. In some cases, for example with negative or zero apparent resistivity, this is not possible, and the linear data space needs to be used.

For borehole data this setting is automatically set to linear as negative resistivities can more often occur during the inversion for borehole data.

9.3.1.3 Use fast Jacobian calculation for dense data sets

This option uses an optimized routine for calculating the Jacobian matrix values for data sets where the number of data points is much greater than the number of electrodes used in making the measurements. It uses an alternative algorithm to calculate the Jacobian matrix values which can be significantly faster than the standard routines (up to 41.8). As a guide, this option should only be used when the expected reduction is more than 20%. Note for some very sparse data sets, this routine can be even slower than the standard method.
If this option is selected, the first two settings “Optimize Jacobian matrix” and “Use fast method to calculate Jacobian matrix” in the “Long survey line” settings will be disabled in the inversion.

9.3.1.4 Always use Finite-element settings*

RES2DINV allows you to use either the finite-difference or finite-element method to calculate the apparent resistivity values. By default, it will use the finite-difference method which is faster if the data set does not contain topography. If the data set contains topography, RES2DINV will automatically use the finite-element method.

9.3.1.5 Use smoothing of model resistivities*

Copyright 2025, Seequent

Apply the smoothness constraint on the model change vector alone, or also on the model resistivity values. Applying the smoothness constraint on the model change vector alone modifies equation (4.1) to the following form which is used by some researchers (Sasaki 1992)

$$(\mathbf{J^T J} + \lambda \mathbf{F}) \Delta \mathbf{q_k} = \mathbf{J^T g_k} \qquad (11.1)$$

where $\Delta \mathbf{q_k}$ is the model parameter change vector.

9.3.1.6 Combine Marquardt & smoothness constraints*

Combining the damped least squares method with the smoothness-constrained method, is intended for use in unusual situations where the data sensitivity values of the model blocks are significantly distorted by large resistivity variations. It modifies the least-squares equation to the following form.

$$(\mathbf{J^T J} + \lambda (\mathbf{F+I})) \Delta \mathbf{q_k} = \mathbf{J^T g} - \lambda \mathbf{F q_{k-1}} \qquad (11.2)$$

In some situations, such as a survey over a very low resistivity body, the current paths could be distorted such that parts of the subsurface are not well mapped and have very low data sensitivity values in the inversion model. This could lead to large distortions just below the low resistivity body. By combining the Marquardt (or ridge regression) and Occam (or smoothness-constrained) inversion methods, the distortions in some cases might be reduced. This option should be used as a last resort if everything else fails! It seems to give better results in resolving compact structures where the width and thickness are slightly smaller than the depth, such as a cave or ore-body whose size is just slightly less than its depth.

9.3.1.7 Local optimization option*

The inversion routine determines the change in the model parameters $\Delta \mathbf{q}$ from solving equation (4.1). It attempts to find the optimum amplitude for the parameter change vector $\Delta \mathbf{q}$ using quadratic interpolation if this option is enabled.

9.3.2 LS solver types

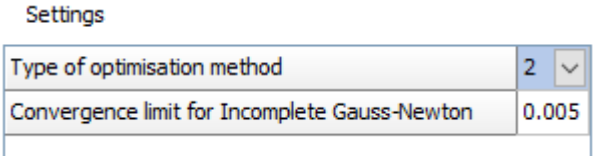

9.3.2.1 Type of optimization method

This option allows you to choose two different methods to solve the least-squares equation (4.1).

The ‘Standard Gauss-Newton least-squares method, that calculates an exact solution of the least-squares equation, should be used if the number of data points and/or model cells is small (less than a few thousand). If the number of data points and/or model cells is large (more than a few thousand), the time taken to solve the least-squares equation could be the most time-consuming part of the inversion process. To reduce the inversion time, an alternative method that calculates an approximate solution of the least-squares equation using the ‘Incomplete Gauss-Newton’ method can be used. This uses an iterative linear conjugate-gradient method to solve the least-squares equation.

9.3.2.2 Convergence limit for Incomplete Gauss-Newton

Set the convergence accuracy of the solution. For most data sets, an accuracy of about 1% (i.e., a convergence limit of 0.01) seems to provide a solution that is almost the same as that obtained by the ‘Standard Gauss-Newton’ method. Setting a higher accuracy, for example 0.5%, will in theory give a result that is even closer to the ‘Standard Gauss-Newton’ method but this is at the expense of a longer inversion time. The incomplete Gauss-Newton method has an option to scale the matrices in order to improve the convergence of the iterative method used.

Copyright 2025, Seequent

9.3.3 Data/model norm

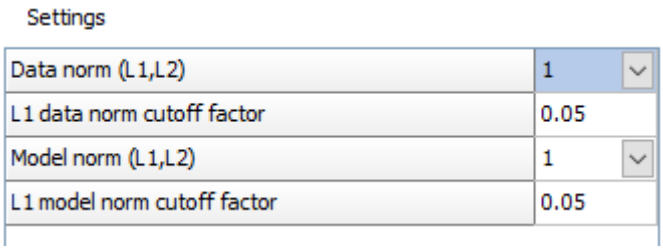

9.3.3.1 Data norm (L1, L2)

This allows you to select the smooth (L2 norm) or the robust/blocky (L1 norm) inversion method.

The conventional least-squares method, L2 norm, ('standard data constraint') will attempt to minimize the square of difference between the measured and calculated apparent resistivity values. This method gives reasonable results if the data contains random or “Gaussian” noise. However, if the data set contains “outlier” data points (where the noise comes from non-random sources such mistakes or equipment problems), this method is less satisfactory. Such “outlier” data points could have a great influence on the resulting inversion model. To reduce the effect of such “outlier” data points, the L1 norm method ('robust data constraint') inversion method where the absolute difference (or the first power) between the measured and calculated apparent resistivity values is minimized can be used (Claerbout and Muir 1973).

9.3.3.2 L1 data norm cutoff factor

There is a cut-off factor which controls the degree in which the L1 constrain is used. If a value of 0.05 is used, this means the effect of data points where the differences in the measured and calculated apparent resistivity values are much greater than 5 percent will be greatly reduced.

9.3.3.3 Model norm (L1/L2)

The conventional smoothness-constrained least squares method (deGroot-Hedlin and Constable 1990) also attempts to minimize the square of the changes (L2 model norm) in the model resistivity values. This will produce a model with a smooth variation in the resistivity values. Such a model is more suitable where subsurface resistivity also changes in a smooth manner (Loke *et al.* 2003). However, if the subsurface bodies have sharp boundaries, such as the soil-bedrock interface or massive homogeneous bodies, the conventional least-squares smoothness-constrain method tends to smear the boundaries. If the robust model constrained inversion method (L1 model norm) is used, the program will attempt to minimize the absolute changes in the resistivity values. This constraint tends to produce models with sharp interfaces between different regions with different resistivity values, but within each region the resistivity value is almost constant. This might be more suitable for areas where such a geological situation exists, such as the soil-bedrock interface.

As an example, Figure 233 shows the inversion results for a synthetic model with a faulted block (with a resistivity of 50 ohm.m) in the bottom-left side and a small rectangular block (1 ohm.m) on the right side within a surrounding medium with a resistivity of 10 ohm.m. A test data set was generated for the Wenner array (Figure 233a). The model produced by the standard least-squares method has a gradational boundary for the faulted block (Figure 233b). In comparison, the model produced by the robust model inversion method has sharper and straighter boundaries (Figure 233c). A field example with sharp boundaries was shown earlier in Figure 14 for the Magusi River resistivity and IP data set. The main structure, the massive sulphide ore body, by nature has a distinct and sharp resistivity/IP contrast with the surrounding igneous/metamorphic country rocks.

Copyright 2025, Seequent

9.3.3.4 L1 model norm cutoff factor

There is a cut-off factor which controls the degree in which this robust model constrain is used. If a large value is used, for example 1.0, the result is essentially that of the conventional smoothness-constrained least-squares inversion method. If a very small value is used, for example 0.001, the result is close to the true L1-norm inversion method.

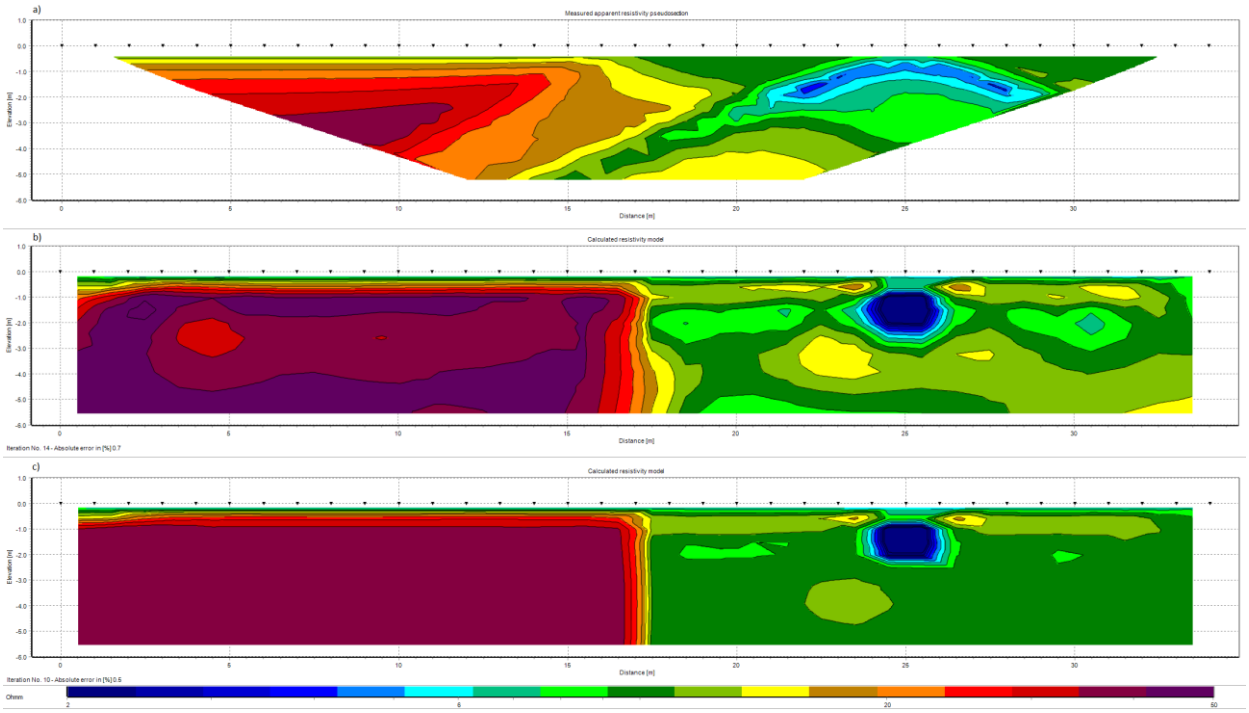

Figure 23. Example of inversion results using the smooth and robust inversion model constraint. (a) Apparent resistivity pseudo section. The inversion models produced by (b) the conventional least-squares smoothness-constrained method (L2) and (c) the robust or blocky inversion method.

9.3.4 Parameter range

Settings

Limit resistivity values	0
DC Upper limit factor	50
DC Lower limit factor	0.02
IP Lower Limit	0
IP Upper Limit	900

9.3.3.1 Limit resistivity values

This option allows you to limit the range of resistivity values that the inversion will give.

9.3.3.2 DC upper limit factor

A value of e.g., 50 gives the upper limit 50 times the average model resistivity value for the previous iteration.

9.3.3.3 DC lower limit factor

A value of e.g., 0.5 gives the lower limit 0.5 times the average model resistivity value for the previous iteration (1/20 times).

Copyright 2025, Seequent

Res2Dinv uses “soft” limits that allow the actual resistivity model values to exceed these limits to a certain degree. However, this option will avoid extremely small or large model resistivity values that are physically unrealistic.

9.3.3.4 IP upper limit

This sets the upper limits of the model IP values that the inversion can use. Although in theory IP values can range up to 1000 mV/V, in practice it is unlikely to be more than a few hundred mV/V.

9.3.3.5 IP lower limit

This sets the lower limits of the model IP values that the inversion can use. The minimum model IP value is usually set at zero, although there have been reports of negative intrinsic IP values (Brandes and Acworth 2003).

9.3.4 Long survey lines

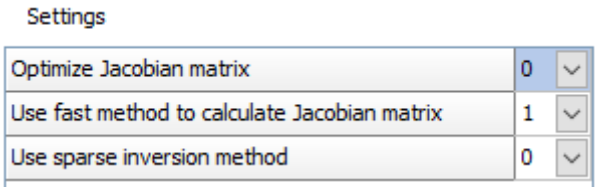

9.3.4.1 Use fast method to calculate Jacobian matrix

Use an optimized method to calculate the Jacobian matrix. This can significantly reduce the calculation time without affecting the accuracy of the values and should give the same inversion model as the default method.

9.3.4.2 Use fast method to calculate Jacobian matrix

Use a fast method to calculate the Jacobian matrix by excluding the model cells that are far away from the electrodes used in an array. The Jacobian matrix values and thus the inversion model will be slightly different from that obtained using the standard method, but the difference is normally small (less than 5%).

9.3.4.3 Use sparse inversion method

Using sparse inversion techniques, is intended for long survey lines with 500 electrodes positions or more. This method will still produce a contiguous model along the entire survey line but takes advantage of the sparse nature of the Jacobian matrix to reduce the number of calculations needed. The results will be slightly different (usually less than 5%) from that obtained using the standard method.

9.3.5 Reference model*

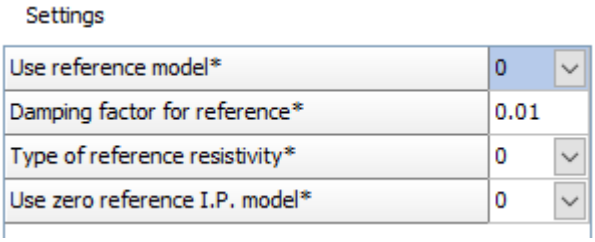

Copyright 2025, Seequent

9.3.5.1 Use reference model*

A background reference model helps to stabilize the inversion model by reducing large departures from a fixed resistivity value. A homogeneous reference model will be used.

The least-squares equation (4.1) minimizes a combination of the model smoothness and the data misfit. Sometimes, an additional constraint is used where the model must be 'close' to some reference model as shown below.

$$(\mathbf{J}^T\mathbf{J} + \lambda (\mathbf{F}+\mu\mathbf{I})) \Delta\mathbf{q}_k = \mathbf{J}^T\mathbf{g} - \lambda\mathbf{F}\mathbf{q}_{k-1} - \lambda\mu (\mathbf{q}_{k-1} - \mathbf{q}_m) \quad (11.3)$$

9.3.5.2 Damping factor for reference*

An additional damping factor μ that controls the degree where the inversion model is 'close' to a reference model $\mathbf{q}_m$ is used. The reference model is usually a homogeneous half-space model.

9.3.5.3 Type of reference resistivity*

By default, the program will use the average of the apparent resistivity values as the constant resistivity reference model. However, this reference resistivity value can be manually set by the user.

9.4 Damping settings

This list of settings controls the damping factor, λ in equation (4.1), used in the smoothness-constrained least-squares inversion equations.

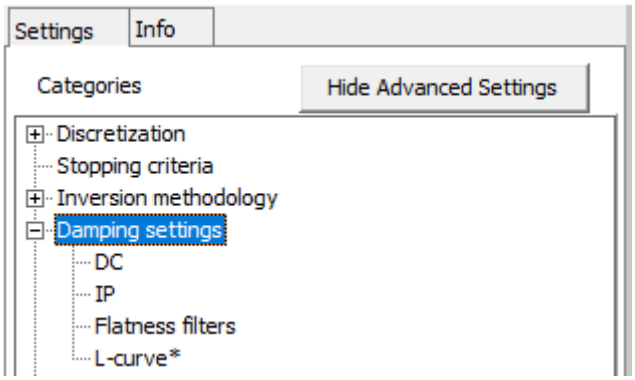

9.4.1 DC

Settings

Initial damping factor	0.15
Minimum damping factor	0.02
Enable first layer damping	0
Extra damping factor for first layer	4
Damping factors for changes in distance between blocks	1
Adjust damping factors for changes in distance between	1
Increase of damping factor	1.05
Automatic calculation of damping factor with depth	0

9.4.1.1 Initial damping factor

You can set the initial value for the damping factor λ in equation (4.1), as well as the minimum damping factor. The inversion program automatically reduces the damping factor by about half after each

Copyright 2025, Seequent

iteration until it reaches the selected minimum value. If the data set is very noisy, you should use a relatively larger damping factor (for example 0.3). If the data set is less noisy, use a smaller initial damping factor (for example 0.1).

9.4.1.2 Minimum damping factor

The inversion subroutine will generally reduce the damping factor but a minimum limit for the damping factor must be set to stabilize the inversion process. The minimum value should usually set to about one-tenth to one-fifth the initial damping factor value.

9.4.1.3 Enable first layer damping

For some data sets, particularly when the Model refinement option under Horizontal Discretization is used to select a model with narrower blocks, the first few layers can show a rippling effect. This can be reduced by using a higher damping factor for the first layer.

9.4.1.4 Extra damping for first layer

Only applies if above setting is on, defines how much extra damping is applied to first layer.

9.4.1.5 Damping factors for changes in distance between blocks

There is usually less data near the ends of the survey line, so an option to use higher damping factor for the model cells at the sides of the model is used.

9.4.1.6 Adjust damping factors for changes in distance between blocks

This option allows the user to adjust the damping factor for the different layers to take into account changes in the distances between the model cells.

9.4.1.7 Increase of damping factor

Since the resolution of the resistivity method decreases exponentially with depth, the damping factor used in the inversion least-squares method is normally also increased with each deeper layer in order to stabilize the inversion process. Normally, the damping factor is increased by 1.05 times with each deeper layer, but you can change it. Use a larger value if the model shows unnatural oscillations in the resistivity values in the lower sections. This will help to suppress the oscillations.

9.4.1.8 Automatic calculation of damping factor with depth

You can also select the choice to allow the program to determine the value to increase the damping factor with depth automatically. This might be a good choice if the thickness of the layers is much thinner than the default values, for example if you had reduced the unit electrode spacing by half in the data file in order to produce a model with smaller model blocks.

9.4.2 IP

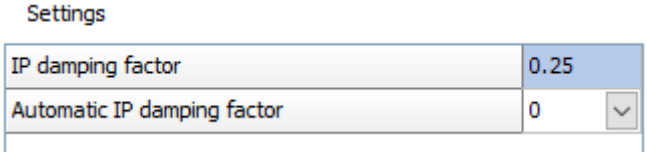

9.4.2.1 IP damping factor

This setting controls the amplitude of the change in the model IP values allowed after each iteration. A smaller IP damping factor can be used to allow a greater change in the IP model values (which is

Copyright 2025, Seequent

normally much smaller than the change in the model resistivity values in the joint inversion method). If a value of 1.0 is used, then the same damping factors will be used for both the resistivity and IP inversion routines. Normally a much smaller value of about 0.10 to 0.25 is used.

9.4.2.2 Automatic IP damping factor

Automatic estimate the IP damping factor from the Jacobian Matrix.

9.4.3 Flatness filters

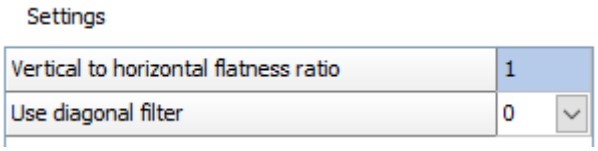

9.4.3.1 Vertical to horizontal flatness ratio

You can select the ratio of the damping factor for the vertical flatness filter ($\mathbf{f_z}$) to the horizontal flatness filter ($\mathbf{f_x}$). By default, the same damping factor is used for both. However, if the anomalies in the pseudo section are elongated vertically, you can force the program to produce models that are also elongated vertically by selecting a higher value (for example 2.0) for the ratio of the vertical to horizontal flatness filter. For anomalies that are elongated horizontally, choose a smaller value (e.g. 0.5).

9.4.3.2 Use diagonal filter

The normal roughness filter used has components in the *x* and *z* directions only (Figure 24a). Thus, it has a tendency to produce structures aligned along the x and z directions. To reduce this effect, the roughness filter used can be modified so that it has components in the diagonal directions (Farquharson, 2008) as well (Figure 244b).

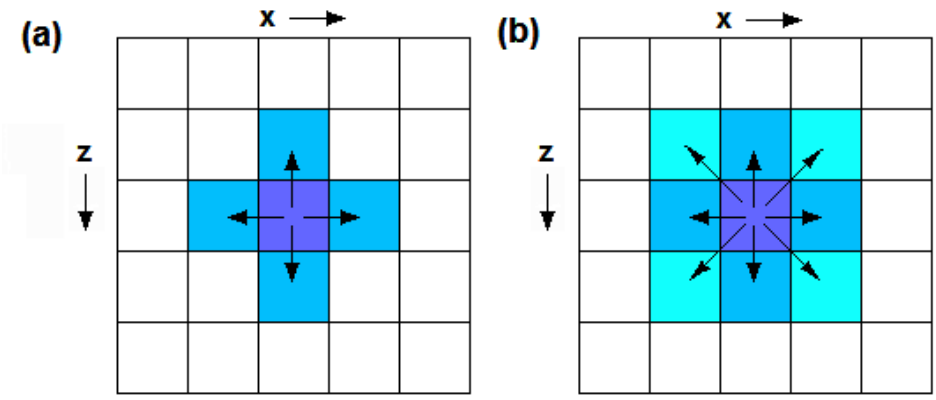

Figure 24. Types of roughness filters. (a) Horizontal and vertical components only. (b) Diagonal components as well.

9.4.4 L-curve*

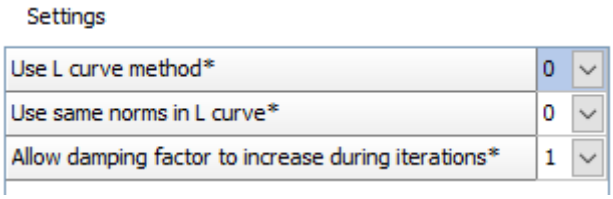

Copyright 2025, Seequent

9.3.4.1 Use L-curve method*

In this option, the optimum damping factor is automatically determined by the program using the L-curve method (Farquharson and Oldenburg 2004). This method essentially estimates the data misfit and the model roughness for a large range of the damping factor values. On selecting this option, the following dialog box is shown.
The L-curve method assumes the data misfit and the model roughness changes in a smooth manner with the damping factor so that a unique point of maximum curvature is obtained (Figure 23). In some cases, particularly with very large resistivity contrasts near the surface, the standard model discretization (where the width of the model cell is the same as the unit electrode spacing) can result in small ‘kinks’ in the curve. To reduce the effect of any single model cell on the total model roughness, it is recommended that the ”Model refinement” setting in Discretization is set to 0.5.

9.4.4.2 Use same norm in L-curve*

This option is only relevant if you use the “Robust” or L1-norm method in the "Data/model norm" setting. This option allows you to use the same L1-norm method within the L-curve routine or use the standard L2-norm method.

9.4.4.3 Allow damping factor to increase during iterations*

For rare cases where the damping factor increases after an iteration. This option allows the user to ensure it does not increase.

In RES2DINV, the damping factor values tested range from 0.01 to 100 times the trial value. Figure 25a shows the variation of the model roughness with the data misfit for the BLUERIDGE.DAT data set for damping factor values ranging from 0.000295 to 2.95. Figure 25b shows a plot of the curvature of the curve against the damping factor value. The optimum value is selected at the point with the maximum curvature value. The calculations are carried out internally by the program for a range of damping factor values. In this example, the trial value used is 0.0295 while the optimum value calculated is 0.0142.

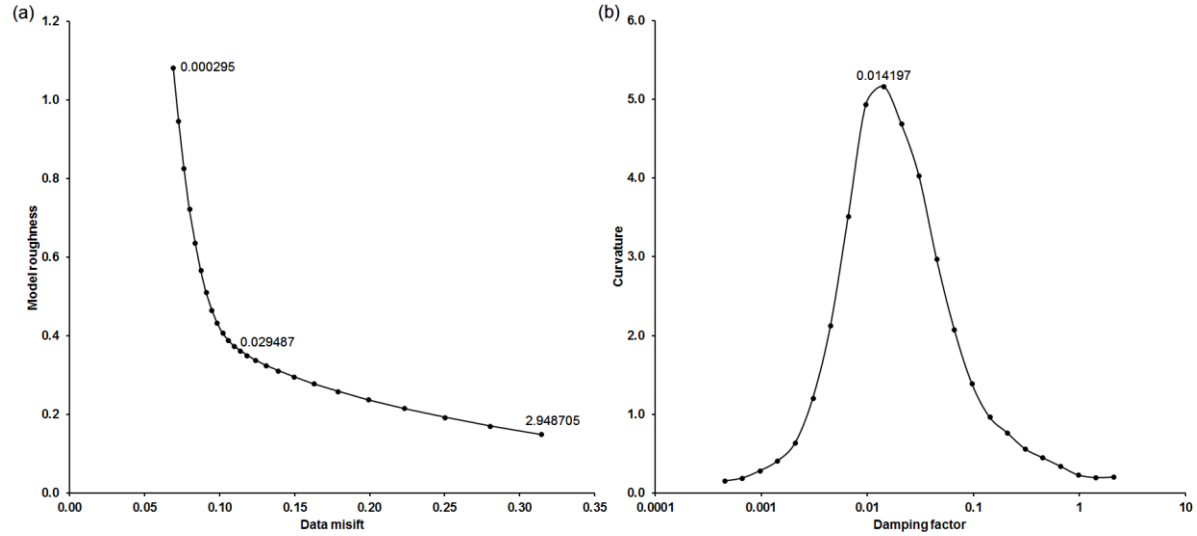

Figure 25. Example L-curve plot to determine the optimum damping factor for the BLUERIDGE.DAT data set. (a) Variation of model roughness with data misfit for a range of spatial damping factor values (a few values are shown near the corresponding points), (b) variation of the curvature of the L-curve with the damping factor.

9.5 Topography

Copyright 2025, Seequent

If there is significant topographical relief along the survey line, the effect of the topographical effects can be accounted for if the horizontal and vertical coordinates of a number of points along the survey line are known. When RES2DINV reads in a data file with topography data it will automatically select the finite-element method that incorporates the topography into the modelling mesh used. In this case, the topographic modelling will be automatically carried out by RES2DINV when you invert the data set

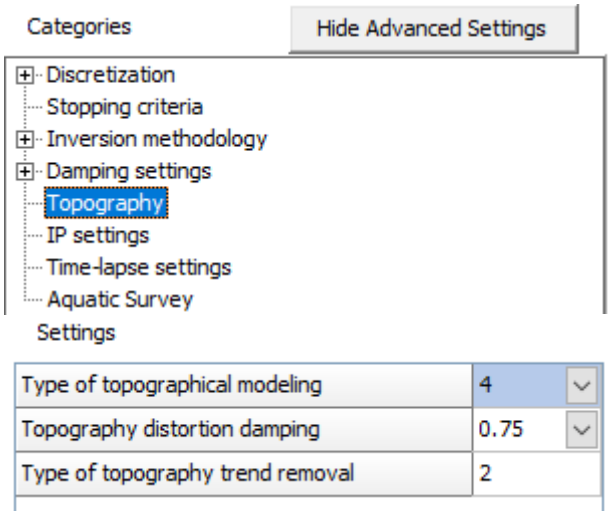

9.5.1 Type of topography modelling

Distorted finite-element grid with uniform distortion: This method, and the next two methods, use a distorted finite-element grid such that the surface nodes of the mesh match the actual topography. This gives more accurate results than the older method of using the correction factors for a homogeneous earth model calculated with the finite-element method (Fox *et al.* 1980) which can cause distortions in cases where large resistivity variations occur near the surface (Tong and Yang 1990; Loke 2000). In this option, the nodes below the surface (and thus also the model layers) are shifted to the same extent as the surface nodes.
Distorted finite-element grid with damped distortion: In this option, the subsurface nodes are shifted to a lesser extent compared with the surface nodes, i.e., the effect of the topography is "damped" with depth. This option is probably a reasonable choice if the curvature of the topography is less than the depth of the deepest model layer. A damping factor that controls the degree of damping with depth (Figure 27) can be modified by the user.
S-C transformation with distorted finite-element grid: This method uses the Schwarz-Christoffel transformation method to calculate the distortion in the subsurface layers. It is probably the best method that produces a more 'natural' looking model section in cases with a comparatively large topography curvature. In such cases, the damped topography approach might produce unusually thick model layers under areas where the topography curves upwards. In some unusual cases where the topography has very sharp acute peaks or valleys and sparse topography data points, the Schwarz-Christoffel transformation method might not work. If this happens, add a few extra topography data points near the places with a sharp curvature in the topography.

Figure 26 shows an example of an inversion model for the Ratchrogan Mound (Waddell and Barton 1995) data set that has topography from Ireland. The burial chamber is the prominent high resistivity region a few meters below the surface below the 20 meters mark. The L1-norm inversion method was used to sharpen the burial chamber and the surrounding soil. A unit electrode spacing of 2 meters was used during the survey, but the inversion model uses model blocks of 1 meter width due to significant lateral variations near the surface.

Copyright 2025, Seequent

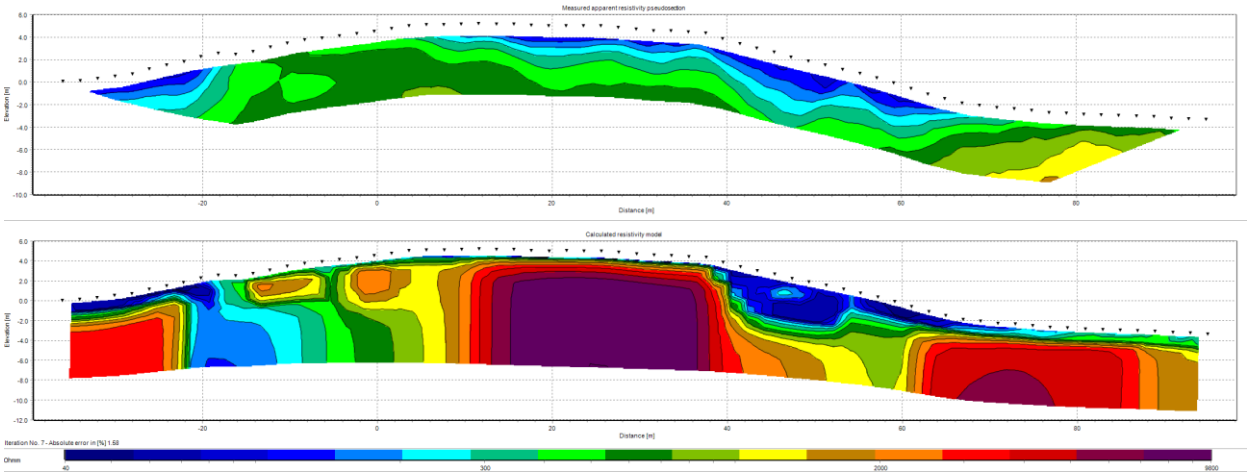

Figure 26. Example of the model for the Rathcrogan Mound data set. (a) Measured apparent resistivity pseudo section. (b) Inverse model section with topography.

Copyright 2025, Seequent

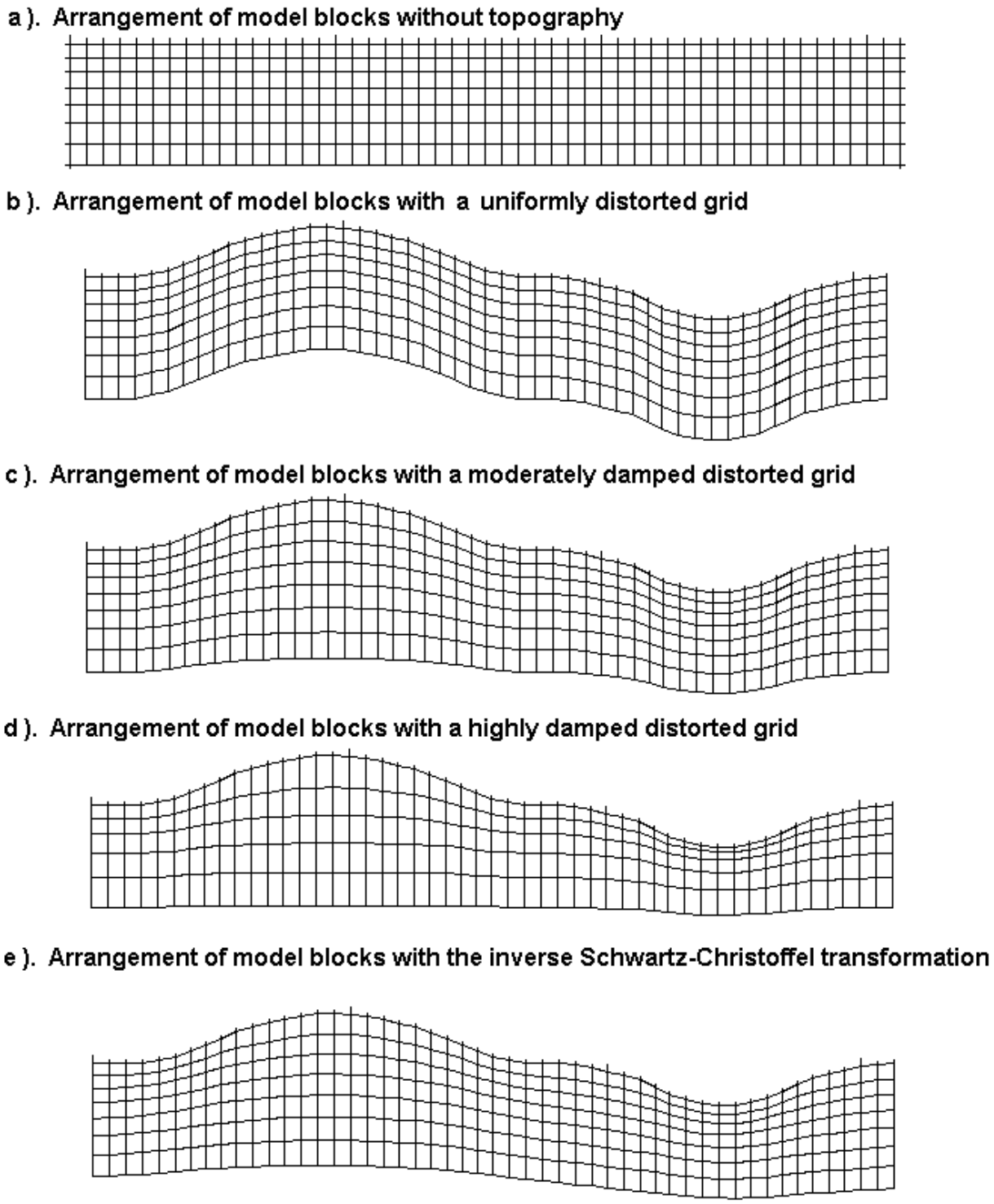

Figure 27. Different methods to incorporate topography into a 2-D inversion model. (a) Schematic diagram of a typical 2-D inversion model with no topography. Model mesh discretization with a distorted grid to match the actual topography where (b) the subsurface nodes are shifted vertically by the same amount as the surface nodes, (c) the shift in the subsurface nodes is gradually reduced with depth or (d) rapidly reduced with depth, and (e) the model obtained with the inverse Schwartz-Christoffel transformation method.

Copyright 2025, Seequent

9.5.2 Topography distortion damping

Set the degree damping factor with depth.

9.5.3 Type pf topography trend removal

You can choose to remove the average elevation, a least-squares linear trend, or a straight line joining the first and last topography data points. If the ground surface along the survey line is generally flat except for a few points, use the option to subtract a constant value from the heights of the electrodes locations. If the survey points are on a slope, choose either a least-squares or an end-to-end straight line for the linear trend. Figure 28 shows an example with topography where the end-to-end straight line trend was removed.

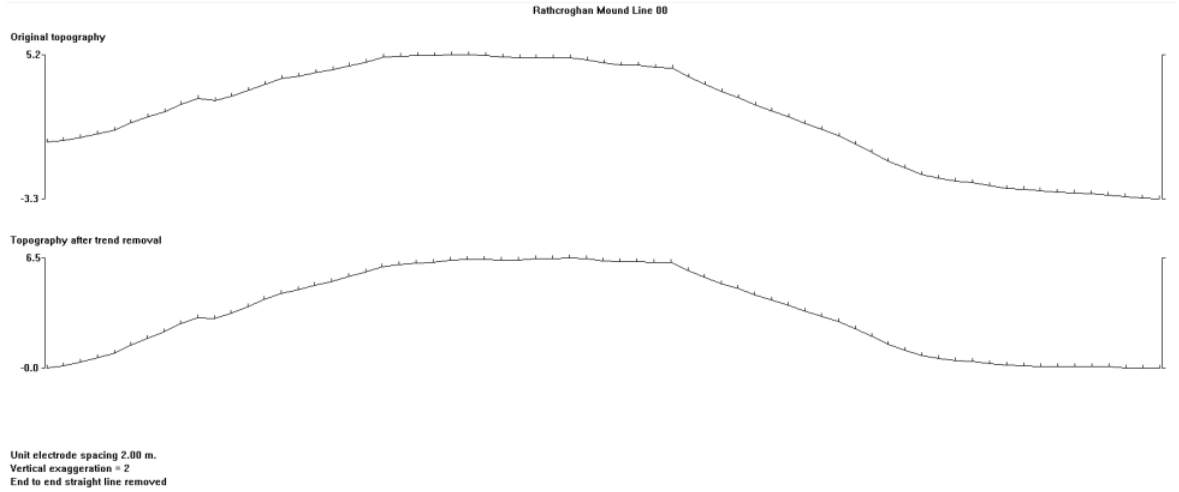

Figure 28. Topography linear trend removal for the Rathcrogan mound data set.

Copyright 2025, Seequent

9.6 IP settings

This list of settings will cover a number of options for the inversion of data sets with IP measurements.

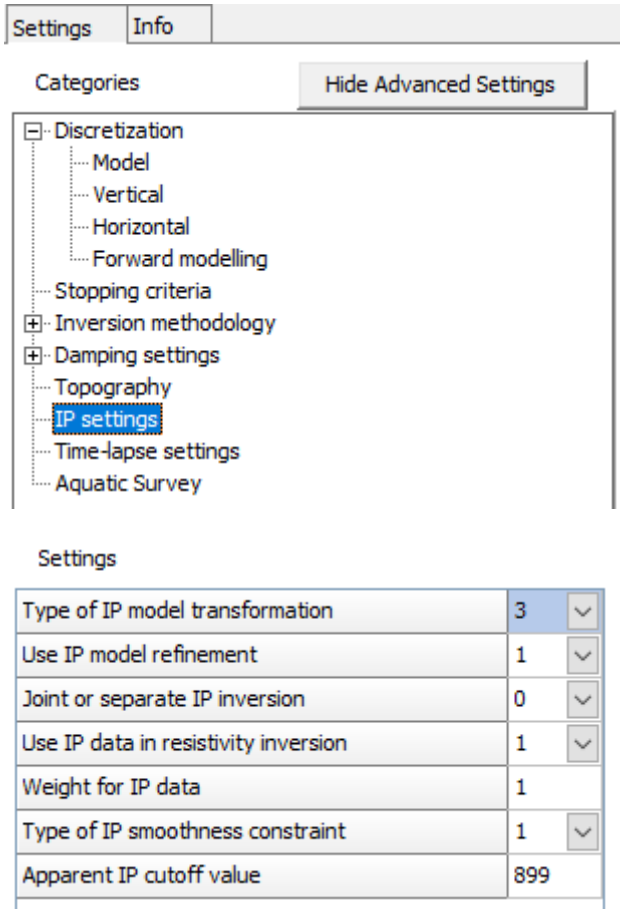

9.6.1 Type of IP model transformation

The ‘Square-root’ or ‘Range bound’ is normally used to ensure the model IP values produced by the inversion program do not exceed the allowed limits. The ‘Square-root’ transformation ensures that the model IP is always positive but does not directly set an upper limit. The ‘Range bound’ method ensures that the model IP values are restricted to the range set in the ‘Parameter range’ option under Inversion methodology.

9.6.2 Use IP model refinement

It is recommended that the IP refinement step is used for most data sets.

RES2DINV uses the complex resistivity method for the inversion of IP data (Kenma *et al.* 2000). The effective conductivity is treated as a complex quantity with real and imaginary components. The complex conductivity is given by:

$$\sigma = \sigma_{DC} - i\, m\sigma_{DC} \tag{11.6}$$

The DC conductivity σ_{DC} forms real part, while $m\sigma_{DC}$ forms the imaginary part. A complex potential is then calculated for this complex model:

$$\phi = \phi_r + i\, \phi_i \tag{11.7}$$

Copyright 2025, Seequent

The complex potential has two components, ϕ_r and ϕ_i. The real (resistivity) and complex (IP) potentials are calculated simultaneously. The inversion method calculates the optimum resistivity and IP models simultaneously using the same least-equation (4.1). In many data sets, the resistivity data misfit has a much larger range than the IP data misfit. This causes the inversion routine to determine a more accurate resistivity model at the expense of the IP model that might show a much smaller change with each iteration. To overcome this problem, after calculating the optimum resistivity and IP model through a joint inversion, a separate inversion to minimize the IP data misfit alone by changing the model IP values only (and keeping the model resistivity values fixed) is commonly carried out in each iteration. This option allows the user to select the IP model refinement step via the following dialog box.

9.6.3 Joint or separate of IP inversion

In the complex resistivity method, the inversion model resistivity together with model IP values are simultaneously calculated. This option allows the user to fix the IP model when the resistivity model is calculated. It then only changes the model IP values during the IP model refinement step which is automatically enabled when the separate inversion option is selected.

9.6.4 Use IP data in resistivity inversion

In the resistivity inversion step, the IP data has a small effect on the resistivity model. However, the effect can be completely removed by choosing the option not to use the IP data in resistivity inversion if the separate inversion option is selected.

9.6.5 Weight for IP data

This sets the weights given to the IP data and model in the joint resistivity-IP inversion method.

This program uses the complex resistivity method (Kenma *et al.* 2000) where the inversion of the apparent resistivity and IP data are inverted jointly. In most data sets, the data misfit for (the logarithm of the) apparent resistivity values have a much larger range than the apparent IP values. This causes the program to give a greater weight to reducing the data misfit for the apparent resistivity compared to the apparent IP The first parameter (weight for IP data) enables the user to compensate for this effect by giving a greater weight to the IP data misfit. The second parameter (IP damping factor) controls the amplitude of the change in the model IP values allowed after each iteration. A smaller IP damping factor can be used to allow a greater change in the IP model values (which is normally much smaller than the change in the model resistivity values in the joint inversion method). If a value of 1.0 is used, then the same damping factors will be used for both the resistivity and IP inversion routines. Normally a much smaller value of about 0.10 to 0.25 is used.

9.6.6 Type of IP smoothness constraint

Normally the program uses the same smoothness constraint for the IP inversion as that used for the resistivity inversion. This option allows you to use a different smoothness constraint for the IP inversion. If the ‘Robust’ (L1-norm) method is used for the resistivity inversion, this option allows you to use the ‘Smooth’ (L2-norm) method for the IP inversion. Selecting the L2-norm constraint for the IP model might be useful for some cases as it has a much smaller range compared to the resistivity values. In theory, the IP model and (magnitude of the) data are limited to values of 0 to 1000 mV/V.

9.6.7 Apparent IP cutoff value

Many modern resistivity meter systems used in engineering and environmental surveys now have IP measurement capability as well. However, the IP data from most multi-electrode systems is probably of limited use for electrode spacings of more than a few meters. Most systems use a battery power source that cannot deliver enough current (usually less than 1 Amp) for reliable IP signals, so the IP data is often extremely noisy. Although in theory the magnitude of measured apparent IP values can range up to 1000 mV/V, in practice natural IP effects produce much smaller values of usually less than

Copyright 2025, Seequent

00 mV/V. This option sets an upper limit on acceptable apparent IP values above which the values are not used by the program to calculate the IP inversion model.

9.7 Time-lapse settings

To study the changes of the subsurface resistivity with time, 2-D surveys are repeated over the same line at different times. Such studies include the flow of water through the vadose zone, changes in the water table due to water extraction (Barker and Moore 1998), flow of chemical pollutants and leakage from dams.

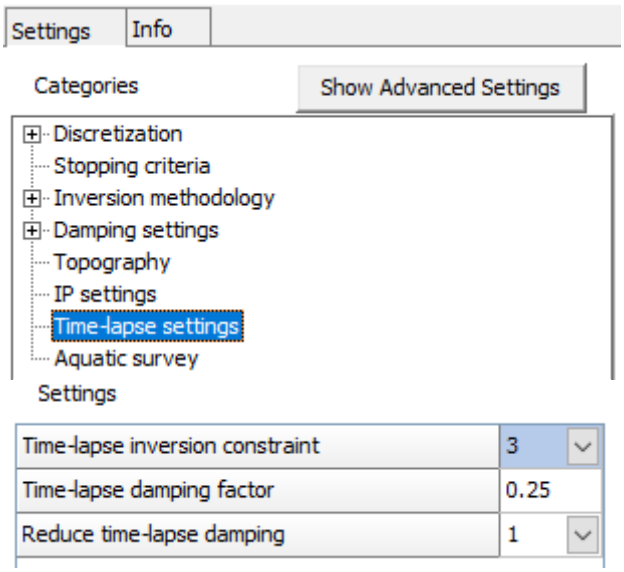

9.7.1 Time-lapse inversion constraint

Type of time-laspe inversion. No constraints make each time data set to be inverted independently. Modify the time-difference roughness filter to select smooth or blocky differences between the time models (Kim 2010; Loke *et al.* 2014).

9.7.2 Time-lapse damping factor

The time-lapse inversion equation (Kim *et al.* 2009, Loke *et al.* 2014) is given by

$$[\ \mathbf{J}^T\mathbf{J} + \lambda\,(\mathbf{F} + \alpha\mathbf{M}^T\mathbf{R}_t\mathbf{M})\ ]\ \Delta\mathbf{q}_k = \mathbf{J}^T\mathbf{g}_k - \lambda(\mathbf{F} + \alpha\,\mathbf{M}^T\mathbf{R}_t\mathbf{M})\mathbf{q}_{k-1} \qquad (11.4)$$

The relative importance given to minimizing the difference between models at different times is controlled by the time lapse damping factor α. A larger value of the time-lapse damping factor will force the different time models to be more similar but at the expense of a larger data misfit (Rucker *et al.* 2011a).

9.7.3 Reduce time-lapse damping

Reduce damping with 40% for each iteration.

9.8 Floating Electrodes

These settings are for data from a survey with floating electrodes where the thickness and resistivity of the water layer was measured during the survey.

Copyright 2025, Seequent

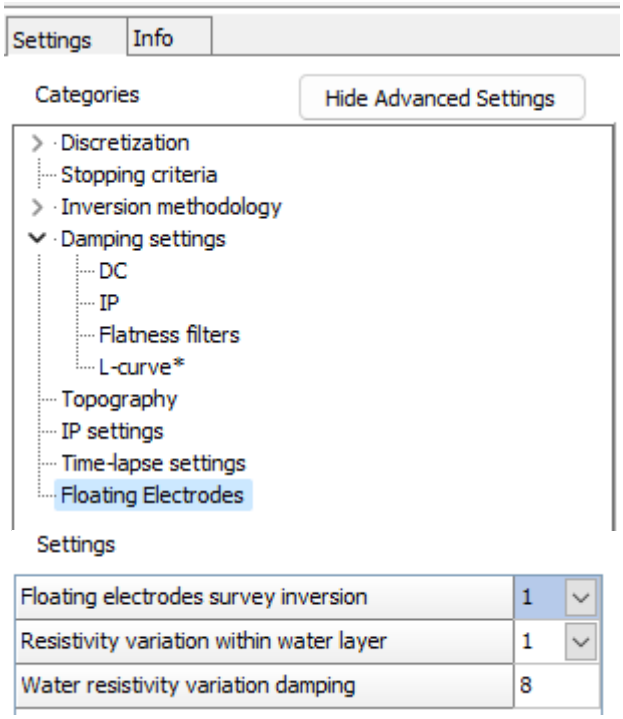

9.81 Floating electrodes survey inversion

There are two methods that can be used for the inversion of the data set. The first method (Use fixed water layer) is more suitable when the maximum thickness of the water layer is small (less than 20%) compared to the maximum depth of investigation of the survey configuration. Figure 29 below shows the inversion of the WATER_FLOAT.DAT data set using this method. A distorted finite-element grid is used to model the water layer. The maximum thickness of the water layer in this example is 2.5 meters that is small compared to the maximum depth of investigation at about 15 meters for the data set.

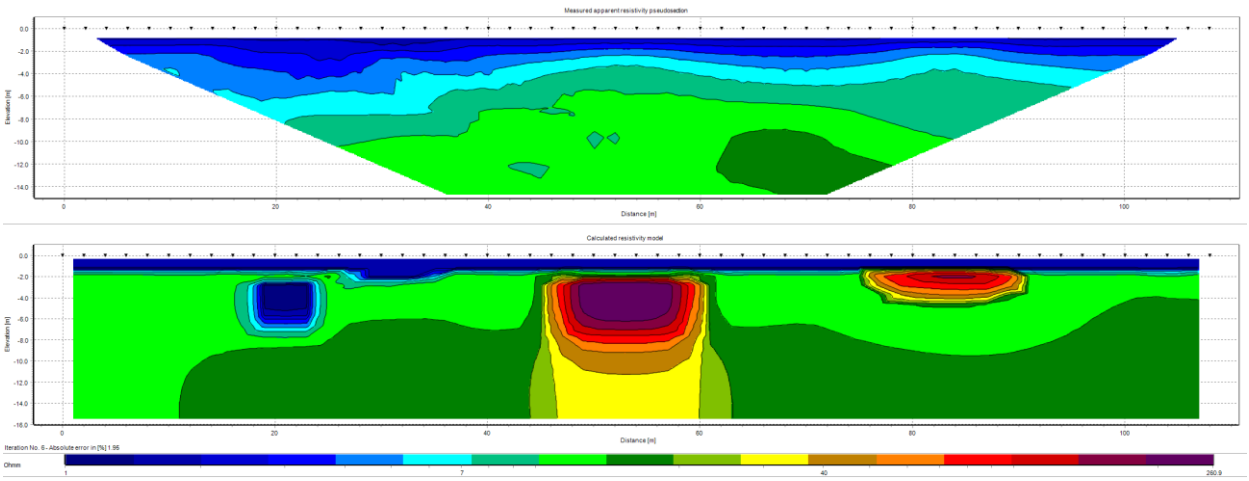

Figure 29. Example of inversion model with a fixed water layer. The inversion results of the WATER_FLOAT.DAT data is shown where the resistivity water layer (represented by the top blue layer in the model section) is fixed and model extends from below the water bottom.

In cases where the thickness of the water layer is significant, a second inversion method (Incorporate the water layer into the model) is more suitable. The water layer section is included into the inversion model.

9.82 Resistivity variation within water layer

The ‘Incorporate the water layer into the model’ method has two inversion settings. In most cases, the resistivity of the water layer does not vary significantly along the survey line or with depth.

Copyright 2025, Seequent

Thus, normally the option ‘Minimize variation of water resistivity’ is selected. However, to accommodate cases where there are significant variations in the water resistivity (such as in a mixing zone between fresh and saline water), the option ‘Allow water layer resistivity to vary freely’ can be used.

The subsurface material below the water layer frequently has a much higher resistivity than the water. The option ‘Select a sharp change across the water bottom boundary’ can be used so that a sharp contrast is allowed between the water layer and the subsurface. This option uses the method described in section 7.10. The program automatically adjusts the thickness of the model layers and divides the model cells into those belonging to the water layer and the subsurface. Figure 300 shows the arrangement of the model cells for one of the survey lines along the São Francisco River, that divides the Bahia (BA) and Pernambuco (PE) states, near the Santa Maria da Boa Vista city (PE), northeast of the Brazil (Rodrigo Machado pers. Comm.). In this survey, a dipole-dipole type of configuration was used with 5 meter dipoles. However, the readings were taken every meter that gives a data set with a nominal unit electrode spacing of 1 meter. To reduce the number of model cells and taking in consideration that the resolution of such a survey is very unlikely to be better than half the dipole length, the width of the model cells was set at 3 times the unit electrode spacing (section 9.1.3.1), i.e., basically 3 meters for almost the entire section. Also, note that the depth of the water at some places is greater than maximum median depth of investigation (as indicated by the data points markers). However, the program sets the depth of the layers such that there is at least one model layer below the water bottom (represented by the dark blue line). The cells below the water layer are marked as light blue in the figure below. A sharp resistivity variation is allowed in the inversion method used between the two sections.

The apparent resistivity pseudo section and inversion model for this data set is shown in Figure 31. In this inversion, the resistivity variation within the water layer was minimized. Thus, the water layer resistivity is generally uniform except towards the left end of the survey line where there is not much data. There is also an indication that between the 190 and 220 meter marks, the near-surface riverbed material consists of low resistivity sediments.

Surveys with floating electrodes are frequently carried out using a cable with a number of electrodes pulled behind a boat, usually with a multi-channel resistivity-meter system controlled by a computer linked to a GPS system. A 5 meter spacing between the electrodes takeouts is commonly used together a dipole-dipole type of array configuration (not necessary symmetrical). The boat moves continuously and the measurements can be made at arbitrary intervals although the dipole length is 5 meters. Frequently, the measurements are digitized to every 1 meter position. Thus, the active electrode positions are 1 meter apart that is much smaller than the dipole length of 5 meters. This can result in very long survey lines, and very large inversion models with the default settings of the RES2DINV. A number of options have been added to RES2DINV to reduce the inversion time for such data sets.

The resolution of the survey setup is unlikely to be very much better than the dipole length particularly if there is water layer of significant thickness between the cable and the subsurface. The program normally uses a model where the widths of the model blocks are set to be the same (or half) as the distance between the electrode positions along the line. This is reasonable for normal land surveys with a static cable setup. For floating electrodes survey, since the distance between the electrodes positions (1 meter) is much smaller than the dipole length (5 meters), this results in a model that is too fine. To avoid this, use the option ‘Width of blocks’ under Horizontal discretization. Since the horizontal resolution of the data is unlikely to be better than half the dipole length, it is recommended that the width of the model cells be set at 3 times the unit electrode spacing (for the situation with 5 meter dipoles and 1 meter data spacing). This will greatly reduce the number of model cells in the inversion model. The time taken to calculate the apparent resistivity (and the corresponding Jacobian matrix) can be greatly reduced by using ‘Use sparse inversion method’ under Long survey line settings within Inversion methodology.

It is assumed that the survey line is straight when a 2-D inversion approach is used. In cases where there are strong water currents this is no longer true so there will be distortions in the resulting inverse model. If there are significant deviations in the direction of the survey line, a better method will be to use a 3-D approach in modeling the data (Rucker *et al.* 2011b).

9.83 Water resistivity variation damping

Controls the degree which the water resistivity can vary. A higher value will result in a smaller resistivity variation.

Copyright 2025, Seequent

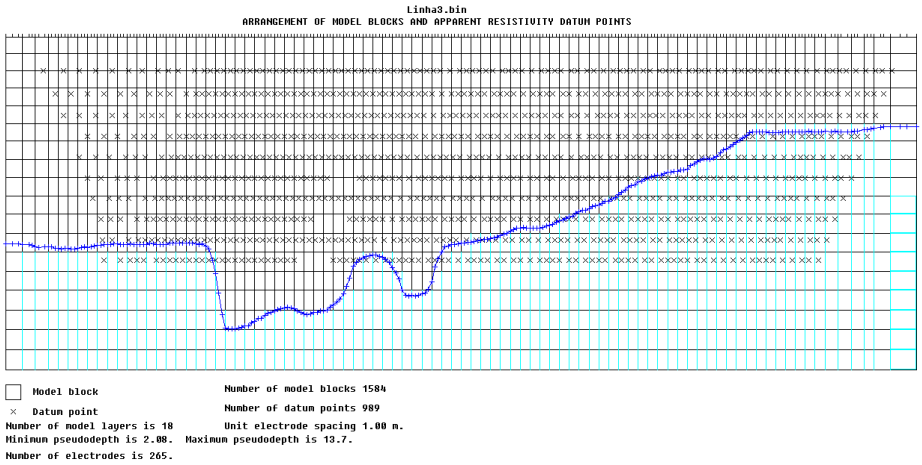

Figure 30. Arrangement of model blocks and the water bottom boundary for an arrangement with the water layer incorporated into the inversion model.

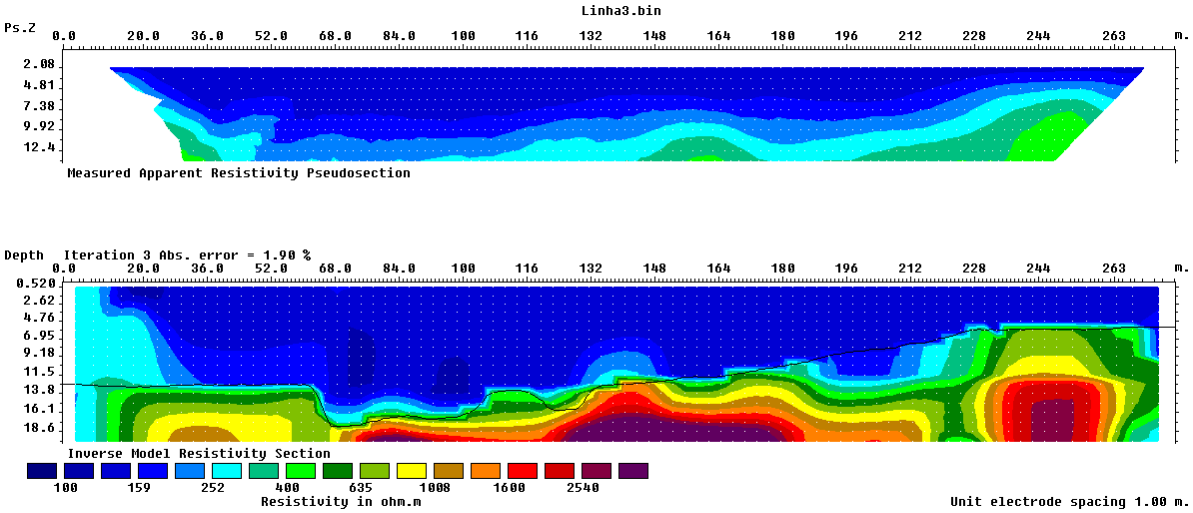

Figure 31. Inversion model for the survey with floating electrodes along the along the São Francisco River in Brazil. The thin black line indicates the water bottom boundary.

9.9 Borehole

These settings are for borehole data. This includes single borehole, cross-borehole and surface-borehole data.

When borehole data is loaded into Res2Dinv, two settings under Inversion Methodology/Settings are changed as default. The two settings are “Reduce effects of side blocks” which is turned off, and “Data space” which is set to linear. These two settings are described in section 9.3.1.

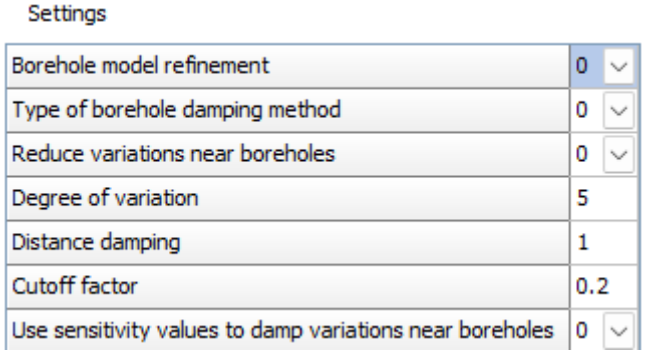

Copyright 2025, Seequent

9.9.1 Borehole model refinement

Default (0) sets the dimensions of the model blocks as the spacing between the electrodes on the ground surface and in the boreholes. Setting it to 1, sets the dimensions of the model blocks where the size of the blocks is half width of the spacing between the electrodes on the ground surface and in the boreholes.

9.9.2 Type of borehole damping method

If set to 0 (default), the damping factor distance is using the horizontal distances of the model cells from the boreholes, if set to 1 the damping factor distance is the distance from nearest active electrode.

9.9.3 Borehole model refinement

For some cases, the model cells near to the boreholes can show very large resistivity variations. This option allows to reduce the variations.

9.9.4 Degree of variation

Set the degree in which the variations near the boreholes are reduced. A larger value will result in smaller variations near the boreholes.

9.9.5 Distance damping

Set the degree the variations near the boreholes are suppressed depending on distance to the borehole. A smaller value will give a larger reduction in the resistivity variations with distance away from the borehole.

9.9.6 Cutoff factor

Only model cells above the cutoff factor will be subjected to a higher damping factor.

9.9.7 Use sensitivity values to damp variations near boreholes

To reduce the resistivity variations near the borehole electrodes, you can use the sensitivity values. This is more useful in cases where not all the boreholes' electrodes are used, for example when the subsurface electrodes are actually arranged along a horizontal line.

Copyright 2025, Seequent

10. Results/Model tab

All tools and functions on the Result/model tab are described on the Wiki page that can be accessed by pressing F1 when on the Result/model tab in Res2Dinv:

https://wiki.ags-cloud.dk/wiki/R2H_InversionTab

Error Statistics Tool

All tools and functions on the Error Statistics Tool are described on the Wiki page that can be accessed by pressing F1 when on the Error Statistics Tool window in Res2Dinv:

https://wiki.ags-cloud.dk/wiki/R2H_ErrorStatisticsTool

This displays the data misfit between the measured and calculated apparent resistivity values in the form of a histogram as shown in Figure 32. This option can be used to filter out data outliers. Data with normal random noise will show an exponential decrease in the number of data points with increasing data misfit, as in the initial part of Figure 32. Data outliers are likely to have much higher data misfit values which can be used to separate them from the other data points, as shown by a data point on the right end of the histogram in Figure 32. In this option, the user selects a data misfit cutoff value. The data points that will be removed are marked in red in the scatter plot on the right. If IP data is present, the scatter plot for the apparent IP data points will also be displayed below.

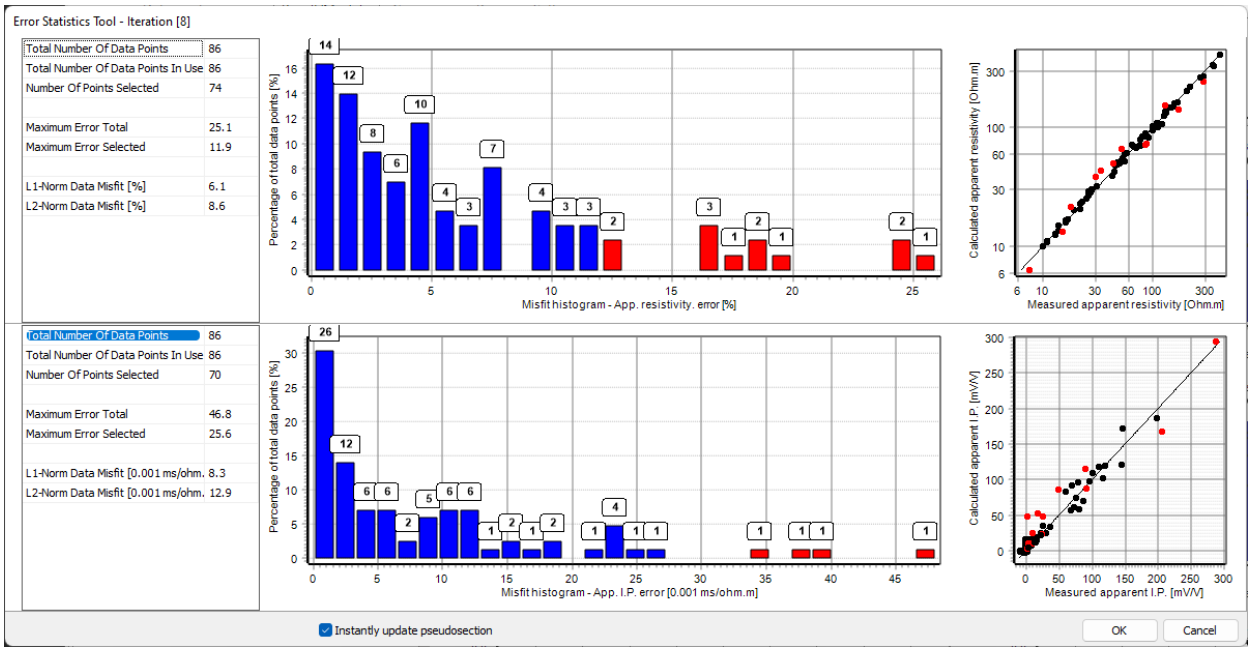

Figure 322. Histogram and scatter plots for the inversion results of the IPMAGUSI.DAT data sets.

10.1 Model export

In the Result/model tab, it is possible to export the inversion model to different formats.

Copyright 2025, Seequent

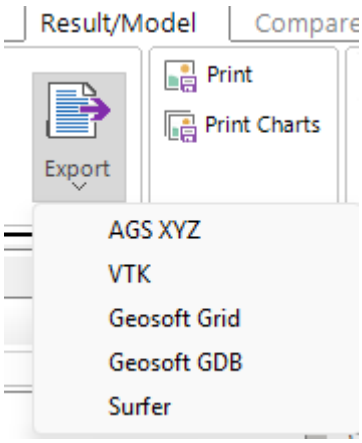

Save data in AGS XYZ format - This saves model values into a simple text file table. Rows in the table each represent a single quadrilateral block of a model. Columns represent different block properties such as resistivity, sensitivity, positions of each 4 corners of a block, and several others. If some block properties are not defined or have not been calculated for a given inversion model, the column will contain entries with asterisks (*). If exporting a time lapse model, additional columns are added to represent resistivities (and IP values if available) from each time step. These additional columns appear furthest to the right in the table.
All column variables are described in the header of the text file. The header also contains information about the size of the model, including e.g. the vertical and lateral number of blocks. The output blocks form a structured grid. This means that blocks always share edges with four other neighboring blocks if not at a boundary. This subdivision may by finer than the coarser set of blocks used to define individual parameters in the inversion procedure. To map from the fine (regular) block grid to the coarser (less regular) block grid, the column called 'blkind' can be employed. It indicates which coarse block a given fine block is part of.

Model output in VTK format - This saves the inverse model into the VTK format used by the free Paraview graphics plotting program. Global coordinates, if present, are also stored in the vtk files so that models from different lines have the same coordinate system. The positions of the electrodes are saved in a separate file with a name that ends with "_Elec.vtk". The vtk files with global coordinates from different 2-D lines in the same area can be displayed together in a fence diagram display using the Paraview program.

Save data in Geosoft GDB format - This saves model values in a Geosoft GDB database file which can be opened and edited in e.g. Oasis montaj. The resulting GDB file will contain exactly the same information as in the AGS XYZ format described in the above paragraph. Saving data to GDB files requires installation of the GeoSoft API. The steps needed for this are described in Appendix G.

Save model in Surfer format - This option allows the user to save the apparent resistivity pseudo sections and model sections in the format used by the SURFER graphics 2-D plotting program by Golden Software. A description of the steps involved is described in Appendix E.

11. Compare tab

All tools and functions on the Compare tab are described on the Wiki page that can be accessed by pressing F1 when on the Compare tab in Res2Dinv:

https://wiki.ags-cloud.dk/wiki/R2H_CompareTab

11.1 Display properties

For each model plot, besides plotting resistivity, conductivity, IP (if IP is inverted), it is

Copyright 2025, Seequent

also possible to display the sensitivity, uncertainty and model resolution (if this option is selected in the inversion settings).

The model property can be selected either in the Plot settings list or by right-clicking on each plot and select Display Property

Model sensitivity

This displays the model with the sensitivity value associated with each model block or contour plot. This gives the integrated sensitivity value associated with each model block as given by the following equation.

$$S_i = \frac{1}{m}\sum_{j=1}^{m}\left|J_{ij}\right| \qquad (14.1)$$

It sums up the Jacobian matrix values associated with the model block for all the data points. It is a very crude measure of the information the data set has on the resistivity value of a model block. A better measure is the model resolution value.

Model uncertainty

This displays an estimate of the uncertainty in the model resistivity values, and the lower and upper limits of the resistivity values based on the estimated uncertainty. If the model resolution was calculated, the uncertainty value is calculated from the diagonal elements of the $\mathbf{(J^TJ + \lambda F)^{-1}}$ matrix. If the model resolution was not calculated, an approximation of the uncertainty is used. The maximum and minimum sections are calculated from the inversion model values and the estimated uncertainty in the model values.

Model Resolution

If the option to calculate the model resolution values was selected (section 9.3.1), the model resolution values will be saved in the INV file. This option displays the saved model resolution values (Figure 33).

12. Program settings

All tools and functions on the Program Settings tab are described on the Wiki page that can be accessed by pressing F1 when on the Program Settings tab in Res2Dinv:

https://wiki.ags-cloud.dk/wiki/R2H_ProgramSettingsTab

Copyright 2025, Seequent

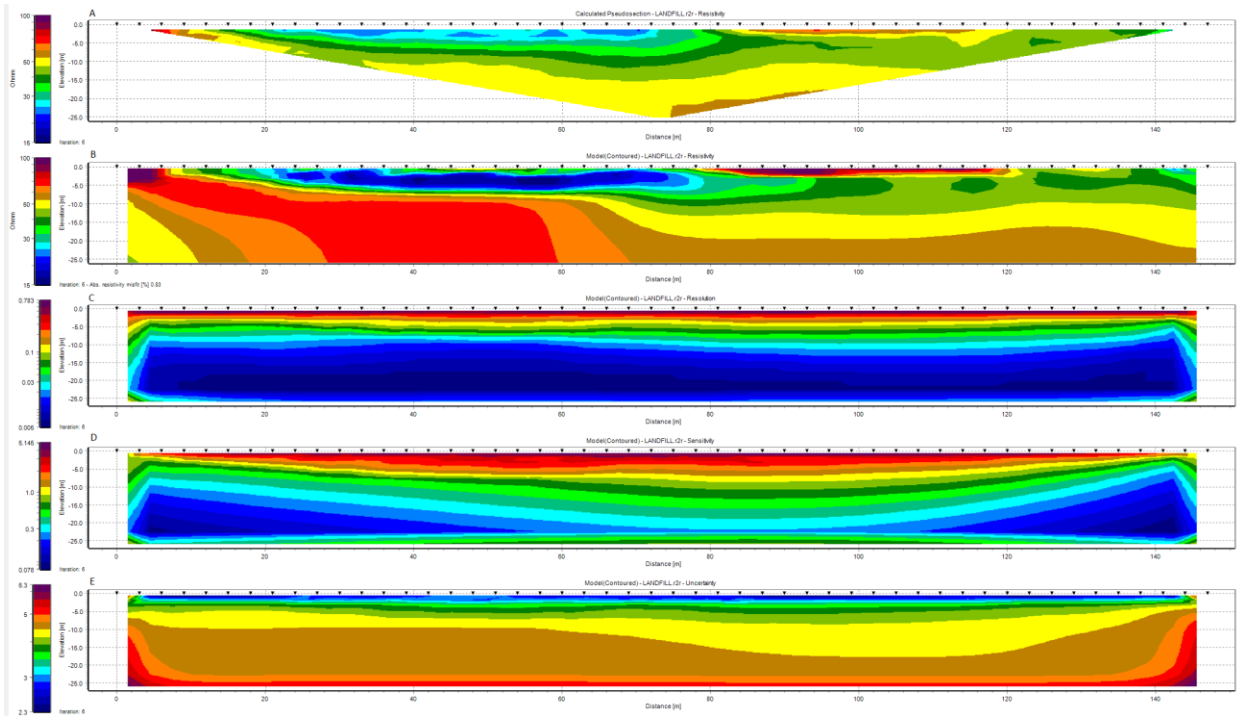

Figure 333. Display properties sections for the LANDFIL.DAT data set. (a) Apparent resistivity pseudo section. (b) Inversion model section. (c) Model resolution section. (d) Sensitivity section (e) Uncertainty section.

.

Copyright 2025, Seequent

Acknowledgements

Dr. Torleif Dahlin of Lund University in Sweden provided the interesting and challenging Odarslov Dyke, Gladkvarn and Knivsas data sets. The Grundfor and Cromer data sets were kindly provided by Dr. Niels B. Christensen of the University of Aarhus in Denmark and Dr. Torleif Dahlin. The Rathcroghan data set was kindly provided by Dr. Kevin Barton and Dr. Colin Brown from data collected by the Applied Geophysics Unit of University College Galway, Ireland. Dr. Andrew Binley of Lancaster University kindly provided the cross-borehole field data set. Mr. Ernst Neiderleithinger of Buro Fur Geophysik Lorenz (Germany) supplied the Landfill data set that provided the initial motivation to write this program to handle large 2-D data sets. I am also grateful to Prof. Douglas Oldenburg of the University of British Columbia in Canada for pointing out the some of the possible advantages of using equation (2). The Bauchi data was provided by Dr. Ian Acworth of School of Civil and Environmental Engineering, The Un. of New South Wales, Australia. Many thanks to Richard Cromwell and Rory Retzlaff of Golder Assoc. (Seattle) for the survey example to map holes in a clay layer. Bill Seaton of ATS, Virginia kindly provided the BLUERIDGE.DAT data set. I would also like to thank Ron Kaufman of Technos Inc. for his permission to use the Lake Lelia underwater field survey example. I would like to acknowledge Michel Ritz of IRD, France for kindly providing the BOREHOLE_TOPO.DAT example data set. The data set for the floating electrodes survey along the São Francisco River in Brazil was kindly provided by Rodrigo Machado. Finally, a special thanks to Ron Barker of The University of Birmingham (U.K.) for the Birmingham time-lapse, Stud Farm bedrock survey and the Clifton (with Julian Scott) data sets.

Copyright 2025, Seequent

References

Acworth, R. I., 1987. The development of crystalline basement aquifers in a tropical environment: Quarterly Journal Engineering Geology, **20**, 265-272.

Barker, R. and Moore, J., 1998. The application of time-lapse electrical tomography in groundwater studies. The Leading Edge, **17**, 1454-1458.

Brandes, I. and Acworth, R.I., 2003. Intrinsic negative chargeability of soft clays. ASEG Extended Abstracts, 2003, 1-4.

Christensen N.B. and Sorensen K.I., 1994. Integrated use of electromagnetic methods for hydrogeological investigations. Proceedings of the Symposium on the Application of Geophysics to Engineering and Environmental Problems, March 1994, Boston, Massachusetts, 163-176.

Claerbout, J.F. and Muir, F., 1973. Robust modeling with erratic data. Geophysics, **38**, 826-844.

Dahlin, T., 1996. 2D resistivity surveying for environmental and engineering applications. First Break, **14**, 275-284.

Dahlin, T. and Zhou, B., 2004. A numerical comparison of 2D resistivity imaging using ten electrode arrays. Geophysical Prospecting, **52**, 379-398.

Dahlin, T. and Zhou, B., 2006. Multiple gradient array measurements for multi-channel 2D resistivity imaging. Near Surface Geophysics, **4**, 113-123.

Dahlin, T., Loke, M.H., Siikanen, J. and Höök, M., 2014. Underwater ERT Survey for Site Investigation for a New Line for Stockholm Metro, in Procs. 31st Nordic Geological Winter Meeting, Lund, Sweden, 8-10 January 2014.

Day-Lewis, F.D., Singha, K. and Binley, A.M., 2004. Applying petrophysical models to radar travel time and electrical resistivity tomograms: Resolution-dependent limitations. Journal of Geophysical Research : Solid Earth, **110**, 1 - 17.

deGroot-Hedlin, C. and Constable, S., 1990, Occam's inversion to generate smooth, two-dimensional models form magnetotelluric data. Geophysics, **55**, 1613-1624.

Edwards, L.S., 1977, A modified pseudo section for resistivity and induced-polarization. Geophysics, **42**, 1020-1036.

Farquharson, C.G., 2008. Constructing piecewise-constant models in multidimensional minimum-structure inversions. Geophysics, **73**, K1-K9.

Farquharson C.G. and Oldenburg D.W. 2004. A comparison of automatic techniques for estimating the regularization parameter in non-linear inverse problems. Geophysical Journal International, **156**, 411-425.

Fox, R.C., Hohmann, G.W., Killpack,T.J. and Rijo, L., 1980, Topographic effects in resistivity and induced polarization surveys. Geophysics, **45**, 75-93.

Hallof, P.G., 1990, Reconnaissance and detailed geophysical results, Granite Mountain Area Pershing County, Nevada. in Fink, J.B., McAlister, E.O., Sternberg, B.K., Wieduwilt, W.G. and Ward, S.H. (Eds), 1990, Induced polarization : Applications and case histories : Investigations in Geophysics No. 4, Soc. Expl. Geophys.

Keller G.V. and Frischknecht F.C.,1966. Electrical methods in geophysical prospecting. Pergamon Press Inc., Oxford.

Kenma, A., Binley, A., Ramirez, A. and Daily, W., 2000. Complex resistivity tomography for environmental applications. Chemical Engineering Journal, 77, 11-18.

Kim, J H., M J. Yi, S G., Park, and J.G. Kim, 2009. 4-D inversion of DC resistivity monitoring data acquired over a dynamically changing earth model. Journal of Applied Geophysics, **68**, 522-532.

Kim, J.H., 2010. 4-D inversion of resistivity monitoring data using L1 norm minimization. *Procs. 16th European Meeting of Environmental and Engineering Geophysics*, 6 - 8 September 2010, Zurich, Switzerland, A15.

Loke, M.H., 1999. Time-lapse resistivity imaging inversion. 5th Meeting of the Environmental and Engineering Geophysical Society European Section Proceedings. Em1.

Loke, M.H., 2000. Topographic modelling in resistivity imaging inversion. 62nd EAGE Conference & Technical Exhibition Extended Abstracts, D-2.

Loke, M.H., 2018. Tutorial : 2-D and 3-D electrical imaging surveys. Geotomosoft Solutions, Malaysia. (Available for download from www.geotomosoft.com)

Loke, M.H. and Barker, R.D., 1996, Practical techniques for 3D resistivity surveys and data inversion. Geophysical Prospecting, **44**, 499-523.

Loke, M.H. and Dahlin, T., 2002. A comparison of the Gauss-Newton and quasi-Newton methods in resistivity imaging inversion. Journal of Applied Geophysics, **49**, 149-162.

Copyright 2025, Seequent

Loke, M.H., Acworth, I. and Dahlin, T., 2003. A comparison of smooth and blocky inversion methods in 2D electrical imaging surveys. Exploration Geophysics, **34**, 182-187.

Loke, M.H. and Dahlin, T., 2010. Methods to Reduce Banding Effects in 3-D Resistivity Inversion. Near Surface 2010 – 16th European Meeting of Environmental and Engineering Geophysics 6 - 8 September 2010, Zurich, Switzerland, A16.

Loke, M.H., Wilkinson, P. and Chambers, J., 2010a. Fast computation of optimized electrode arrays for 2D resistivity surveys. Computers & Geosciences, **36**, 1414-1426.

Loke, M.H., Wilkinson, P. and Chambers, J., 2010b. Parallel computation of optimized arrays for 2-D electrical imaging. Geophysical Journal International, **183**, 1202-1315.

Loke, M.H., Chambers, J.E., Rucker, D. F., Kuras, O. and Wilkinson, P. B., 2013. Recent developments in the direct-current geoelectrical imaging method. Journal of Applied Geophysics , **95**, 135-156.

Loke, M.H., Dahlin, T. and Rucker, D.F., 2014. Smoothness-constrained time-lapse inversion of data from 3-D resistivity surveys. Near Surface Geophysics, **12**, 5-24.

Loke, M.H., Kiflu, H., Wilkinson, P.B., Harro, D. and Kruse, S., 2015. Optimized arrays for 2-D resistivity surveys with combined surface and buried arrays. Near Surface Geophysics, **13**, 505-517.

Maurer, H. and Friedel, S., 2006. Outer-space sensitivities in geoelectrical tomography. GEOPHYSICS, 71(3), 1942-2156.

Nelson, G.D. and Van Voorhis, 1973, Letter to the editor regarding the paper "Complex resistivity spectra of porphyry copper mineralization". Geophysics, **38**, 984.

Niederleithinger, E., 1994, Use of high resolution geomagnetics, 2D-DC-geoelectrics and induced polarisation in environmental investigations. Paper presented at SAGEEP '94, Boston, USA.

Oldenborger, G.A., and P.S. Routh, 2009, The point-spread function measure of resolution for the 3D electrical resistivity experiment, Geophysical Journal International, **176**, 405-414.

Oldenburg, D.W. and Li., Y., 1999. Estimating depth of investigation in dc resistivity and IP surveys. Geophysics, **64**, 403-416.

Olivar, A., de Lime, L. and Sharma, M.M., 1990. A grain conductivity approach to shaly sandstones. Geophysics, **55**, 1347-1356.

Robain, H., Albouy, Y., Dabas, M., Descloitres, M., Camerlynck, C., Menchler, P. and Tabbagh, A., 1997, The location of infinite electrodes in pole-pole electrical surveys: consequences for 2D imaging. Journal of Applied Geophysics, **41**, 313-333.

Rucker, D., Fink, J.B. and Loke, M.H., 2011a. Environmental Monitoring of Leaks using Time Lapsed Long Electrode Electrical Resistivity. Journal of Applied Geophysics, **74**, 242-254.

Rucker, D.F., Noonan, G.E. and Greenwood, W.J., 2011b. Electrical resistivity in support of geological mapping along the Panama Canal. Engineering Geology, 117, 121-133.

Sasaki, Y., 1992, Resolution of resistivity tomography inferred from numerical simulation. Geophysical Prospecting, **40**, 453-464.

Scott, J.B.T., Barker, R.D. Peacock, S., 2000. Combined seismic refraction and electrical imaging. Procs. 6th Meeting of the European Association for Environmental and Engineering Geophysics, 3-7 Sept. 1997, Bochum, Germany, EL05.

Seaton, W.J. and Burbey, T.J., 2000. Aquifer characterization in the Blue Ridge physiographic province using resistivity profiling and borehole geophysics : Geologic analysis. Journal of Environmental & Engineering Geophysics, **5**, no. 3, 45-58.

Silvester, P.P. and Ferrari, R.L., 1990, Finite elements for electrical engineers (2nd. ed.). Cambridge University Press.

Slater, L., Binley, A.M., Zaidman, M.D. and West, L.J., 1997, Investigation of vadose zone flow mechanisms in unsaturated chalk using cross-borehole ERT. Proceedings of the EEGS European Section 3rd Meeting, Aarhus, Denmark, 17-20.

Summer, J.S., 1976, Principles of induced polarization for geophysical exploration. Elsevier Scientific Publishing Company.

Tong, L. and Yang, C., 1990, Incorporation of topography into two-dimensional resistivity inversion. Geophysics, **55**, 354-361.

Van Voorhis, G.D. Nelson, P.H. and Drake, T.L., 1973, Complex resistivity spectra of porphyry copper mineralization. Geophysics, **38**, 49-60.

Waddell, J. and Barton, K, 1995, Seeing beneath Rathcroghan. Archaeology Ireland, Vol. **9**, No. 1, 38-41.

White, R.M.S., Collins, S. and Loke, P., 2003. Resistivity and IP arrays, optimised for data collection and inversion. Exploration Geophysics, **34**, 229-232.

Copyright 2025, Seequent

Wilkinson, P. B., Chambers, J. E., Lelliot, M., Wealthall, G. P. and Ogilvy, R. D., 2008. Extreme Sensitivity Of Crosshole Electrical Resistivity Tomography Measurements To Geometric Errors. Geophysical Journal International, 173, 49-62.

Witherly, K.E. and Vyselaar, J, 1990, A geophysical case history of the Poplar Lake Copper-Molybdenum deposit, Houston Area, British Columbia. in Fink, J.B., McAlister, E.O., Sternberg, B.K., Wieduwilt, W.G. and Ward, S.H. (Eds), 1990, Induced polarization : Applications and case histories : Investigations in Geophysics No. 4, Soc. Expl. Geophys.

Zhou B. and Dahlin, T., 2003, Properties and effects of measurement errors on 2D resistivity imaging surveying, *Near Surface Geophysics*, 1, 105-117.

Copyright 2025, Seequent

Appendix A Array types in RES2DINV

A list of the arrays supported by the RES2DINV program together with their number codes is given below.

Table 35. Array types and their number codes.

Array name	Number code	Number of electrodes
Wenner (Alpha)	1	4
Pole-Pole	2	2
Inline Dipole-Dipole	3	4
Wenner (Beta)	4	4
Wenner (Gamma)	5	4
Pole-Dipole	6	3
Wenner-Schlumberger	7	4
Equatorial dipole-dipole	8	4
Offset pole-dipole (only used as sub-array number with data in the general array format)	10	3
Non-conventional or general array	11	2 to 4
Cross-borehole survey (apparent resistivity values)	12	2 to 4
Cross-borehole survey (resistance values)	13	2 to 4
Gradient array (only used as sub-array number with data in the general array format)	15	4

A description of the different arrays types is given in the free tutorial notes on electrical imaging (Loke 2018). Figure 34 shows the arrangement of the electrodes for some commonly used arrays. In general, for an array with 4 electrodes, there are 3 possible arrangements for the electrodes. The Wenner array has three different variations. The "normal" Wenner array is actually the Wenner alpha array. The Wenner beta array is a special case of the dipole-dipole array where the "n" factor is always 1. The RES2DINV program will automatically convert a Wenner beta array data file into a dipole-dipole array data set.

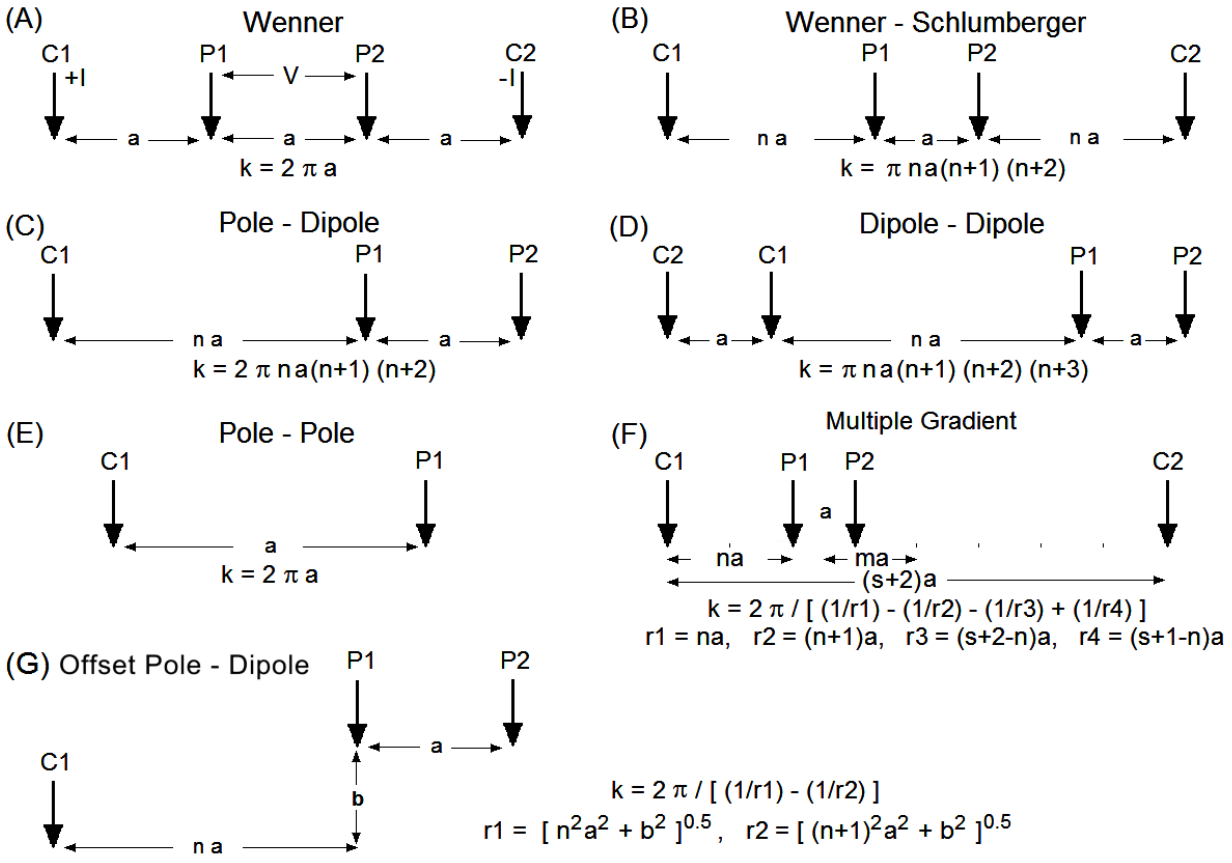

Figure 344. Arrangement of the electrodes for some commonly used arrays and their geometric factors.

Copyright 2025, Seequent

The general array with number code 11 is always given with a secondary sub-array number code. If the arrays are actually one of the conventional arrays, the number code for the conventional array is used as the sub-array number (for example if it is a dipole-dipole array the sub-array number is then 3). If it is not one of the conventional arrays, or if it is a mixture of different arrays (such as the dipole-dipole and gradient), the sub-array number is given as 0.

The ‘forward’ and ‘reverse’ variations of the pole-dipole array are shown in Figure 355. If an offset dipole-dipole array is used, the general array data format should be used with a sub-array type of 0.

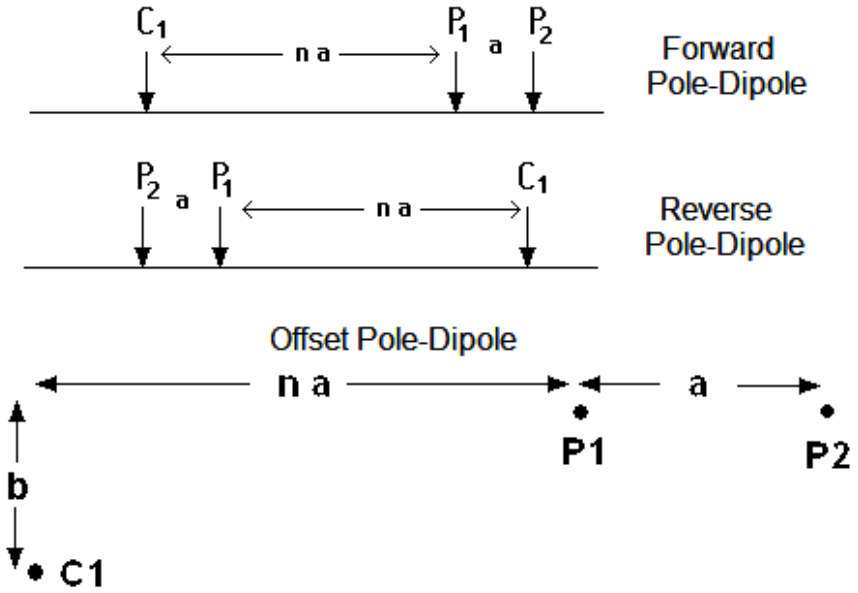

Figure 355. Normal, reverse and offset pole-dipole array arrangements.

Copyright 2025, Seequent

Appendix B Special OhmMapper Note

Data collected by the OhmMapper system can be converted into the format used by the RES2DINV program using the 'DataMap for OhmMapper' program provided by Geometrics, Inc. This is a Windows based program. After starting the program, please click the EXPORT option to carry out the data conversion. For further details, please refer to the OhmMapper manual provided by Geometrics. The figure below shows an example of a data set collected by the OhmMapper system together with the inversion model produced by the RES2DINV. The survey was conducted over an area with weathered granite. The data set is given in the file OHMMAPPER.DAT. The measurements were made using the dipole-dipole array with a dipole length "a" spacing of 10 metres and with n values of 0.5 to 3.5. The data set has 732 data points while the inversion model consists of 1240 cells.

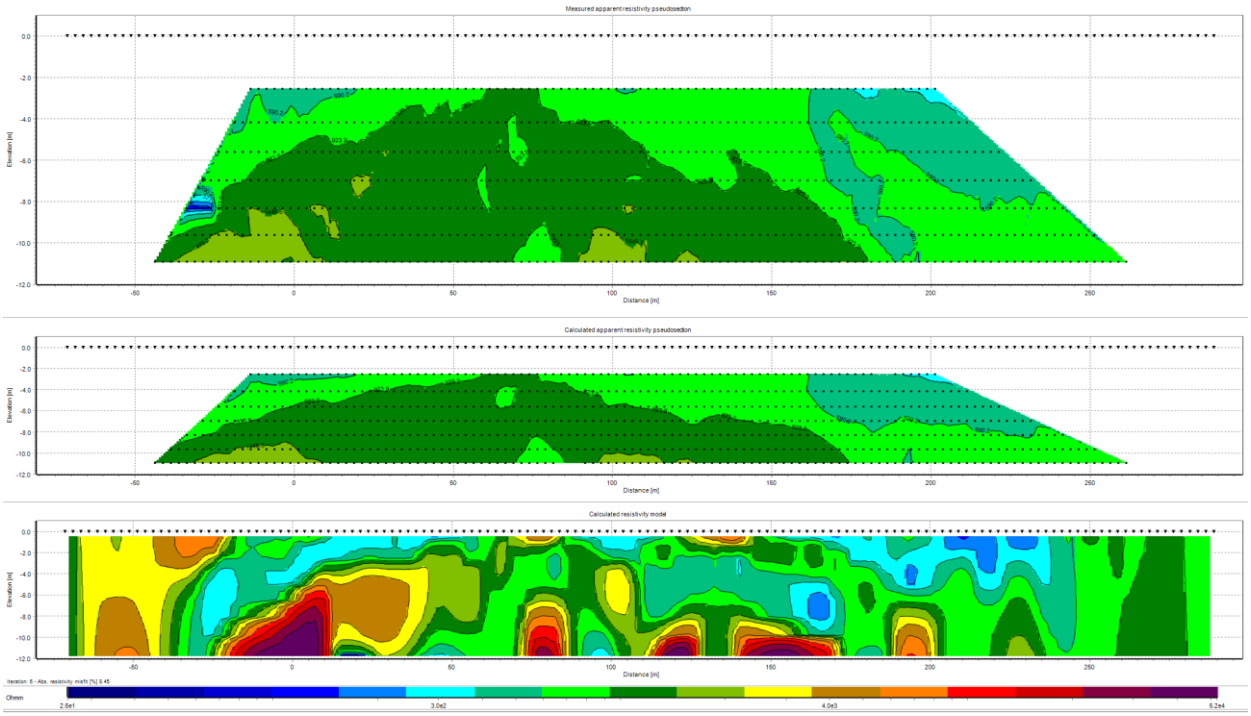

Figure 366. Example OhmMapper data set and inversion model. (a) Apparent resistivity pseudo section measured with an OhmMapper mobile resistivity surveying system. (b) Model section obtained by RES2DINV

Copyright 2025, Seequent

Appendix D Surveys with electrodes suspended in a water layer

The two arrangements for aquatic surveys have the electrodes on the seabed (section 7.9.1) or floating on the water surface (section 7.9.2) have disadvantages if a mobile system is used. If the water layer is thick, the resolution will be very poor with floating electrodes as most of the current will flow within the water layer and very little penetrates into the sub-bottom materials which are of interest. Dragging the cable along the bottom might lead to other problems, such as the cable being snagged by debris on the seabed. The third possible arrangement is to have the cable suspended a short distance (such as 1 meter) above the seabed. This has the advantage of better resolution with the electrodes closer to the targets of interest while avoiding obstacles on the seabed. The example file Suspended-Streamer-Aquatic-Survey.dat file (37) shows the data format for this type of situation. After the section with the water layer parameters, a header 'Suspended streamer used' is used to indicate that the electrode are not on the water bottom but suspended in the water layer. This is followed by the main section giving the elevation of the streamer along the profile. This data set is from a synthetic model with the cable 4 meters below the water surface and 1.0 to 1.5 meters above an uneven seabed with a depth of 5.0 to 5.5 meters below the surface. The water region is modeled by a finite-element mesh. The vertical positions of the nodes in the mesh are automatically adjusted to take into account variations in the water thickness (Figure 377) with adjustments at the appropriate nodes to fit the actual depths of the electrodes along the profile. Figure 38 shows the pseudo section and inversion model for the example data file.

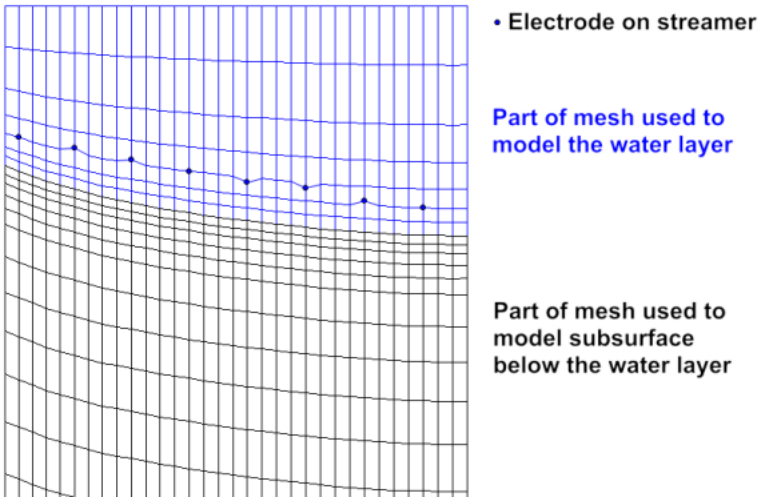

Figure 377. Mesh used to model water layer.

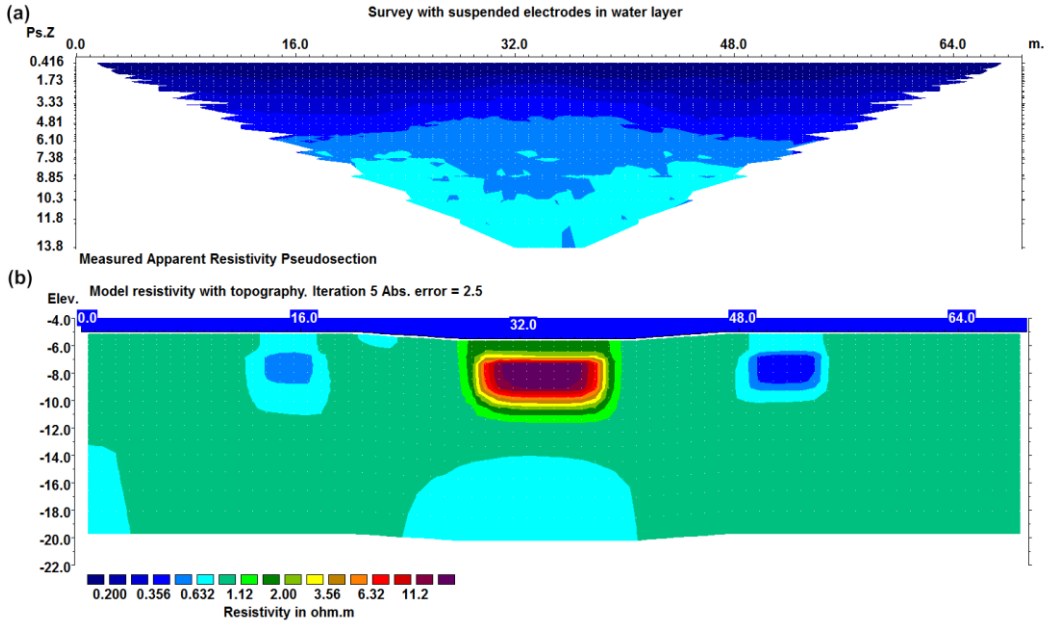

Figure 388. Example data set and inversion model for a survey with a streamer suspended in a water layer. (a) Apparent resistivity pseudo section and (b) inversion model section.

Copyright 2025, Seequent

Table 36. Example data file for a survey electrodes suspended in a water layer.

Suspended-Streamer-Aquatic-Survey.dat file	*Comments*
Survey with suspended electrodes in water layer	*Title*
1.0	*Unit electrode spacing*
11	*General array type*
3	*Non-specific sub-array*
Type of measurement (0=app. resis, 1=resistance)	*Header*
0	*0 to indicate apparent resistivity given*
2172	*Number of data points*
1	*Indicates true horizontal x-distances*
0	*No IP data*
4 1.0,0.0 0.0,0.0 2.0,0.0 3.0,0.0 0.15426	*First 3 data points in general*
4 2.0,0.0 1.0,0.0 3.0,0.0 4.0,0.0 0.15422	*array data format. Note water*
4 3.0,0.0 2.0,0.0 4.0,0.0 5.0,0.0 0.15409	*surface at 0.0 meter elevation*
..	
..	*Similar format for other data*
..	*points*
4 12.0,0.0 4.0,0.0 60.0,0.0 68.0,0.0 0.53350	*Last 2 data points*
4 13.0,0.0 5.0,0.0 61.0,0.0 69.0,0.0 0.78482	
Topography in separate list	*Topography information header for general array*
1	*True x-distance*
8	*Number of topography values*
0.000,-5.000	*Topography x and z values*
20.00,-5.000	*Note this is the elevation of the true water bottom.*
28.00,-5.500	
30.00,-5.500	
34.00,-5.500	
40.00,-5.500	
47.00,-5.000	
69.00,-5.000	*Last topography data point.*
0	*No fixed regions*
1	*1 indicates survey with submerged electrodes*
0.300,-100.000, 200.000,0.0	*Resistivity, left and right limits of water layer, elevation at top of water layer*
1	*Indicates surface geometric factor used*
Suspended streamer used	*Header to indicate survey with suspended streamer*
Type of suspended streamer information (0=streamer,1=true water bottom)	*Header, to provide options for other types of information in future*
0	*Use 0 for now*
Number of streamer elevation data points	*Header*
7	*Number of values for streamer elevation profile*
x and z coordinates of points on streamer	*Header*
0.000,-4.000	*This section lists the x and z coordinates for*
10.00,-4.000	*points along the streamer profile*
30.00,-4.000	
35.00,-4.001	
40.00,-4.000	
60.00,-4.00	
69.00,-4.000	
0,0,0,0	*End with a few zeros*

Copyright 2025, Seequent

Appendix G Setup for GDB import/export

Importing or exporting from GDB files requires installation of a set of files (Geosoft redistributables). An installer for these files can be downloaded from https://www.aarhusgeosoftware.dk/download-additional-software. Furthermore, in some cases it will also be necessary to install the Microsoft Visual C++ Redistributable. This is often the case, if Res2DInv reports that one or dll-files are missing. The redistributable can be downloaded from here: https://docs.microsoft.com/en-us/cpp/windows/latest-supported-vc-redist?view=msvc-170 (choose the installer for x64 architecture).

First time a GDB file is attempted imported or exported, the conversion program will start a licensing app called Seequent Connector. This will take the user to a web browser showing a login form requiring a Seequent ID login:

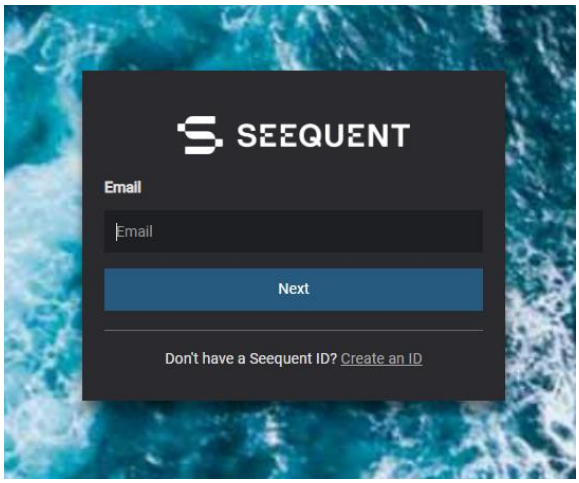

If the user does not already have a Seequent ID, it can be created for free by using the provided link. After signing in, accept the web browser's attempt to open Seequent Connector. Once this step is completed, GDB import/export will work without the need for additional Seequent Connector logins.

Copyright 2025, Seequent

DISCLAIMER

This software is provided "as is" without any express or implied warranties including its suitability for a particular purpose. Neither this company nor the subagent will assume responsibility for any damage or loss caused by the use of this program. In the event of program bugs, every effort will be made to correct the bugs. Users with a license under maintenance are entitled to free software updates and support for the first year. After the first year, there is an annual fee for software updates and technical support.

See user terms:

https://www.seequent.com/legal-privacy/online-services-user-terms/

SUPPORT

A frequent source of queries is when the results obtained are not what you expect, or the program refuses to accept your data file. In such a case, support will only be provided if a copy of the data file is sent together as an attachment with your email, preferably compressed into a ZIP file. The most common causes of problems are (a) the data in the DAT file is not given in the correct RES2DINV format (b) excessive noise in the data set (particularly for dipole-dipole surveys and/or IP data sets) (c) instrument malfunction or field survey errors. It is only possible to trace the source of the problem if a copy of the data file is provided. Please note that support is only available for users with a license under maintenance.

For technical support, you can contact.

ags.support@seequent.com

The following information will be required before technical support is provided.

1). Your license serial number.

2). The name of your company or institution.

Copyright 2025, Seequent

What's New

Version 3.00 - Major upgrade to Windows 3.1 and 95. Maximum number of electrodes increased to 500. Multi-tasking support for Windows 95. Support for any Windows compatible graphics card and printer.

Version 3.01 - Improvements to finite-difference subroutine to calculate the Jacobian matrix which is now about twice as fast as the earlier versions.

Version 3.10 - Support for underwater surveys. Direct incorporation of topography into inversion model using a distorted finite-element grid.

Version 3.11 - The time taken by the finite-element subroutine to calculate the Jacobian matrix is reduced. An option to use a finer mesh for the finite-difference or finite-element forward modelling method is added.

Version 3.12 - Non-integer values for the "*n*" factor for the dipole-dipole, pole-dipole and Wenner-Schlumberger arrays supported (please refer to Appendix A). The maximum limits for the number of data levels and model layers increased to 52 and 17 respectively.

Version 3.13 - The ratio of the largest electrode spacing to unit electrode spacing for the Wenner and pole-pole array was increased from 32 to 64. The maximum number of data levels is now 64. The maximum number of model layers was also increased to 18.

Version 3.20 - Support for IP data added.

Version 3.21 - The maximum number of electrodes was increased to 650. Improvements has been made to the disk-memory swapping subroutines so that for a given amount of RAM the number of datum points the program can handle is increased. For computer systems with more than one hard-disk drive, the program will automatically select the drive with the most free disk space to store the temporary disk swap files.

Version 3.22 - Slight improvements to the use of memory in the IP inversion section. The size of the IP data set that can be handled for a given amount of memory was increased. An option to optimise the damping factor automatically during the inversion process was added. Support for the "reverse" pole-dipole array added (see Appendix A). Support for a command line batch mode included (see Appendix I). An option to plot the model section in the form of rectangular blocks was also added.

Version 3.30 - Support for cross-borehole surveys added. An option to allow the number of model parameters to exceed the number of datum points was also added.

Version 3.31 - An option for a used defined model added. In this model, the user specifies the thickness of the first layer and the factor to increase the thickness for each subsequent deeper layer. The program will also automatically update the directory used for the input data files and the output inversion files listed in the RES2DINV.INI file.

Version 3.32 - An option to extend the subdivision of the subsurface into blocks to the edges of the survey line was added. Option to display the uncertainty in the model resistivity values was also added.
Version 3.33 - An option to incorporate the effects of the remote electrodes used in surface resistivity surveys with the pole-pole and pole-dipole arrays was added.

Version 3.34 - A few bug fixes. The user can now scale the depths of the model layers so that the depth to the last layer can be much greater than the default limit allowed by the program. When the program saves the model values in the XYZ format, it will now also save the coordinates of the corners of the blocks in the model. An option to use a very fine mesh in the vertical direction for resistivity contrasts of greater than 250:1 was added, as well as an option for 6 nodes in the horizontal direction between adjacent electrodes.

Copyright 2025, Seequent

Version 3.35 - The user can now set the maximum number of electrodes, from 150 to 1500, via the JACOBWIN.EXE program. Drawing of colour contour sections is now significantly faster on most computers.

Version 3.36 - A robust least-squares inversion option was added. For very noisy data with ‘outliers’, the resulting model will be less sensitive to such datum points when the robust data inversion method is selected. For areas where the subsurface geology has sharp interfaces, the robust model inversion method will give better results.

Version 3.40 - Support for non-conventional arrays for resistivity surveys.

Version 3.41 – Two new methods for topographic modelling using a damped distorted grid and the inverse Schwartz-Christoffel transformation added.

Version 3.42 - Support for remote electrodes for IP surveys.

Version 3.43 - Support for the Wenner Gamma array, and underwater surveys with non-conventional arrays. Maximum number of electrodes increased to 2000. The program has also been optimised for data sets where the unit electrode spacing has been reduced by half of the actual value so as to get a model where the width of the blocks is half the usual size. This helps in cases where there are very large lateral resistivity variations near the surface.

Version 3.44 - Support for IP surveys with non-conventional arrays. This feature is useful in some cases where data from a series of overlapping collinear 1D sounding survey lines can be combined into a single 2-D data set to obtain a 2-D model.

Version 3.45 - Option to save results in SURFER format added. Also support for surveys with some electrodes underwater and some electrodes above the water surface level added.

Version 3.46 - Minor additions for data in general array format. Option to use a model with half the unit electrode spacing for data in general array format is added (see the file RATCMIX2.DAT for an example). It is now possible to carry out the inversion of data in the general array format with the demo version, but the results will only be displayed temporarily on the screen during the inversion. The damped distorted grid finite-element method is set as the default method for topographic modelling.

Version 3.47 – An option to carry out the inversion of IP data sequentially was added. Slight changes in the menu structure.

Version 3.48 – Support for up to 4 boreholes in cross-borehole option.

Version 3.49 – Incomplete Gauss-Newton inversion option added. Maximum number of electrodes increased to 4000, and maximum number of data points to 20000. Option to combine a number of 2-D data files in RES2DINV format into a single 3-D data file in RES3DINV format added.

Version 3.50 – Bedrock edge detection and time-lapse options added.

Version 3.51 – Option to include data noise estimates included.

Version 3.52 – Option for surveys with floating electrodes added. Support for topography in cross-borehole surveys included.

Version 3.53 – Sparse inversion option for very long survey lines (2000 to 16000 electrode positions) added. This method inverts the entire data set and model at a single time to produce a continuous and seamless model. New format for batch mode option script file which makes use of the files containing the inversion parameters produced by the RES2DINV program.

Version 3.54 – Option to include boundaries of layers from seismic or borehole surveys added.

Copyright 2025, Seequent

Version 3.55 – Support for the multiple gradient array added.

Version 3.56 – Support for the offset pole-dipole array added.

Version 3.57 – Support to incorporate water layer into the inversion model for surveys with floating electrodes added.

Version 3.58 – Support for global coordinates added.

Version 3.59 – Support for time-lapse cross-borehole data added. Support for inclined boreholes added.

Version 3.70 Beta - Trial version with support for multi-core PCs. New inversion algorithm for time-lapse data. Complex resistivity inversion method for IP data.

Version 3.71 - Option to calculate model resolution values. New time-lapse method support for cross-borehole data.

Version 4.00 - 64-bit version that can access more than 4 GB RAM. This greatly increases the maximum size of the data set and model that can be handled. Supports up to 30 time series for time-lapse surveys.

Version 4.01 – Options to extend the horizontal range of inversion model and fast calculation of Jacobian matrix for dense data sets added.

Version 4.02 – Option to collate data from 2-D lines that are not parallel or orthogonal in the RES3DINV arbitrary electrodes format. Option for using L-curve method to estimate optimum damping factor added.

Version 4.03 – Support for more than one water layer for underwater surveys added.

Version 4.04 – Support for survey with electrodes on the ground surface and water bottom across water layer with a limited extent (such as a dam) added. Support for time-lapse IP data.

Version 4.05 – Support for underwater surveys with electrodes on a streamer suspended in the water layer with the entire water layer modeled by the finite-element mesh. Option to fix resistivity of regions above and below sharp boundary added.

Version 4.06 – Depth of investigation (DOI) calculations added. Option to display sequential changes in time-lapse display.

Version 4.07 – Options to display correlation plots for the data misfits added. Support for BMP, JPEG, PNG, TIFF and GIF bitmap graphics file formats.

Version 4.08 – Option to remove a series of data points using the ‘Exterminate bad data points’ option by using mouse right click the first and last data point in a profile. Model with borehole electrodes saved to xyz file with global coordinates if present. Option to save output model in Paraview vtk format. IP model values automatically saved with resistivity values and a second vtk file is automatically generated if global coordinates present. Aarhus GeoSoftware online copy protection system implemented to replace USB dongle system.

Version 4.09 – Options to calculate and display the model resolution point-spread function values. Model resolution values are included in xyz output file for data with global coordinates. VTK output files with coordinates of electrodes are also created together with the files with the model resistivity and IP values.

Version 4.10 – Output the positions of all 4 electrodes in xyz file. Different plotting order of general array data in ‘remove bad data points’. Results in less messy plots.

Version 5.0 –New user interface with many new visualization and processing options. Inversion speed is optimized.

Copyright 2025, Seequent

See release history log in installation folder for all update information from version 5.0 and forward.

Copyright 2025, Seequent